Synthesis, Characterization and Application of PEGylated Bimetallic Oxide Snail Shell Based Adsorbent for Remediation of Methylene Blue Polluted Wastewater

Abisoye Abidemi ADARAMAJA

LCU/PG/002217

Being a MSc Thesis Submitted to the Department of Chemical Science, Faculty of Applied Sciences, Lead City University, Ibadan, Oyo State, Nigeria

In Partial Fulfillment of the Requirement for the Award of Master of Science Degree (MSc) in Industrial Chemistry

2023

Certification

This is to certify that Abisoye Abidemi, ADARAMAJA with matriculation number LCU/PG/002217 carried out this research work titled "Synthesis, Characterization and Application of PEGylated Bimetallic Oxide Snail Shell-based Adsorbent for Remediation of Methylene Blue Polluted Wastewater" in the Department of Chemical Science, Faculty of Applied Sciences, Lead City University, Ibadan, Oyo State, for the award of Master Degree in Industrial Chemistry and that this has not been previously submitted.

_____ _____

Dr. A. O. Bamisaye **Date**

(Supervisor)

_____ _____

Dr. O. M. Ighodaro **Date**

(Head of the Department)

Dedication

The entire thesis is a thank-you to Almighty God and my loving parents, Mr. and Mrs. Adaramaja, for their unfailing love and guidance throughout my life.

Acknowledgement

I would not have been able to finish my research without the help of the research facilities provided by the Faculty of Applied Sciences at Lead City University in Ibadan.

I would be like a boat that got lost in the water if I wasn't properly guided. I would like to extend my profound gratitude to my supervisor, Dr. A.O. Bamisaye, for exposing me to the exciting topic of material science, for thoroughly outlining all the instructions I required for my experiments, and for providing me with insightful feedback on the results. I would want to thank the entire Chemistry Department faculty, especially the Department head, Professor O.M. Ighodaro. Without the kind help of Miss R.E. Morenike, Dr. A.A. Ige and Dr. A.B. Labintan, may God abundantly reward them; this research would not have been possible. I must express my sincere gratitude to the Faculty of Applied Sciences laboratory workers.

I am incredibly appreciative of and deeply admire Mr. & Mrs. Adaramaja's support and parental advice, both of which I respect. I want to express my gratitude to my sister and brother, in particular Yetunde Obasuye and Kolade Onola, for their inspiration and assistance. My coworkers, notably Mr. S. Abati, Dr. I. Bankole, deserve a great deal of credit for their encouragement and support.

Even though the above-mentioned institutions and persons have assisted in the process of this research work, I alone stand responsible for the errors, if any found in the work.

Abstract

Dyes polluted waste water has been shown to be catastrophic and lethargic to the environment; flora and fauna, resulting to an imbalance in the eco-system. This study focuses on the synthesis of bimetallic oxide and PEGylated biomass based adsorbent for effective uptake of methylene blue (MB) dye from waste water. The snail shell-based sorbents were synthesized through wet impregnation followed by calcination, which were characterized using FTIR, XRD, SEM and EDX. The batch adsorption experiment of methylene blue was carried out by varying the operating parameters such as contact time, temperature, pH, adsorbent dose, and initial adsorbate concentration. The optimum pH for this study was found at pH 3 with dosage of 10 mg, at 25 °C uptake of MB at 93.5% (CaO), 94.19% (Al_2O_3/Fe_2O_3-CaO) and 91.91% (PEGylated Al_2O_3/Fe_2O_3-CaO). SEM images of the catalysts showed well-organized rod-like and cubic aggregates, while XRD showed a highly crystalline bio-sorbent material. The EDX confirms an effective impregnation of the biomass material with the metal oxide while FTIR spectra showed the presence of O-H, N-H, C=O and C-O moiety available for the efficient adsorption of MB. Langmuir-Freundlich isotherm model best described the adsorption data for all the catalysts: CaO with R^2 value=0.994 and Q_{max}= 349.37mg/g. Al_2O_3/Fe_2O_3-CaO; with R^2 value = 0.986 and Q_{max} = 218.5 mg/g and PEGylated Al_2O_3/Fe_2O_3-CaO; with R^2 value = 0.984 and Q_{max} = 1570 mg/g The study is best fitted into Brouers Sotolongo sractals kinetics at a recorded R^2 = 0.991 and Q_{max}= 78.91 mg/g (CaO). R^2 = 0.995 and Q_{max} = 52.10 mg/g (Al_2O_3/Fe_2O_3-CaO), and R^2= 0.992 and Q_{max} =27.69 me/g (PEGylated Al_2O_3/Fe_2O_3-CaO). This study revealed that snail shell based adsorbent could be regarded as a promising biosorbent for the remediation of methylene Blue polluted wastewater.

Keywords: Waste water, Methylene blue, Catalysts, Biomass based adsorbent.

Word Count: 284

Table of Contents

List of Tables

List of Figures

List of Figures

List of Figures

List of Acronyms

Abbreviation	Meaning
AC	Activated Carbon
AOP	Advanced Oxidation Process
MB	Methylene Blue
MIP	Molecular Imprinted Polymers
MOF	Metal Organic Framework
nm	Nano Meter
PEG	Polyethylene Glycol
pH	Potential Of Hydrogen
PPM	Parts Per Million
REDOX	Reduction-Oxidation
SS	Snail Shell
UV	Ultraviolet
Zpc	Point Of Charge

Chapter One

Introduction

1.1 Background to the Study

The most significant and necessary element on Earth is water, but due to human activity, the quality of our water resources is constantly declining. There have been reports of thousands of organic, inorganic, and biological pollutants in water[1]. A few of them are deadly and carcinogenic, and some have harmful side effects and toxicities. These pollutants pose a serious threat to the continuous, aquatic life, and the planet's ecosystem as a whole. The four most popular techniques for treating wastewater are boiling, filtration, distillation, and chlorination. However, water treatment for industrial effluent water is done based on the pollutants present in it. Adsorption, membrane separation, activated sludge process, etc. are frequently the used method for waste water remediation[1].

Water pollution has become a serious issue for immediate attention due to the incessant release of harmful contaminants into water bodies, owing to the sporadic rise in industrial, economic, and technological development globally[2]. Among the numerous contaminants released into water bodies are effluents discharged from pharmaceutical and agro-industries wastewater plants and are endangering biotic and aquatic life[3].

Furthermore increasing population and anthropogenic activity are typically associated with the presence of ubiquitous pollutants in the ecosystem[4]. Water resource contamination is a hotly debated issue on a global scale because it harms living things in the long run, sometimes fatally[5]. More than one-third of the world's renewable freshwater resources are used for domestic, industrial, and agricultural purposes, and the majority of

these uses contaminated water with a variety of synthetic and geogenic substances like pesticides, dyes, fertilizers, heavy metals, and radionuclides[6].

Water pollution resulting from dye and dying materials requires a keen approach because it causes changes in the natural appearance of water even at low concentrations. Diverse industries, including textile, paint, pulp, paper, food, plastics, cosmetics, rubber, tannery, and others, uses dyes[7]. These industries use a significant number of dyes and produce dye-laden effluent, which is ultimately released directly into the ecosystem. Since dyes are poisonous and unappealing, dye-loaded wastewater poses serious environmental problems[8]. Dye also affects aquatic plants negatively by increasing sunlight absorption and lowering photosynthetic activity. Additionally, dyes and the by-products of their breakdown are frequently toxic and even carcinogenic. They also react in some health challenges which includes mucous membrane irritation, contact dermatitis, respiratory illnesses, and skin rashes[9,10]. There are many different types of dyes, and they are produced in about 1.6 million tons annually[11].

Methylene blue (MB) is one of the most popular known dyes. It is a heterocyclic compound with the formula $C_{16}H_{18}N_3SCl$[11]. In order to dye cotton for use in the textile industry; Heinrich Caro first created it in 1876 as an aniline-based synthetic dye. Its ability to stain and inactivate various microbial species was quickly realized following this research[12]. Additionally, it was discovered to be a cyanide and carbon monoxide antidote in 1932. It is a dark green powder that turns water blue when it comes into contact with it at room temperature. It exhibits maximum light absorption at about 668 nm. MB is one of the typical synthetic cationic dyes that have been used extensively in dying papers, cottons, and wools[13]. Due to its non-biodegradability, thermal and light

stability, MB is challenging to break down in the environment[14]. Meanwhile, MB-containing waste water would be harmful to humans, aquatic life, animals, and plants. Therefore, it is essential to create such cutting-edge approaches that can remove such dangerous pollutants from water bodies.

Over the years, conventional methods including coagulation, precipitation, ion exchange, membrane filtration, and oxidation have been employed in the treatment of wastewater[15]. Biological processes have also been investigated using phytoremediation. However, a major drawback with these techniques could be traced to sludge production and high operational cost, thereby making the process economically appealing. Moreover, phytoremediation may be time-consuming and hence not very suitable for immediate remediation[16]. Interestingly, the cost-friendly and effectiveness of the adsorption process for wastewater remediation have gained more attention due to the possibility to develop sorbent materials that are ecosystem friendly with increased adsorption capabilities at a low cost[17,18,19]. Nowadays, simpler methods are designed to process new carbonaceous materials with a wide range of applicability to meet consumers' demands, overcome the environmental crisis and address energy shortages.However, due to the high cost, cost-friendly nanoporous adsorbent materials with high adsorption efficiencies are garnering awareness aimed at adsorbent dose reduction and disposal problem solutions. Moreover, most available porous adsorbents also suffer from other limitations such as small particle size, low capacity, slow adsorption kinetics, and/or time-consuming separation process as well as poor physical stability[20,21]. Thus, the quest for innovative composite materials with perfect sorption and fast separation properties is paramount for environmental reclamation. Therefore, hierarchically bimetallic nanoporous composite materials, having

well-structured organized pores with different size levels, appears to be more prospective as ideal adsorbents. These materials are characterized by nanoporous geometry with the ability to change the mechanism and efficiency of intraparticle mass transport of dyes, thereby facilitating an enhanced adsorption rate and increased adsorption efficiency in practical wastewater remediation applications.

1.2 Statement of the Problem

The regular technologies employed in wastewater treatment appear to be highly expensive especially for small-scale industries in developing countries because it requires high capital investment, high reagent, and high energy requirement for release of toxic wastes that require proper disposal[22,23]. Therefore, necessity demands alternative low-cost and eco-friendly adsorbent materials, with good adsorbent properties. To date, there are quite a several prospective reports on the adsorption of dyes in wastewater using single-phase nanoporous compounds such as superhydrophobic nanoporous polymers, Magnetic carboxyl functional nanoporous polymer, nanoporous metal-organic frameworks (MOFs), multi-walled carbon nanotubes and so on[24]. However, information on the bimetallic nanosorption of the dyes polluted wastewater is an emerging technology that is gaining serious impetus in this decade. Thus, not much information has been explored in this field. Therefore, the gainful application of PEGylated bimetallic nanoporous adsorbent for the remediation of dyes-polluted wastewater will expand the prospects of nanomaterials and bring about the practical exploitation of these compounds to solve environmental problems.

1.3 Aim and Objectives of the Study

The broad objective of the study is to synthesize and characterize PEGylated bimetallic nanoporous adsorbent for remediation of methylene blue-polluted wastewater.

The specific objectives of the study include to:

i. calcinated Snail shell and PEGylated bimetallic nanoporous adsorbent preparation
ii. calcinated Snail shell and bimetallic nanoporous material that has been PEGylated is characterized using instruments.
iii. calcinated Snail shell and bimetallic nanoporous adsorbent is being used to study the adsorption of MB-contaminated wastewater under various circumstances.
iv. examine and learn about the adsorption isotherm and kinetics mechanism

1.4 Scope of the Study

Considering the advancement of nanoporous materials, the prepared nanoadsorbent will be examined for the immediate remediation of MB-polluted wastewater. Typical adsorption parameters such as effects of adsorbent dosage, contact time, pH, temperature, and initial analyte concentration as environmental parameters affecting the sorption process of MB from wastewater will be explored. More also, the study covers the examination of the adsorption isotherm and kinetics with emphasis on Langmuir and Freundlich isotherms to evaluate the sorption process as well as the use of pseudo-first-order and pseudo-second-order kinetics to describe the mechanism of the sorption process.

1.5 Justification of the Study

The contamination of wastewater by dyes cannot be over-emphasized. These contaminants are frequently released from industrial effluents, sewage plant, hospital effluent and contaminated irrigation ground/surface water[25]. Nevertheless, the superiority of adsorption using bimetallic nanoporous materials has been well noted in comparison to chemical and physical methods for wastewater remediation with respect to the range of pollutants it can efficiently and effectively absorb, accelerated adsorption kinetics, and design simplicity. The treatment process becomes attractive based on the availability and cost-effective adsorbent employed. However, an activated carbon-based material that is commercially available is expensive because the starting materials are costly and non-renewable nanoparticles[26]. Among the various methods used for remediation of antibiotics-polluted wastewater, special emphasis on the preparation of nanoporous materials has been given due to the growing interest.

The porous geometry of materials is a major aspect influencing the adsorption characteristics of carbonaceous adsorbents, while the increase in the total surface area attributed to nanoporous structures enhances high adsorption capacity[27]. Moreover, incorporating bimetallic nanoporous structures with a PEGylated network could offer low-resistance transport pathways with significantly improved adsorption performance.

Endnotes

1. V. Subha, K. Divya, S. Gayathri, E. Jagan Mohan, N. Keerthanaa, M. Vinitha, S. Kirubanandan, & S. Renganathan. *Applications of iron oxide nanocomposite in waste water.* **Water, Air, and Soil Pollution,** 2018, 21-22.

2. E. Zabłocka-Godlewska, W. Przystaś, & E. Grabińska-Sota. *Possibilities of obtaining from highly polluted environments: new bacterial strains with a significant decolorization potential of different synthetic dyes*. **Water, Air, and Soil Pollution,** 2019, 229.

3. K. Samal, S. Mahapatra, & M. Hibzur Ali. *Pharmaceutical wastewater as emerging contaminants (EC): treatment technologies, impact on environment and human health.* **Energy Nexus**, 6, 2022, 100076.

4. F. Mashkoor, & A. Nasar. *Magsorbents: Potential candidates in wastewater treatment technology–a review on the removal of methylene blue dye.* **Journal of magnetism and magnetic materials,** 500, 2020, 166-408.

5. S. Inamuddin. *Xanthan gum/titanium dioxide nanocomposite for photocatalytic degradation of methyl orange dye*. **International Journal of Biological Macromolecules**, 121, 2019, 1046-1053.

6. K. Qamruzzaman, & A. Nasar. *Degradative treatment of bispyribac sodium herbicide from synthetically treatment–dye decolourisation and anti–microbial activity*. **MOJ Drug Des. Dev. Ther,** 2019.

7. M.K. Uddin, & Z. Rehman. *Application of nanomaterials in the remediation of textile effluents from aqueous solutions in Nanomaterials in the wet processing of textiles.* **Hoboken, NJ, USA: John Wiley & Sons, Inc.** 2018, 135-161.

8. M. Ahmed, F. Mashkoor, & A. Nasar. *Development, characterization, and utilization of magnetized orange peel waste as a novel adsorbent for the confiscation of crystal violet dye from aqueous solution.* **Groundwater for sustainable development,** 10, 2020, 100322.

9. S. Shakoor, & A. Nasar. *Adsorptive treatment of hazardous methylene blue dye from artificially contaminated water using cucumissativus peel waste as a low-cost adsorbent.* **Groundwater for Sustainable Development**, 5, 2017, 152-159.

10. G.K Sarma, S. Sen Gupta, & K.G. Bhattacharyya. *Removal of hazardous basic dyes from aqueous solution by adsorption onto kaolinite and acid-treated kaolinite: kinetics, isotherm and mechanistic study.* **SN Applied Sciences**, 1(3), 2019, 1-15.

11. F. Mashkoor, & A. Nasar. *Magsorbents: Potential candidates in wastewater treatment technology–A review on the removal of methylene blue dye.* **Journal of magnetism and magnetic materials,** 500, 2020, 166408.

12. Z.P. Hu, Z.M. Gao, X. Liu, & Z.Y. Yuan. *High-surface-area activated red mud for efficient removal of methylene blue from wastewater.* **Adsorption Science & Technology,** 36(1-2), 2018, 62-79.

13. L. Sheng, Y. Zhang, F. Tang and S. Liu. *Mesoporous/microporous silica materials: preparation from natural sands and highly efficient fixed-bed adsorption of methylene blue in wastewater.* **Microporous and Mesoporous Materials**, 257, 2018, 9-18.

14. A. Pohl. *Removal of heavy metal ions from water and wastewaters by sulfur-containing precipitation agents.* **Water, Air, and Soil Pollution**, 2020, 231.

15. S. Ida & T. Eva. *Removal of heavy metals during primary treatment of municipal wastewater and possibilities of enhanced removal: a review.* **Water (Switzerland),** 2021, 13.

16. W. Polińska, U. Kotowska, D. Kiejza, & J. Karpińska. *Insights into the use of phytoremediation processes for the removal of organic micropollutants from water and wastewater; a review.* **Water (Switzerland),** 2021, 13.

17. C. R. Delgado-González, A. Madariaga-Navarrete, J. M. Fernández-Cortés, M. Islas-Pelcastre, G. Oza, H. M. N. Iqbal, & A. Sharma. *Advances and applications of water phytoremediation: a potential biotechnological approach for the treatment of heavy metals from contaminated water.* **International Journal of Environmental Research and Public Health,** 2021, 18.

18. N. A. A. Qasem, R. H. Mohammed, & D. U. Lawal. *Removal of heavy metal ions from wastewater: a comprehensive and critical review.* **npj Clean Water**, 2021.

19. J. B. Huo, K. Gupta, C. Lu, H. C. Bruun Hansen, & M. L. Fu. *Recyclable high-affinity arsenate sorbents based on porous $Fe_2O_3/La_2O_2CO_3$ composites derived from Fe-La-C frameworks. Colloids and surfaces A:* **Physicochemical and Engineering Aspects,** 585, 2020, 124018.

20. Y. Chao, B. Tang, J. Luo, P. Wu, D. Tao, H. Chang, X. Chu, Y. Huang, H. Li, & W. Zhu. *Hierarchical porous boron nitride with boron vacancies for improved adsorption performance to antibiotics.* **Journal of Colloid and Interface Science,** 584, 2021, 154–163.

21. S. Gupta, Y. Mittal, R. Panja, K. B. Prajapati, & A. K. Yadav. *Conventional wastewater treatment technologies.* **Curr. Dev. Biotechnol. Bioeng.** 2021, 47–75.

22. G. Gangaraju, R. Uma, & K. J. Shah. *Introduction to conventional wastewater treatment technologies: limitations and recent advances. adv. wastewater treat.* **I (Materials Research Foundations LLC**, 2021, 1–36.

23. H. Su, W. Li, Y. Han, & N. Liu. *Magnetic carboxyl functional nanoporous polymer: Synthesis, characterization and its application for methylene blue adsorption.* **Scientific Reports**, 2018, 1–8.

24. G. Jalloul, I. Keniar, A. Tehrani, & C. Boyadjian. *Antibiotics contaminated irrigation water: an overview on its impact on edible crops and visible light active titania as potential photocatalysts for irrigation water treatment.* **Frontiers in Environmental Science**, 2021, 1–29.

25. M. M. Sabzehmeidani, S. Mahnaee, M. Ghaedi, H. Heidari, & V. A. L. Roy. *Carbon based materials: A review of adsorbents for inorganic and organic compounds.* **Materials Advances,** 2, 2021, 598–627.

26. L. Xu, M. Zhang, Y. Wang, & F. Wei. *Highly effective adsorption of antibiotics from water by hierarchically porous carbon: effect of nanoporous geometry.* **Environmental Pollution,** 274, 2021, 116591.

Chapter Two
Literature Review

2.1 Dyes

They are colored aromatic organic compounds that absorbs light and give visible matter colouration[1,2]. Worldwide, over 100,000 commercial dyes have been reported, weighing between 7 and 109 kilograms per year[3]. In 1856, William Henry Perkin named the first artificial dye, an organic aniline dye he called Mauveine[4]. In order to permanently colour the substrates, dyes are applied. These dyes can withstand exposure to water, light, oxidizing agents, sweat, and microbial attacks without fading[5].

The uncontrolled discharge of industrial effluent into aqueous reservoirs as a result of the excessive use of synthetic dyes, which are frequently used in a variety of industries, is an unfavorable and dangerous phenomenon[5]. These dyes are frequently utilized as coloring agents in the paint, paper, leather, textile, pharmaceutical, and food industries. A documented estimate places the annual production of dyes and pigments at around 7 x 10^5 tons for the entire world[6]. These dyes cause hypertrophication, which severely harms aquatic flora and fauna and lowers the capacity for oxygenation for marine life. The bioaccumulation and biomagnification of these toxic dyes in the aquatic environment have an indirect impact on humans because they consume aquatic food[6].

2.2 Methylene Blue (MB)

MB is a well-known, highly carcinogenic thiazine pollutant. It has been produced and used in numerous industries for a variety of purposes; for instance: dyeing of cotton, wool and fabrics; coloring of paper, as a hair coloring agent and redox reaction indicator

in outer space, etc. When consumed, MB poses a serious risk to human health and has been linked to eye and nervous system damage. Breathing issues, gastritis infections, diarrhea, vomiting, and other related illnesses are also common.

The well-known primary thiazine dye MB has the molecular formula $C_{16}H_{18}N_3Cl_3$ and a maximum wavelength of 665 nm. It forms a stable solution with water at room temperature due to its high-water solubility[7,8,9,10]. MB is a positively charged compound that belongs to the class of polymethine dyes with an amino autochrome unit[11]. The International Union of Pure and Applied Chemistry (IUPAC) lists the compound's chemical name as (3,7-bis(dimethylamino) phenothiazine chloride tetramethylthioninechloride) with a colour index (CI) of 52015. MB is not a pH indicator but a redox indicator.

2.2.1 Properties of MB

When MB is dissolved in water, it turns into blue colour. At 25 °C, MB exhibit molecular diffusivity (Dmol) of 4.7 106 (cm^2/s)[12]. The MB molecule has a length of 13.82 or 14.47 and a width of roughly 9.5[13]. ThepKa of MB dye is 3.8. It is dispersible in water, ethanol, acetone, methanol, 2-propanol, and ethyl acetate. At 25 °C; it dissolves in water at a rate of 43.6 g/L.[15] MB has a melting point (Tm) between 100 and 110 °C[14]. MB is typically deep blue in color when it is oxidized and colorless when it is reduced; leucoMB. The chromophoric and auxochrome groups in MB determine its color. The central aromatic heterocycle of MB serves as the chromophore group, and the auxochrome group is composed of N-containing groups with lone pair electrons on the benzene ring. Since almost all calculations are made using the UV-Visible spectra of MB, UV-analysis of MB is crucial for photodegradation and adsorption studies[16].

The MB's absorption spectra show that an MB monomer exhibits the strongest absorption peak at about 665 nm, while an MB dimer exhibits a shoulder peak at about 612 nm. Two more bands with peaks around 292 and 245 nm (connected to substituted benzene rings) also show up in the ultraviolet region[17]. As the photodegradation reaction advances, these absorption peaks gradually decline[18]. For the investigated dyes, Fourier transform infrared spectroscopy (FTIR) offers significant quantitative and qualitative analysis. Part of which is identifying the study sample's chemical bonds and functional groups[14].

2.2.2 Uses and Application of Methylene Blue (MB)

An effective therapeutic agent for treating anaemia, malaria, and Barrett's oesophagus, MB is an alluring molecule with a variety of properties useful for biomedical applications. MB has mainly been applied to a variety of therapeutic and diagnostic procedures in both human and veterinary medicine[19]. MB was the first synthetic antimalarial used in the late 19th and early 20th centuries to treat all forms of malaria and has the additional ability to sensitize people to chloroquine[20]. The photodynamic therapy of cancer employs MB dye. It is frequently utilized as a photosensitizing agent to photodynamically inactivate RNA viruses in plasma, such as HIV, hepatitis B, and hepatitis C viruses[21]. Recent research indicates that MB may help with Alzheimer's disease and memory enhancement[22].

It is currently used clinically to treat a variety of ailments, including methemoglobinemia, uTIs, plaque psoriasis, thyroid surgery, cancer chemotherapy, and ifosfamide-induced encephalopathy[23]. MB was the key ingredient in the creation of chlorpromazine, the first tricyclic antidepressant[14]. Additionally, it has been used to identify neuroendocrine tumors like insulinomas[24].

MB dye has numerous potential applications in the textile, pharmaceutical, paper, dyeing, printing, paint, medicine, and food industries[25,26]. It is one of the most widely used clothing colourants and the most widely used dye in the textile industry[27]. In the textile industry, MB is fixed firmly to fabric and adheres firmly in the spaces between cotton fibres[28]. Rock swelling is calculated using the MB method, which is used in foundries as a quick test to determine the caliber of the foundry sand[29]. Additionally, MB dye is used in analytical chemistry as a photosensitizer, oxidation-reduction indicator, optical redox indicator, and in the trace analysis of anionic surfactants.Furthermore, it is employed as a prospective component in dye-sensitized solar cells, capacitors, sensors and microbial fuel cells[15,30].

2.2.3 Toxicity of MB

The majority of MB dyes released into natural water sources by the textile industry are harmful to both humans and microorganisms[31]. Due to its significant toxicity, MB dye is dangerous to human health above a certain concentration[9]. Because MB is toxic, cancer-causing, and not biodegradable, it poses a serious risk to human health and negatively affects the environment[32]. Multiple health risks are brought on by MB, including respiratory distress, digestive and mental disorders, blindness, and abdominal disorders[33,34]. Likewise, it results in vomiting, diarrhoea, cyanosis, shock, gastritis, jaundice, methemoglobinemia, tissue necrosis, and an accelerated heart rate, which kills premature cells in tissues and irritates the skin and eyes[35]. Skin redness and itching could result from MB contact with skin.

Both humans and animals are affected by the toxicity effects of MB[36]. The environmental release of MB poses a serious risk for both toxicological and aesthetic reasons.

Additionally, it hinders light penetration and provides toxic food to organisms' food chains[37]. Even at very low concentrations, MB in water bodies produces highly coloured by-products. Its high molar absorption coefficient (8.4 104 L mol1 cm1 at 664 nm) lowers sunlight permittivity, reduces oxygen solubility, affects aquatic life's capacity for photosynthetic activity, and diminishes the biological community's diversification and aesthetic appeal[38,39].

2.3 Adsorption

One of the common and effective methods in wastewater treatment is the adsorption technique which is based on the transfer of pollutants from the solution phase to the solid phase.[40] Applying adsorption procedure originating from green and non-poisonous absorbent featuring high reactive surface atom and high surface area demand is on the increase[41]. This method is preferable to other techniques of environmental remediation due to its low cost, design simplicity, easy operation, and non-toxic adsorbents in comparison to other conventional environmental decontamination techniques[42]. To eliminate MB from wastewaters, it is necessary to consider less expensive, readily available, and improved absorptive characteristics[43].

Adsorption, being a surface phenomenon involves two components:

i. The attached compound to the solid surface, i.e. adsorbate.
ii. The compound on which adsorption occurs, is known as the 'adsorbent'.

Adsorption delivers a high-quality product through a financially feasible process. Considering less expensive absorbents that are readily available, adsorption is a reliable alternative for wastewater. Furthermore, one advantage of this method is that operation is

free from sludge and diluted solution, so it is possible to completely eliminate contaminants[44]. Some common examples of adsorption materials are carbonaceous compounds and they have been used extensively to remove antibiotics from wastewater to a very large extent[45,46].

2.4 Classification of Adsorption

2.4.1 Physical Adsorption (Physisorption)

Van der Waal's attractive force is responsible for the binding of the gas molecules to the solid surface. Physical adsorption occurs on all surfaces provided that pressure and temperature are favorable and it is easily reversed[47]. Under proper conditions, adsorbed molecules could form multiple layers in the process of physical adsorption (Figure 2.1a).

The ability to remove almost all absorbed molecules at adsorption temperature is one feature of physical adsorption. The energy needed for the molecules to escape the adsorption site is provided by heating which facilitates desorption. At temperatures below or close to boiling point and at adsorptive pressure, physisorption is likely to[48].

2.4.2 Chemical Adsorption (Chemisorption)

In chemisorptions, chemical bonds are responsible for the binding of the gas molecules or atoms to the solid surface. Ionic or covalent bonds are features of this adsorption[49] . Chemisorption is a single-layer process because it only continues with adsorptive direct contact with the surface. The escape of chemical bound is connected to the influx of a relatively high amount of energy when compared to that needed to liberate a physically bound molecule. The availability of this energy is made possible by heat and often very high temperatures are required to purify a surface of chemically adsorbed molecules.

Chemisorption commonly occurs at temperatures above the boiling point of the liquefied adsorptive.[50]

The possibility of electron sharing between the adsorbate and the solid surface (chemical bond) based on the adsorption phenomenon, depends on the gas and solid. Unlike physisorption, it is challenging to reverse chemisorption. In removing chemically absorbed molecules, a substantial amount of energy is usually required.

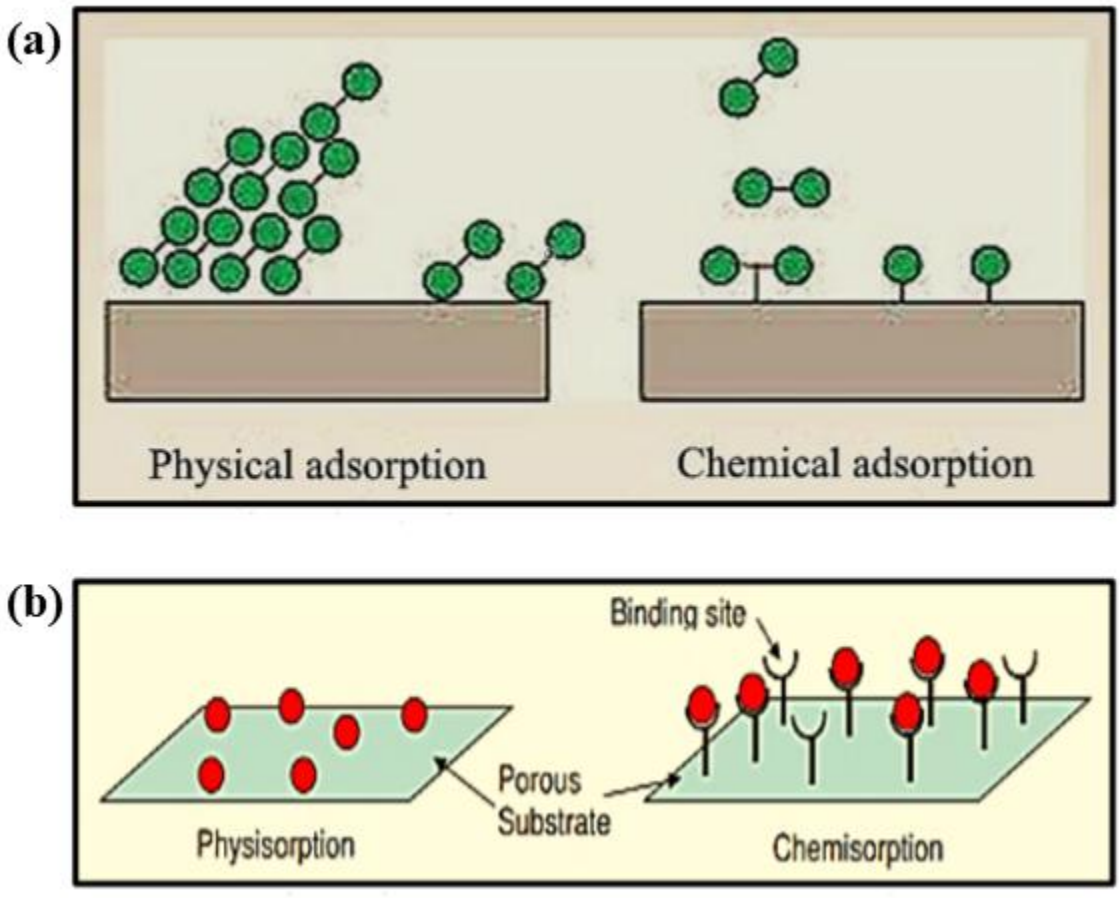

Figure 2.1: (a) Physical and Chemical adsorption (b) Mechanism of physical and chemical adsorption on the surface.

Source[51]

2.4.3 Biosorption

Biosorption can be defined as the union of molecules of gas, liquid, or dissolved solids to a surface of biological origin. This is due to attraction between the molecules on the surface referred to as adsorbent and those of the liquid or gas referred to as adsorbate.

The processes involved in biosorption include diffusion of reactant to the surface of the adsorbent, chemical reaction on the surface, biosorption of reactant to the surface, desorption of product on the surface, and diffusion of product away from the surface[52,53]. The first and last processes are the fastest meaning that the rate-determining step will be one of the middle processes.

2.5 Adsorption Process

The occurrence of the adsorption process takes place in different ways which are influenced by a range of factors. Batch, fixed-bed column and continuous processes are the three most prevalent methods employed. In a batch adsorption experiment, a known mass of adsorbent is added to a known volume of solution. The mixture is mixed gently for a specific time[54]. The particles are removed from the liquid by decantation or filtration after the contact period, and the liquid component is then analyzed to determine the residual final adsorbate concentration. The batch column setup consists of a cylindrical column with the adsorbent packed firmly over a specific depth through which wastewater is permitted to flow. Most of the solute will be adsorbed as it is exposed to the new adsorbent bed at first, resulting in a near-zero concentration at the column exit.

For laboratory trials, however, the column should only be turned off when the inlet solute concentration is roughly equivalent to the outlet solute concentration. This is because

determining the properties and dynamic response of an adsorption column requires total column saturation, which results in an S-shaped breakthrough curve[55]. Based on the adsorbate concentration, the process of adsorption can be positive or negative and it is controlled by several mechanisms

- **Positive adsorption:** This takes place when the adsorbate concentration on the surface is higher than the concentration in the bulk phase. When a concentrated solution of KCl is shaken with blood charcoal, for example, positive adsorption is observed[55].
- **Negative adsorption:** This takes place when bulk concentration is higher than that of the adsorbate. For example; negative adsorption is observed when a dilute solution of KCl is shaken with blood charcoal[55].

2.5.1 Factors Affecting Adsorption

Adsorption significance of a surface material depends on certain parameters as outlined below

2.5.1.1 Surface Tension

This is the force acting parallel on the surface of a liquid. Chemicals that lower the surface tension of the solvent or adsorbate in which they are dissolved concentrate on the surface layer, whereas substances that enhance surface tension concentrate less on the surface than in the bulk solution[55].

2.5.1.2 Concentration

Adsorption occurs when the concentration of one substance at the surface of another substance differs from the surrounding bulk or inner phase. Adsorption reduces as the adsorbate's starting concentration rises[55].

2.5.1.3 pH of Solution

The pH of a solution has a strong effect on the adsorption efficiency of the adsorbent. This is because pH indeed influences surface chemistry and surface charge on the material. For example, because the surface is positively charged at low pH, the performance for adsorbing cations will be poor due to electrostatic repulsion. However, a pH that low is not ideal for applications or even handling the material because it will be extremely corrosive[55].

2.5.1.4 Adsorbent Dosage

Adsorbent dosage is a critical variable in the adsorption process since an adsorbent's capacity for a particular starting adsorbate concentration depends on it.

2.5.1.5 Initial Metal Concentration

This parameter appears to have an effect on the adsorption process, with larger initial metal ion solution concentrations resulting in increased metal ion absorption. This is because the ratio of the initial number of moles of the metal ion to the accessible surface area is low at lower initial concentrations. As a result, it is critical to identify the adsorbent's maximum adsorption capacity, for which studies should be carried out at the greatest feasible initial metal ion concentration[55].

2.6 Adsorbent

Adsorbents are materials that may extract specific compounds from gases, liquids, or solids by forcing them to stick to their surface without affecting their physical properties. There are so many examples of absorbent materials that have been extensively explored for the adsorption of antibiotics and other wastewater contaminants (Figure 2.2)[56,57].

All of the constituent atoms of an adsorbent's bonding requirements (whether ionic, covalent, or metallic) are fulfilled by other atoms in the material's bulk[58]. However, because atoms on the adsorbent's surface are not completely covered by other adsorbent atoms, they can attract molecules from the adsorbate. The nature of the connection is determined by the species involved[59].

2.6.1 Activated Carbon (AC) Adsorbent

Activated carbon has been heavily explored as an absorbent in many wastewater treatments, and it is developed from a micro-porous and homogenous framework with high surface area and radiation stability[60]. The processing and production of high-efficiency activated carbon materials is still growing in many developing countries[61].

Although there are several challenges with the regeneration of used activated carbon adsorbents, recent interest has shown the quest for low-cost and efficient alternatives to the currently available commercial activated carbon[62].

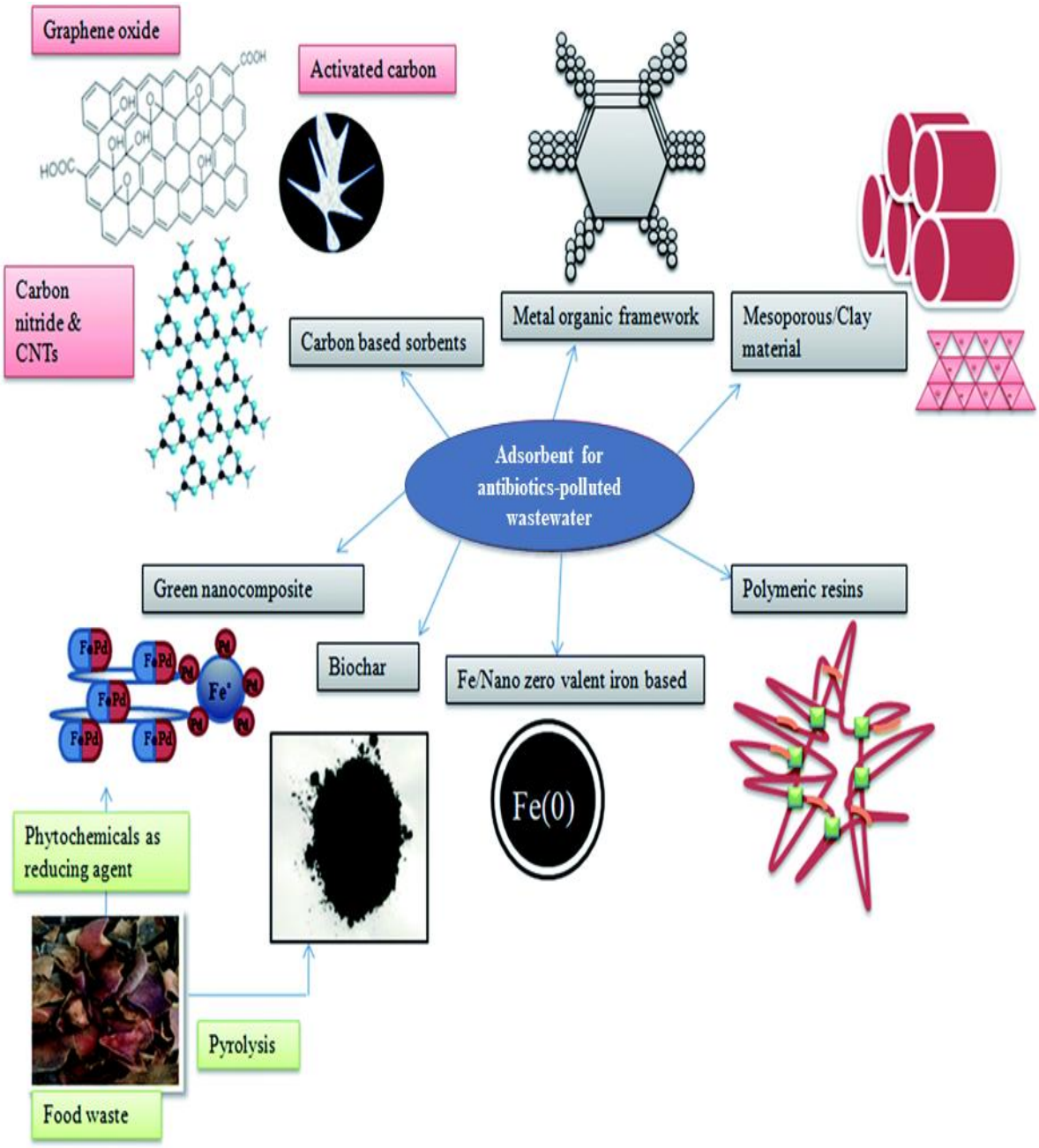

Figure 2.2: Adsorbent for the remediation of MB-polluted wastewaters.

Source[59]

Activated carbon is developed to have minute, low-volume pores that enlarge the surface area available for adsorption or chemical reactions[63]. A wide range of feedstock can be employed for the production of activated carbon; these include anthracite and bituminous coal, lignite, peat, wood and coconut shells[64,65,66]. The ability of activated carbon to adsorb hazardous species is determined by the type of organic material utilized in its production as well as the experimental parameters used during the activation process[67].

On the surface of an AC, there is the existence of certain functional groups which influences the solution pH, and subsequently the adsorption process[68,69]. This allows the wide application of AC in wastewater remediation and purification, wherein physisorption and/or chemisorption can be used to monitor the contaminant's shift from the liquid to the solid surface[70,71]. The extensive application of AC in wastewater remediation could be traced to its relatively high adsorption performance and usability, thereby showing huge prospects as an alternative to the conventional and advanced wastewater treatment technologies[72].

The preparation of AC is often achieved by two basic processes of carbonization and activation. Firstly, the precursor feedstocks are pyrolyzed at high temperatures, between 400 and 850°C, to remove the volatile non-carbon components such as hydrogen, oxygen, and nitrogen which could be present in the form of gases and tars. This method creates char with a high carbon content but low porosity and surface area. The synthesized char is activated in the second phase to produce a substance exhibiting increased porosity. Opening previously inaccessible pores, new pore formation by selective activation, and expansion of existing pores are all examples of pore size augmentation during the activation process. The activation of the carbon material can be achieved either by

physical or chemical means[73]. In physical activation, the carbonized char is subjected to oxidizing gases such as air, carbon dioxide, and steam at high temperatures, usually between 650 and 900 °C. In this approach, CO_2 is the most ideal activating agent owing to its pure nature, ease of handling, and controlled activation process at 800 °C. More also, uniformly high porosity is often found with CO_2 activation than with steam. Howbeit, steam is highly sorted for during physical activation than CO_2 since it produces AC with comparatively high surface area. Diffusion inside the char structure is effective due to the lower molecule size of water, resulting in an activation process two to three times higher than CO_2 with the same degree of conversion.

Chemical activation, on the other hand, involves mixing the carbonized precursor with chemical activating agents e.g. NaOH, KOH, $FeCl_3$, etc which act as oxidants and dehydrating agents. At a relatively low temperature of 300-500 °C, the carbonization and activation processes are carried out simultaneously. These have an effect on pyrolytic decomposition, as well as improving the porosity structure and increasing the carbon yield. Chemical activations are preferable over physical activations because they use less heat, have higher microporosity structures, have a larger surface area, and take less time to complete[74,75].

2.6.2 Polymer-Based Adsorbent

Polymer microspheres have demonstrated promising adsorption qualities for a wide range of contaminants in wastewater since they can improve the stability and mechanical characteristics of adsorbents by forming a network or providing protection for other materials, as well as increasing sorption capacity[76]. Natural polymers such as cellulose, chitin, starch, alginate, chitosan, etc. are often employed for wastewater treatment owing

to their biodegradability, non-toxicity, cheapness, and eco-friendliness[77]. They are widely used in industrial and commercial applications because they can afford high adsorption rates, thermal stability, and recyclability[78].

The molecular imprinting technique, which is being used to fabricate polymer-based absorbents, is an emerging technology in which a substance is synthesized in the presence of a template molecule, and then the template is removed, leaving a material with "memory" sites competent of selectively recognizing and re-binding to the initial template of a mixture[79,80]. Basically, molecularly imprinted polymers (MIP) are obtained from cross-linking polymers having specific voids to target the analyte[81]. Copolymerization of bridging monomers and functional monomers with an imprinting molecule or template creates open gaps. The template is eliminated after the polymerization process, allowing the void to efficiently target the analyte[82]. The major benefits of MIP include the easy method of fabrication and the ability to recreate “tailor-made” sites for binding the desired target molecule (Figure 2.3). MIP is usually more porous, with a larger surface area, and higher binding efficiency. Moreover, non-imprinted polymers comprise cross-linked polymeric networks that have macropores with suitable adsorption sites for organic molecules.

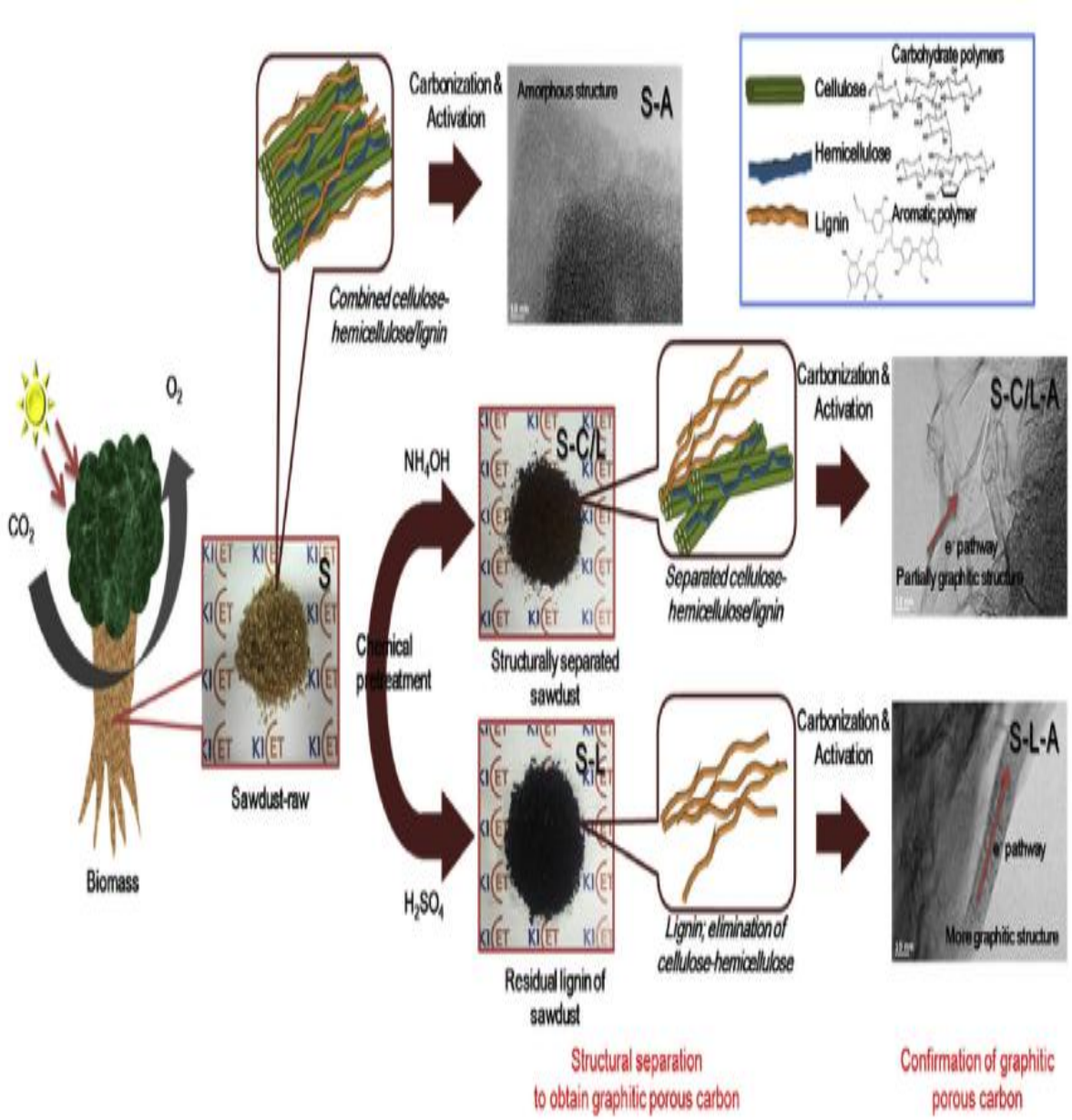

Figure 2.3: Chemical treatment and carbonization of activated carbon material from biomass.

Source[81]

The preparation strategies for imprinted and non-imprinted polymers are the same in which templates are not required. Thus, they possess the same chemical features but with the absence of specific voids for the target molecules.

However, non-imprinted polymers demonstrate a stronger hydrophobic interaction (owing to their non-specific binding) between organic pollutants and polymers. Several authors have explored the use of MIP and non-imprinted polymers with promising prospects for water and wastewater treatment (Figure 2.4)[83]. For instance, a chitosan-based composite hydrogel with tuneable properties and controllable adsorption capacity has been used for the adsorption of trace pharmaceuticals in wastewater showing the removal efficiency of 91% to 100% within 48 h[83]. The adsorption efficiency could be ascribed to the simple alteration of the bio-based modifiers used to fine-tune the properties of the absorbent. The studies of Gao used lignin and cross linked lignin-based adsorbents and found that they have a high adsorption capacity (0.828 mmol/g), good anti-interference to some inorganic salts, and efficient regeneration and reuse performance, but the adsorption is dependent on the cross-linking density and degree of carboxymethyl substitution, as well as the pH of the solution[84,85].

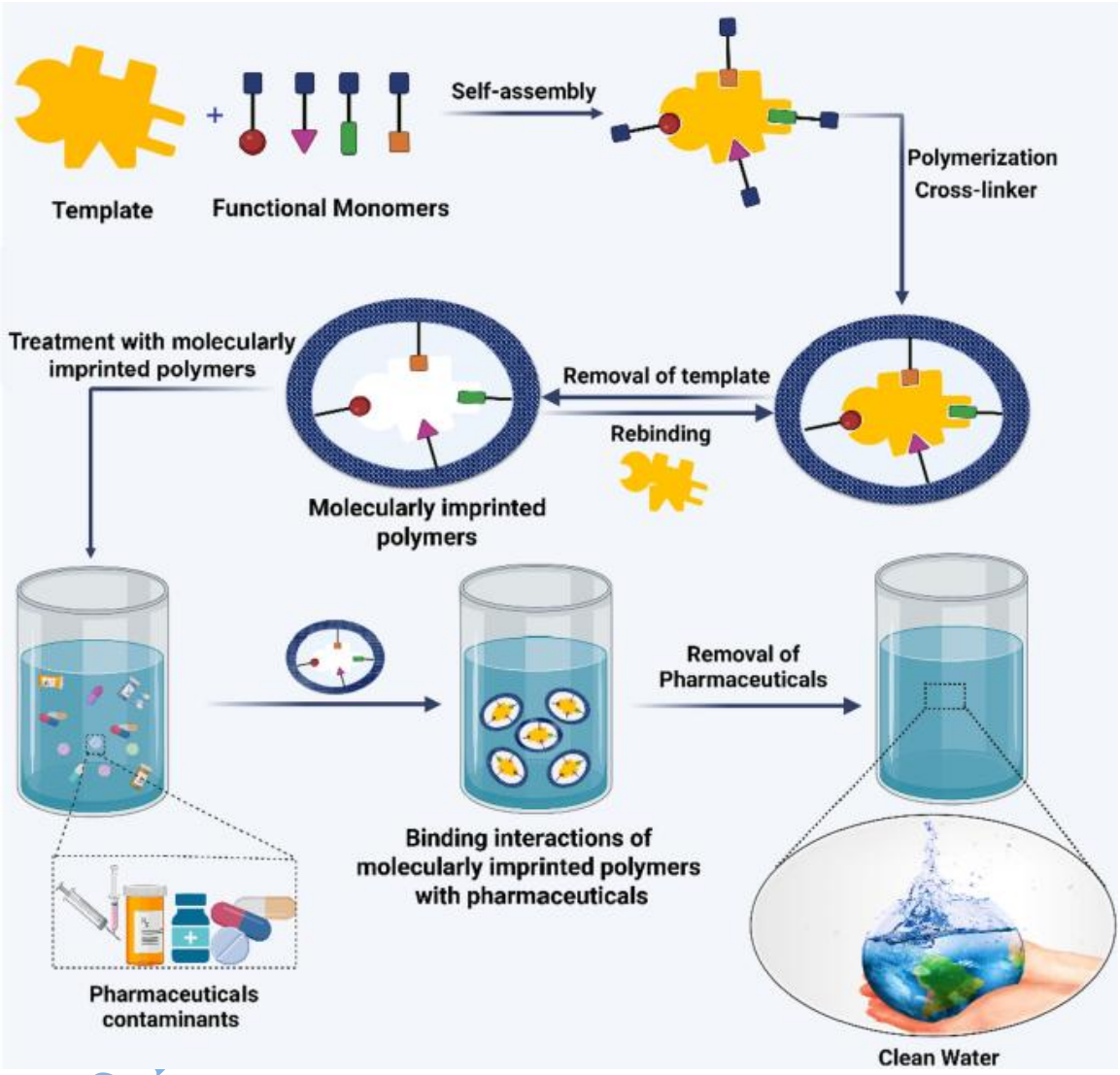

Figure 2.4: Designing strategies for MIP for pharmaceutical-polluted wastewater remediation.

Source[83]

2.6.3 Inorganic Adsorbent

Inorganic materials such as metal oxides, hydroxyapatite, zeolites, clays, and hybrid materials have found tremendous application in the adsorption of cations and anions, intended mainly for solving environmental problems[86]. These materials are highly considered owing to their very high surface area, well-structured properties, tunable surfaces for easy modification, and a regular channel structure[87,88]. In general, sorption onto solid surfaces and associated heterogeneous electron transfer (redox) reactions are important factors influencing contaminant distribution and fate in environmental matrixes[89,90].

During the pollutant removal at the surface, oxidation can be initiated at the inorganic material (metal)/wastewater interface by direct coordinative (inner-sphere) binding with free metals at the active surface sites, via ligand exchange reactions. Nevertheless, this coordination mode propagates electron transfer processes between sorbed molecules and metal active sites, which is usually a time-dependent process that can occur within many hours.

2.6.4 Metals and Metal Oxides Adsorbent

Numerous references to metals and their oxides as adsorbents in both homogeneous and heterogeneous systems have been made. Their surface hydroxyl groups and Lewis acid sites were said to be the primary active sites in AOPs[90]. Recently, several altered types of metal oxides were effectively evaluated as nanocatalysts for the treatment of wastewater. It has been extensively investigated how to degrade pollutants in aqueous solutions using metal oxide nanoparticles including ZnO, TiO_2, and CeO_2[91].

Figure 2.5 shows the mechanism of the photocatalytic oxidation process. TiO_2 nanotube arrays (TNAs) were used in photocatalytic degradation of pharmaceuticals to remove the -blocker metoprolol (MTP) from aqueous solution utilizing free hydroxyl radicals. Experiments with the addition of particular scavengers were conducted to clarify the degradation mechanism[91].

According to this study, free hydroxyl radicals (•OH) in bulk solution contributed the most reactive species to MTP degradation, 88%, and photo-generated holes (h^+), 9%, respectively. As a scavenger for •OH and h^+, tert-butanol and formic acid were added.

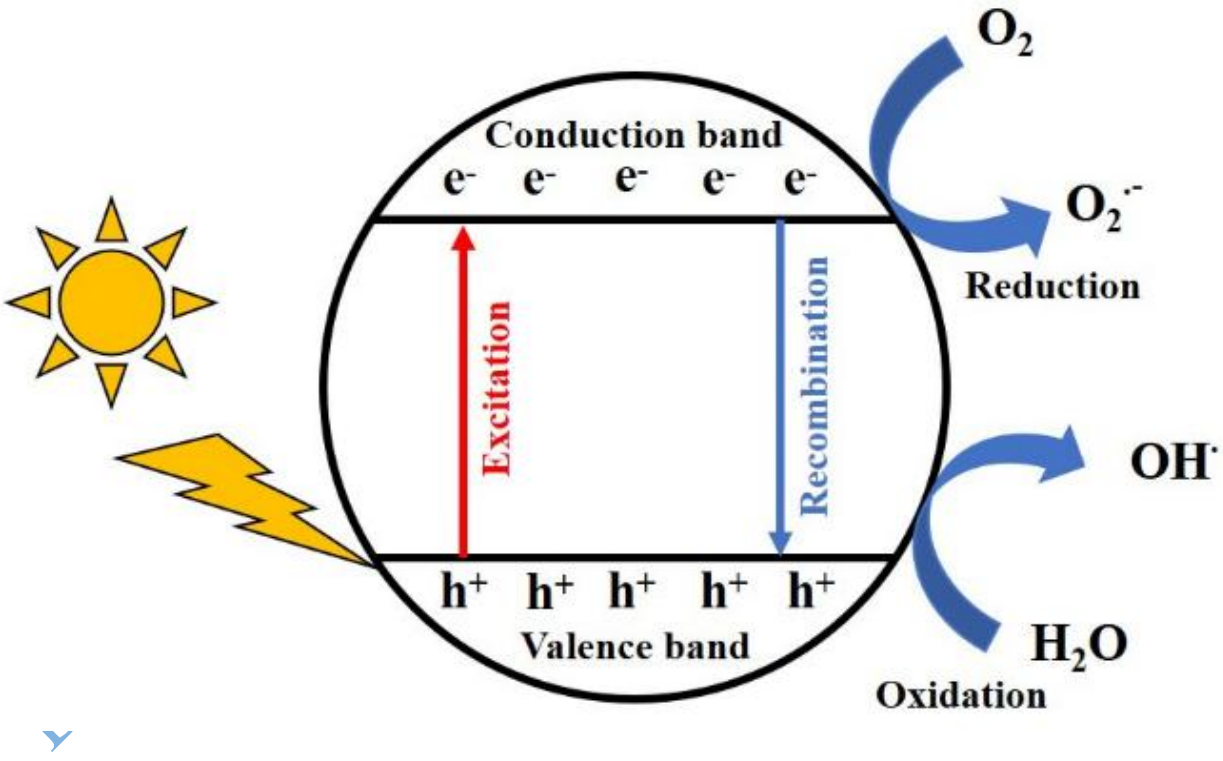

Figure 2.5: Mechanism for photocatalytic degradation.

Source[91]

Free hydroxyl radicals caused the majority of the MTP degradation, whereas the interaction between h^+ and •OH adsorbed on catalyst surfaces caused little degradation on the catalysis surface. About 3% of the MTP over TNAs was somewhat degraded by other reactive species such photo-generated electrons and superoxide radical anions. Metal oxide nanoparticles are thought to be superior photocatalysts for water purification due to their improved photocatalytic efficacy and large surface area. Among the metal oxides, iron-based catalysts have received substantial study and have proven to be quite efficient in the oxidation of a variety of environmental pollutants[92]. Recyclability, reusability, and comparatively lower usage costs and environmental concerns are benefits of iron oxides. For instance, greater efficiencies were attained when utilizing -Fe_2O_3 in a batch mode photocatalyst advanced oxidation process to degrade salicylic acid (20 g)[93].

In watery conditions, it's possible that the metals, metal oxides, and all of their many forms cannot live separately. They may hydrate and form various complexes when there are water molecules present; this process may be pH-dependent[94]. Additionally, the pH of water may change as a result of the presence of metal oxides and the pollutants found on them. Because the AOPs are pH-dependent activities, the effectiveness of their mechanism depends on the pH of the water[95]. pH is a factor in UV-based reactions, Fenton-like activities, and catalytic ozonation. For instance, ozonation requires an alkaline pH. Contrarily, the Feton-like process of catalytic hydrogen peroxide breakdown needs an acidic pH to effectively produce the hydroxyl radicals required for the degradation of contaminants. No matter the target contaminant, a pH of 3 is thought to be the best and most appropriate pH for this operation[96]. Higher pH causes Fe^{3+} to become $Fe(OH)_3$, which reduces the Fenton process' effectiveness since there is less Fe^{3+}

available to react with hydrogen peroxide to produce hydroxyl radicals[97]. However, if the pH is below 3, Fe complex ($[Fe(H_2O)_6•]^{2+}$) forms and reacts with the hydrogen peroxide in the solution, reducing the amount of hydrogen peroxide that is accessible for use as an oxidant. In addition, hydrogen peroxide produces stable oxonium ions $[H_3O_2]+$ at very low pH levels, which are less reactive and stable than hydroxyl radicals, decreasing its ability to oxidise contaminants[97,98]. The type of active sites and the efficiency of the catalysts may both be impacted by the pH of the water. For instance, a material's point of zero charge is a crucial characteristic since it can affect the surface charges on a material at a given pH and the type of active sites (involving Lewis and Bronsted acid sites).As a result, different materials have a distinctive point of zero charge[90]. Therefore, it is crucial to research how different materials are affected by pH in order to determine how well they can function as a catalyst for wastewater treatment. However, the pH fluctuations that occur during the process and as a result of impurities on catalysts were frequently disregarded in published publications. In order to continue using metals and metal oxides as nanocatalysts in the treatment of wastewater, the aforementioned issue should be taken into account. The research using metal oxides to remediate wastewater are compiled in Table 2.1. For instance, sono catalysis was used to remove 44% of the COD from textile wastewater using ZnO nanoparticles (catalyst dosage of 6 mg/L) at pH 9 for 150 minutes of reaction time[99].

2.7 Advances in Nanoporous Adsorbents

Nanotechnology is a multidisciplinary field concerned with the design, production, and manipulation of particle structures with diameters ranging from 1 to 100 nm.This field

encompasses the separation, consolidation, and deformation of material by one atom or molecule. It is divided into three interdependent aspects;

i. wet nanotechnology is concerned with biological systems like enzymes, membranes, and cellular components.
ii. surface science, physical chemistry, and the manufacturing of structures in carbon, silicon, and inorganic materials are all important aspects of dry nanotechnology.
iii. computational nanotechnology deals with modeling and stimulating the complex nanometer-scale structure.

Over the years, the remarkable advancement in this scientific technology has opened many avenues for the designing and fabrication of novel materials which have been extensively applied in health care, cosmetics, agriculture, environmental health, biomedicine, chemical industries, electronics, sensors, environmental remediation, and so on[91,92]. Nanotechnology is considered an interdisciplinary field in which existing/natural materials, man-made materials, and systems, can acquire different properties rendering them suitable for numerous applications varying from structural and functional to advance in-vivo biomedical applications[93,94].

Nanostructured materials have attracted a lot of attention in recent decades because of their unique size-volume ratio and tunability. They have been used as photocatalysts and adsorbents for water treatment, and have been touted as a solution to a lot of technological and environmental problems[95,96]. Nanoparticles are viewed as the fundamental building blocks of nanotechnology; which is the foundation for preparing many nanostructured materials. In the synthesis and assembly of nanoparticles or

nanomaterials; precursors of liquid, solid, or gases are used and can be tailored readily from 1 nm to 100 nm in diameter which can be controlled by oversize uniformity[97].

Nanoparticles are unique because nano-size increases surface-to-volume ratio, also its physical and chemical properties are different from bulk material, with distinct crystallography phases and morphologies such as spheres, cylinders, rods, tubes, etc[98].

Nanoparticles are a thin layer of material that connects bulk materials with molecular (atomic) structures. Because bulk materials have separate structures from random-grained individuals, their physical properties remain consistent; they are oriented in space and have contact with each other herby oriented in a crystalline lattice[99]. Nanomaterials differ from bulk materials in that they have a large number of surface atoms, high surface energy, spatial confinement, and fewer flaws. Metals, metal oxides, silicates, non-oxide ceramics, carbon, and polymers are some of the most frequent materials used to make nanoparticles[100]. The broad chemical composition of the particles, their form and size, the medium in which they are present, the state of dispersion of the particles, and, most crucially, the multiple conceivable surface modifications, all contribute to their immense diversity[101,102].

Table 2.1: Metal oxides adsorbent in wastewater treatment.

Adsorbent	Wastewater type	Target contaminants	Removal efficiency	References
TiO_2 nanotube arrays (TNAs)	Aqueous solution	β-blockermetoprolol (MTP)	87.09±0.09% in 120 min, Ph range = 3–11, nanotube diameter = 53 nm	[92]
Fe_2O_3 nanoparticles	Aqueous solution	Salicylic acid (SA)	53% of SA	[93]
TiO_2 nanoparticles	Petroleum refinery wastewater	COD	83% in 120 min, pH = 4,COD = 100 mg/L	[94]
ZnO nanoparticles	Textile wastewater	COD	44% in 150 min, pH = 9,catalyst = 6 mg/L	[95]
CeO_2nanoparticles	Aqueous dye solution	Eriochrome black-T(EBT), Alizarin redS (ARS)	100% in 120 min, dye = 100 mg/L, catalyst = 0.6 g/L	[96]

Source: Field survey

Nanoparticles show different properties such as large surface-area-to-volume ratio as compared to the bulk equivalent, quantum confinement, short-range ordering, plasmon excitation, low coordination sites, decrease in melting temperature, and transition between molecular and metallic sites provide specific electronic structure[103]. They are made up of very small particles because they help to achieve super miniaturization, which allows nanostructures to be packed very tightly together, which is important for commercial applications. Nanoparticles have a huge specific surface area due to their small size, which amplifies the interactions between them and the environment in which they are found. Nanoparticles have a wavelength that is often less than the critical wavelength of light, making them helpful in a variety of applications[104].

Nanoparticles can be broadly grouped into three which are; Organic nanoparticles including carbon nanoparticles (fullerenes), Inorganic nanoparticles which include magnetic nanoparticles and noble metal nanoparticles (3d and 4d transition metals), and Semi-conductor nanoparticles (titanium dioxide and zinc oxide).

Inorganic nanoparticles are gaining popularity due to their superior material characteristics and functional diversity. Inorganic nanoparticles have been investigated as potential instruments for medical imaging and illness treatment due to their size properties and benefits over current chemical imaging pharmacological agents and medicines. Inorganic nanomaterials have been found to contain remarkable porous surface and pore volume which allows for the adsorption of many environmental contaminants. Thus, owing to their rich functionality and good biocompatibility, they can be incorporated with other materials to form intriguing super adsorbent compounds.

2.8 Adsorption Process

The occurrence of the adsorption process takes place in different ways which are influenced by a range of factors. Batch, fixed-bed column and continuous processes are the three most prevalent methods employed. In a batch adsorption experiment, a known mass of adsorbent is added to a known volume of solution. The mixture is mixed gently for a specific time[105]. The particles are removed from the liquid by decantation or filtration after the contact period, and the liquid component is then analysed to determine the residual final adsorbate concentration. The batch column setup consists of a cylindrical column with the adsorbent packed firmly over a specific depth through which wastewater is permitted to flow. Most of the solute will be adsorbed as it is exposed to the new adsorbent bed at first, resulting in a near-zero concentration at the column exit. For laboratory trials, however, the column should only be turned off when the inlet solute concentration is roughly equivalent to the outlet solute concentration. This is because determining the properties and dynamic response of an adsorption column requires total column saturation, which results in an S-shaped breakthrough curve[106,107]. Based on the adsorbate concentration, the process of adsorption can be positive or negative and it is controlled by several mechanisms (Figure 2.6)[108].

(a) Positive adsorption: This takes place when the adsorbate concentration on the surface is higher than the concentration in the bulk phase. When a concentrated solution of KCl is shaken with blood charcoal, for example, positive adsorption is observed.

(b) Negative adsorption: This takes place when bulk concentration is higher than that of the adsorbate. For example; negative adsorption is observed when a dilute solution of KCl is shaken with blood charcoal.

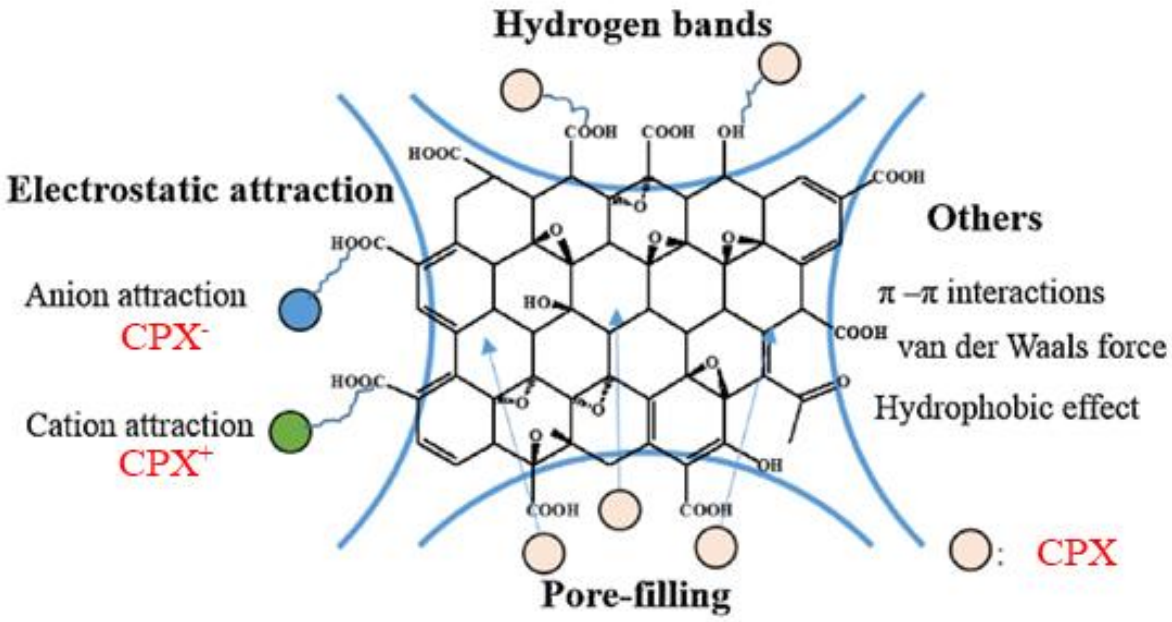

Figure 2.6: The mechanisms of adsorption of MB.

Source[108]

2.9 Adsorption Isotherms

A distribution of weak surface energy sites is a distinguishing feature of solid materials. These sites might become clogged with gas or vapor molecules. This is a broad description of the adsorption phenomena. Temperature, pressure, surface energy distribution, and the solid's surface area all influence the number of molecules taken by the surface. An adsorption isotherm is a relationship between a gas's equilibrium pressure and the amount of gas adsorbed on a solid adsorbent at any constant temperature. It could be presented as an equation or a graphical curve[109].

2.9.1 Langmuir Adsorption Isotherm

Irving Langmuir developed an isotherm for gases adsorbed on solids in 1918, which he named after himself. It's an empirical isotherm generated from a kinetic mechanism that's been postulated.

The basic assumptions on which the model is based include:

i. The molecules are absorbed in a fixed number of well-defined localized sites.
ii. Each site can hold one adsorbate molecule.
iii. All sites are energetically equivalent.
iv. There is no interaction between molecules adsorbed in neighboring sites.

The Langmuir Isotherm quantifies the creation of a monolayer adsorbate on the adsorbent's outer surface, after which no further adsorption occurs. As a result, the Langmuir isotherm represents the distribution of metal ions in the solid and liquid phases at equilibrium. For monolayer adsorption onto a surface with a finite number of identical sites, the Langmuir isotherm is true. The model assumes uniform energies of adsorption onto the surface and no transmigration of adsorbate in the plane of the surface[109]. Based on these assumptions, Langmuir came up with Equation 2.1.

$$q_e = \frac{Q_o K_L C_e}{1 + K_L C_e} \qquad \text{Equation 2.1}$$

Langmuir adsorption parameters were determined by transforming the Langmuir equation into linear form as shown in Equation 2.2.

.

$$\frac{1}{q_e} = \frac{1}{Q_0} + \frac{1}{Q_0 K_L C_e}$$ Equation 2.2

Where Ce = the equilibrium concentration of adsorbate (mg/L-1); qe = the amount of metal adsorbed per gram of the adsorbent at equilibrium (mg/g); Qo = maximum monolayer coverage capacity (mg/g); KL = Langmuir isotherm constant (L/mg).

The values of q_{max} and K_L can be computed from the slope and intercept of the Langmuir plot of $1/q_e$ versus $1/C_e$. The Langmuir isotherm's key characteristics can be stated in terms of the equilibrium parameter RL, which is a dimensionless constant known as the separation factor or equilibrium parameter.

$$R_L = \frac{1}{1 + (1 + K_L C_o)}$$ Equation 2.3

Where; Co = initial concentration; K_L = the constant related to the energy of adsorption (Langmuir Constant); RL value indicates the adsorption nature to be either unfavourable if RL> 1), linear if RL = 1, favourable if $0 < R_L < 1$ and irreversible if RL = 0.

2.9.2 Freundlich Adsorption Isotherm

This is a term that is frequently used to describe the adsorption properties of a heterogeneous surface. These data frequently match Freundlich's empirical equation (Equation 2.4)[110]:

$$Q_e = K_f C_e^{\frac{1}{n}}$$ Equation 2.4

Where K_f = Freundlich isotherm constant (mg/g); n = adsorption intensity; Ce = the equilibrium concentration of adsorbate (mg/L); Qe = the amount of metal adsorbed per gram of the adsorbent at equilibrium (mg/g). On linearizing Equation 2.4, we have Equation 2.5.

$$\log Q_e = \log K_f + {}^{1}\!/_{n} \log C_e \qquad \text{Equation 2.5}$$

The constant K_f is a rough estimate of adsorption capacity, whereas 1/n is a function of the adsorption process's adsorption strength. When n = 1, the partitioning between the two phases is unaffected by concentration. If the value of 1/n is less than one, the adsorption is normal. Conversely, a value of 1/n greater than one suggests cooperative adsorption. As pressure increases without bound, the function reaches an asymptotic maximum. The constants K and n changes as the temperature rises, reflecting the empirical finding that the quantity adsorbed climbs more slowly as the temperature rises, requiring higher pressures to saturate the surface. K_f and n, on the other hand, are sorbent-sorbate system parameters that must be established through data fitting, whereas linear regression is commonly employed to find the parameters of kinetic and isotherm models[111]. The linear least-squares method and linearly transformed equations, in particular, have been widely used to correlate sorption data, where 1/n is a heterogeneity parameter, and the smaller the value of 1/n, the higher the expected heterogeneity. When 1/n = 1, this expression reduces to a linear adsorption isotherm. If n is between one and ten, the sorption process is likely to be favorable.

2.9.3 Temkin Adsorption Isotherm

The Temkin isotherm is used to characterize the adsorption process on heterogeneous surfaces, assuming that adsorption heat reduces linearly with coverage due to adsorbate-adsorbent interactions[112]. The Temkin isotherm proposes that chemical adsorption occurs due to strong electrostatic interactions between adsorbate molecules and the adsorbent surface in principle[113].

Temkin isotherm can be presented by the expression in Equation 2.6:

qe=B lnA + B lnC_f

Equation 2.6

Where qe: equilibrium value of sorbate uptake (mg/g); C_f: equilibrium (final) concentrations of the adsorbate (mg/L); B (mg/g) and A (L/mg) known as Temkin model's constants are related to the heat of adsorption and maximum binding energy, respectively.

2.10 Adsorption Kinetics

Adsorption kinetic studies are useful in ascertaining the equilibrium time, adsorption rate, and adsorption potential rate-limiting steps. For adsorbents targeted to be used in wastewater treatment facilities, a high adsorption rate is an important parameter of initial concern[114]. The frequently ascertained adsorption kinetics includes;

2.10.1 Pseudo-First-order Kinetic Model

The pseudo-first-order kinetic model indicates the rate of adsorption is directly correlated to the difference of uptake at equilibrium and time t, shown as (qe -qt) in equation 2.7[115]. The equation is as shown;

$dqt/dt = k_1(qe - qt)$ Equation 2.7

Where qe: adsorption capacity at equilibrium (mg/g); qt: adsorbate uptake at time t (mg/g); k_1: rate constant of pseudo-first-order adsorption model (1/hr).

Equitation 2.8 is obtained when equation 2.6 is integrated with boundary conditions of qt=0 and $qt = qt$ at time t=0 and t=t, respectively:

$\ln (qe - qt) = \ln (qe) - k_1 t$

Equation 2.8

2.10.2 Pseudo-Second-Order Model

The pseudo-second-order kinetic model has been effectively employed in systems where chemisorption is the rate-controlling step. This model is expressed by equation 2.9. Given k_2 (g/mg.hr) is the rate constant of the pseudo-second-order adsorption model; qe and qt are the amount of antibiotics adsorbed (mg/g) at equilibrium and time t, respectively.

$dqt/dt = k_2 (qe - qt)2$

Equation 2.9

Equation (2.10) is obtained by integration of (equation 2.9) with the boundary conditions of qt=0 and qt=qt at time t=0 and t=t, respectively:

$1/qe - qt = 1/qe + k_2 t$

Equation 2.10

Equation (2.11) can be rearranged in a linear form, as shown below:

$t/qt = 1/k2.qe2 + 1/qe\ t$ Equation 2.11

Based on equation (2.11) by plotting the value of (t/qt) versus (t) equilibrium concentration (qe) can be determined.

However, in the pseudo-first-order kinetic model, the equilibrium concentration should be known before fitting the experimental data to the model. Whether the experimental data are reasonably fitted by the predicted model or not is generally evaluated based on the correlation coefficient (R^2). The higher the correlation coefficient, the more acceptable the predicted model.

In addition, based on the rate constants of pseudo second order kinetic model activation energy can be determined using the equation (2.12):

$\ln k_2 = -Ea/(1/T) + \ln D$

Equation 2.12

where k_2: pseudo second-order model rate constant; Ea: activation energy (kJ/mol); R: universal gas constant (kJ/mol. K); D: Arrhenius constant (kJ/mol).

In general, the activation energy for a physical adsorption process is lower than 4.2 kJ/mol, while for a chemical adsorption process is higher than 4.2 kJ/mol

2.10.3 Elovich Model

When the nature of adsorption is chemisorption and the adsorbent surface is heterogeneous, the Elovich equation can be used[116]. The equation corresponding to this is given in equation (2.13):

$$qt = 1/\beta \ln(\alpha\beta) + 1/\beta \ln(t)$$

Equation 2.13

Where; 1nt: adsorbate uptake at time t (mg/g) α: initial adsorption rate (mg/ g. hr) β: Elovich constant (g/mg).

2.11 Desorption of Adsorbents

Desorption is the physical process that involves the removal of a previously adsorbed substance from the surface of the adsorbent. The desorption and reusability of adsorbents in adsorption-desorption cycles make the process acceptable economically and environmentally[115]. Regeneration of adsorbents using different methods such as thermal, electrochemical, ultrasonic, and chemical methods, etc. has been revised by Kulkarni and Kaware (Figure 2.7) [116].

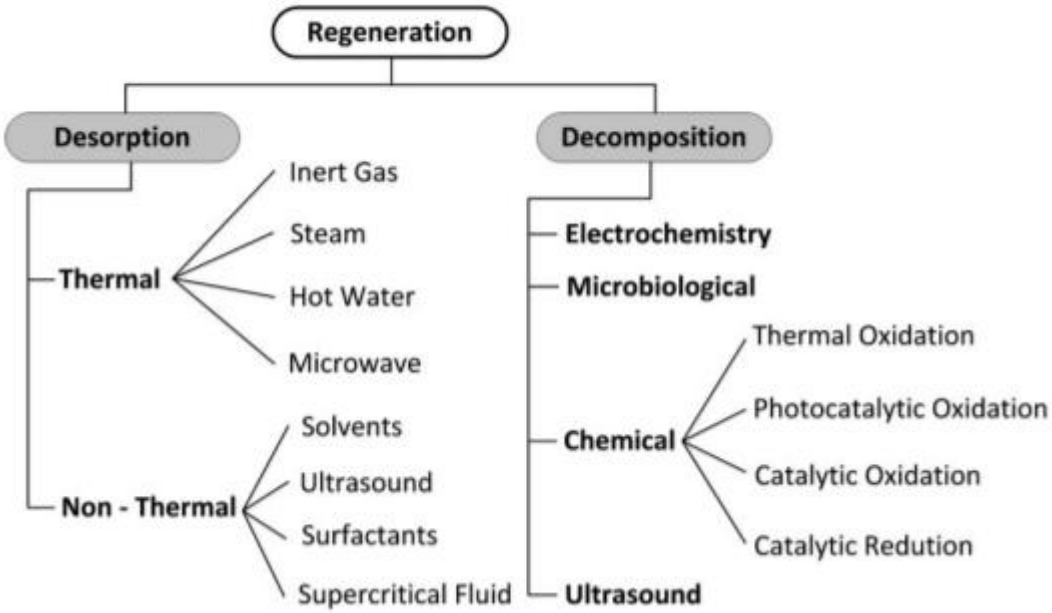

Figure 2.7: Regeneration techniques used in adsorption processes.

source[116]

Chemical regeneration offers several advantages in comparison with other methods. For instance, in chemical regeneration, loss of adsorbents due to burn-off that occurs in thermal regeneration is prevented. Also, further recovery of adsorbate is feasible by applying additional separation methods such as distillation. In the chemical desorption process, adsorbents are set in desorption agents at specific operating conditions such as pH value and temperature for a predetermined time. The desorption agents should be non-destructive for adsorbents, environmental-friendly, efficient, and inexpensive. The selection of the appropriate eluents for the process is highly dependent on the nature of adsorbents in use and the mechanism of adsorption. For instance, an alkaline solution was used when negatively charged adsorbate molecules have adhered to the positively charged surface of adsorbents through electrostatic attractions. Using an alkaline solution

causes the surface of the adsorbent to become negative, and hence repulsion of adsorbate molecules and solid surface to occur[117].

2.12 Adsorption of Methylene Blue

Adsorption has been discovered to be a successful treatment innovation for dye removal among cutting-edge treatment methods[118,119]. Adsorption treatment technology is fundamentally adaptable, easy to design, relatively simple to use, affordable, highly efficient, recyclable, and environmentally friendly. Commercial activated carbon is also a universal adsorbent but is prohibitively expensive for use in many countries around the world. Thus, efforts to find precursor materials with high carbon content, low cost, and local availability are still being made[120,121]. Locally available materials like cassava peel, cotton, orange peel, moringatinctorial bark, vitexnegundo bark, wheat straw, sawdust, avocado seed, and crocus sativus leaves have been used to produce unconventional activated carbon. The difficulty of preparing adsorbents and the numerous limitations of these materials' adsorption performance however remain[122].

Since MB dye has negative effects on water quality and perception, treating wastewater before releasing it into the environment is crucial[123,124]. MB and other textile dyes are reportedly removed from industrial wastewater using a variety of techniques. These include liquid-liquid extraction, coagulation, electrocoagulation, vacuum membrane distillation, adsorption/biosorption., nanofiltration, microwave treatment, and biodegradation, Due to its non-biodegradability, thermal and light stability, MB dye is difficult to break down into smaller inorganic molecules using conventional techniques[125,126].

Every one of these treatment options has benefits and drawbacks in terms of price, viability, effectiveness, and environmental impact[127,128]. Strong redox processes were used in the development of advanced oxidation processes (AOPs) to treat toxic organic pollutants like MB without the production of any additional harmful substances. Ozonation, UV/H_2O_2 oxidation, electrochemical oxidation/degradation, catalytic oxidation, heterogeneous photo-Fenton, and photocatalytic degradation are AOPs approaches used for the photodegradation of MB[121].

The AOPs' treatment modalities have a few benefits. The low solubility of ozone in water, high energy costs, and production of dangerous byproducts are ozonation's main drawback. Poor UV light absorption properties apply to H_2O_2[122]. So, the majority of the light input is being wasted in this situation. A significant drawback of the Fenton process is the creation of sludge that contains iron hydroxide as a byproduct[123]. The electrochemical process's primary flaw is its high operating costs, which result from its high energy consumption. In order to remove MB, photocatalytic degradation techniques are the most popular AOPS techniques. Sonocatalysis, nanofiltration, adsorption, and biodegradation are only a few new photocatalytic degradation techniques that are hybrid or integrated[124,125]. These combined techniques were found to be more effective than using just one process.

MB adsorption has been examined in a number of important papers over the past ten years from various angles. The most significant MB adsorption was reviewed by Liu and Le[126]. The range of the various adsorbent types was not fully covered because the emphasis was only on inexpensive adsorbents. As a result, the analysis of methylene blue adsorption concentrated on inexpensive adsorbents[127,128].

2.13 Other Methods and Materials for Remediating MB in Wastewater

The remediation of MB in wastewater involves the breakdown of the harmful high molecular weight compounds into small harmless molecular weight compounds or the complete removal of these substances by different degradation approaches such as chemical oxidation, biodegradation, catalytic, and photodegradation, amongst others, etc. (Table 2.2).

An effective remediation approach is strongly influenced by factors such as the choice of remediating material, chemical composition/structure of the dyes, and nature of absorbent (porosity). During the process of degrading MB, different transformation products may be formed as the dyes compound interacts with the environmental compartment. In this case, the dyes metabolites may still retain their pharmacological activity, while the dye transformation products may wreak harmful havoc in the ecosystem[129]. The microbial biotransformation of a target pollutant is often associated with oxidation and hydrolysis reactions which give rise to new compounds with lower molecular weight than the parent compound.

Besides, photodegradation is a strategy that has also been explored for the decomposition of MB in wastewaters. This usually occurs in the presence of solar radiation, where MB and associated metabolites can undergo photochemical degradation in environmental matrixes[129]. Generally, the UV light can cause the direct photolysis, photosensitization, and phototransformation of many dyes[130,131]. Considering that some antibiotics are highly sensitive to light, therefore, they tend to be activated and degraded when they absorb direct light[132]. In other cases, the dyes compounds may form reactive oxidant species (ROS) like hydroxyl radicals, peroxides, superoxide or peroxyl radicals, and triplet

excited-state dissolved organic matter generated by photosensitizers under light irradiation[133,134].

In some cases, microorganisms such as algae and their secretions can be exploited as photosensitizers, in the indirect photolysis of residual dye[135]. Their photodegradation reaction is actualized by the secretion of extracellular organic matter (EOMs) and the production of active species that can absorb a sufficient amount of light energy[136,137]. The rate of degradation could be largely influenced by the chemical structure or elemental composition of the dye compound.

In addition, the photocatalytic degradation of dyes in wastewater involves the reduction of large molecular weight dye compounds to small molecular weight, thereby producing water and carbon dioxide, the comprehensive degradation and mineralization are seldomly actualized[138]. Different materials such as semiconducting transition metal oxides, and metal/polymer-based nanocomposites have been widely explored as photocatalysts owing to their large surface areas that promote the separation and transfer of charge carriers and offer abundant active sites for photocatalytic redox reactions[139,140]. The general mechanism of photodegradation involves the generation of electron-hole pairs when the semiconducting photocatalyst is irradiated with light. In many cases, the loss of photogenerated electron-hole pairs by mass recombination mitigates the efficiency and activity of photocatalytic reaction[141,142]. These lead to the formation of reactive OH radicals, superoxide anion radicals, and singlet oxygen which are very important in the photo-degradation of the target dyes (Figure 2.8).

Table 2.2: Recent Advanced Technologies for the Remediation, Degradation, and Removal of MB for Water Treatment

Absorbent	Remediation approach	Removal efficiency or capacity	Other remarks	Ref.
Calcium peroxide	Ozonation	95.6 % and 80.1 % for synthetic and simulated wastewater respectively	Endothermic thermodynamic process	[143]
High rate algal ponds	Continuous photobioreactors	82 %	Photodegradation mechanism	[144]
Persulfate	Electrochemical activation	94 %	Electrocoagulation process played a basic role in CPX removal	[145]
Boron-doped diamond/polymer electrolyte	Ultrasound irradiation	91.36 %	Ultrasound irradiation has a significant impact on energy demand, and it only helps to improve pollutant removal when a low current is used.	[146]
$FeWO_4$/Nitrogen-doped carbon	Photocatalysis	92.23 %	Large surface area and pore structure of the adsorbent enabled photodegradation by photogenerated holes and radicals	[147]

NB: Bp: Black phosphorus; US: Ultrasonic; PS: Persulfate

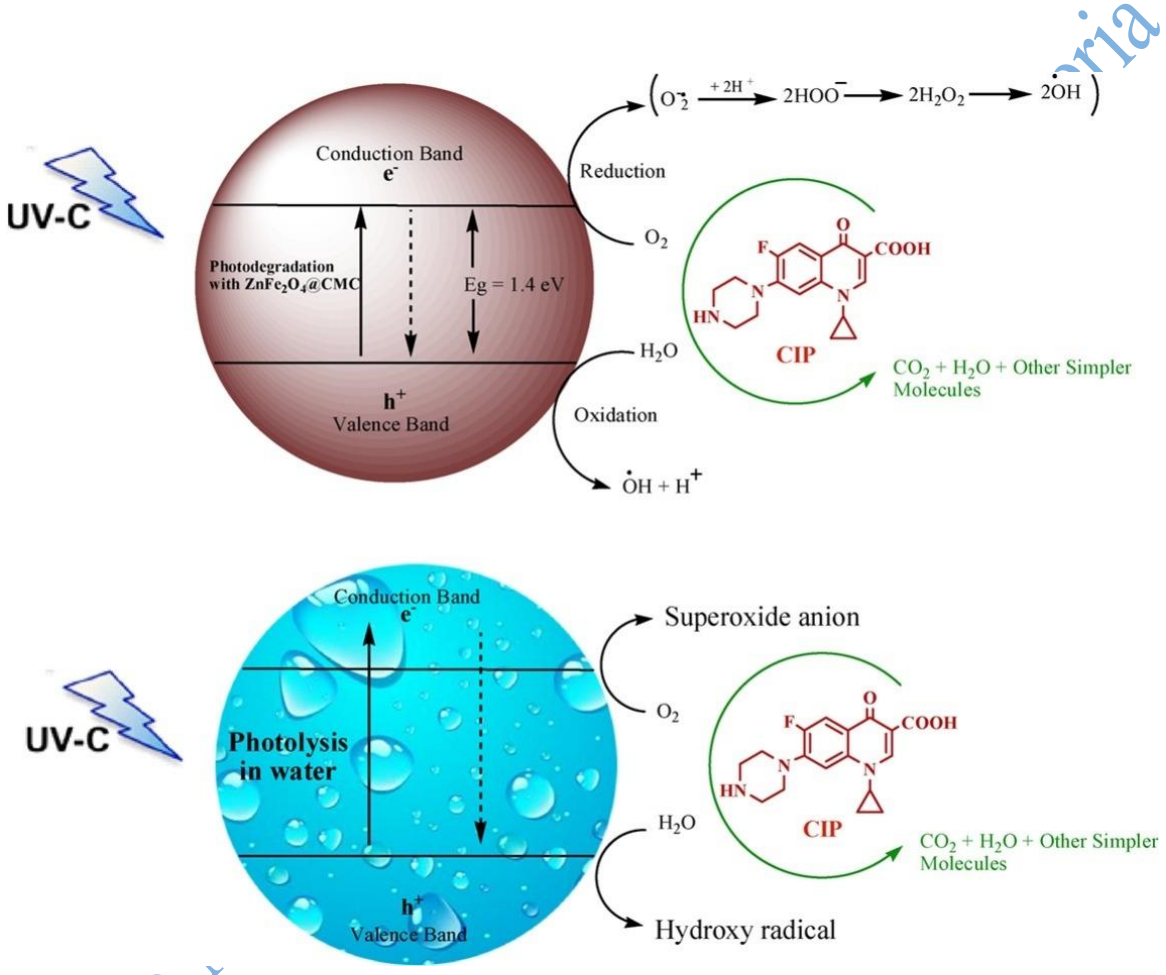

Figure 2.8: The mechanism for photodegradation of MB by metallic nanobiocomposite. Source[140]

Endnotes

1. S. Benkhaya, A. M'rabet, & A. El Harfi. *A review on classifications, recent synthesis and applications of textile dyes.* **Inorganic Chemistry Communications**, 115, 2020, 107891.

2. A.I. Abd-Elhamid, M. Emran, M.H. El-Sadek, A.A., El-Shanshory, H. Soliman, M.A. Akl, & M. Rashad. *Enhanced removal of cationic dye by eco-friendly activated biochar derived from rice straw.* **Applied Water Science**, 10(1), 2020, 1-11.

3. H. D. Bouras, Z. Isik, E.B. Arikan, A.R. Yeddou, N. Bouras, A. Chergui, L. Favier, A. Amrane, & N. Dizge. *Biosorption characteristics of methylene blue dye by two fungal biomasses.* **International Journal of Environmental Studies**, 78(3), 2021, 365-381.

4. N. Tara, S.I. Siddiqui, G. Rathi, S.A. Chaudhry, & A.M. Asiri. Nano-*engineered adsorbent for the removal of dyes from water: a review.* **Current Analytical Chemistry**, 16(1), 2020, 14-40.

5. I. Khan, K. Saeed, N. Ali, I. Khan, B. Zhang, & M. Sadiq. *Heterogeneous photodegradation of industrial dyes: an insight to different mechanisms and rate affecting par*. **Current Analytical Chemistry**, 2(1), 2020, 16-70.

6. M.I. Din, R. Khalid, J. Najeeb, & Z. Hussain. *Fundamentals and photocatalysis of methylene blue dye using various nanocatalytic assemblies-a critical review*. **Journal of Cleaner Production**, 298, 2021, 126567.

7. M. Makeswari, & P. Saraswathi. *Photo catalytic degradation of methylene blue and methyl orange from aqueous solution using solar light onto chitosan bi-metal oxide composite.* **SN Applied Sciences**, 2(3), 2020, 1-12.

8. S. Sabar, H.A. Aziz, N.H. Yusof, S. Subramaniam, K.Y. Foo, L.D. Wilson, & H.K. Lee. *Preparation of sulfonated chitosan for enhanced adsorption of methylene blue from aqueous solution*. **Reactive and Functional Polymers,** 151, 2020, 104584.

9. J. Cheng, C. Zhan, J. Wu, Z. Cui, J. Si, Q. Wang, X. Peng, & L.S. Turng. *Highly efficient removal of methylene blue dye from an aqueous solution using cellulose acetate nanofibrous membranes modified by polydopamine*. **ACS omega**,5(10), 2020, 5389-5400.

10. X. Wei, Y. Wang, Y. Feng, X. Xie, X. Li, & S. Yang. *Different adsorption-degradation behavior of methylene blue and congo red in nanoceria/H_2O_2 system under alkaline conditions*. **Scientific reports,** 9(1), 2019, 1-10.

11. C. Anushree, & J. Philip. *Efficient removal of methylene blue dye using cellulose capped Fe3O4 nanofluids prepared using oxidation-precipitation method.* **Colloids and Surfaces A: Physicochemical and Engineering Aspects,** 567, 2019, 193-204.

12. I. Khan, K. Saeed, I. Zekker, B. Zhang, A.H. Hendi, A. Ahmad, S. Ahmad, N. Zada, H. Ahmad, L.A. Shah, & T. Shah. *Review on methylene blue: its properties, uses, toxicity and photodegradation.* **Water,** 14(2), 2022, 242.

13. P. Jia, H. Tan, K. Liu, & W. Gao. *Removal of methylene blue from aqueous solution by bone char.* **Applied Sciences**, 8(10), 2018, 1903.

14. V.L. Pham, D.G. Kim, & S.O. Ko. *Mechanisms of methylene blue degradation by nano-sized β-MnO_2 particles.* **KSCE Journal of Civil Engineering**, 24(5), 2020, 1385-1394.

15. J. Lin, Z. Luo, J. Liu, & P. Li. *Photocatalytic degradation of methylene blue in aqueous solution by using ZnO-SnO^2 nanocomposites*. **Materials Science in Semiconductor Processing,** 87, 2018, 24-31.

16. C. Hou, B. Hu, & J. Zhu. *Photocatalytic degradation of methylene blue over TiO_2 pretreated with varying concentrations of NaOH.* **Catalysts,** 8(12), 2018, 575.

17. G. Lu, M. Nagbanshi, N. Goldau, M. Mendes Jorge, P. Meissner, A. Jahn, F.P. Mockenhaupt, & O. Mueller. *Efficacy and safety of methylene blue in the treatment of malaria: a systematic review.* **BMC medicine**, 16(1), 2018, 1-16.

18. M.K. Uddin, & A. Nasar. *Decolorization of basic dyes solution by utilizing fruit seed powder*. **KSCE Journal of Civil Engineering**, 24(2), 2020, 345-355.

19. B. Saha, S. Chowdhury, D. Sanyal, K. Chattopadhyay, & G. Suresh Kumar. *Comparative study of toluidine blue O and methylene blue binding to lysozyme and their inhibitory effects on protein aggregation*. **ACS omega,** 3(3), 2018, 2588-2601.

20. M. Marimuthu, B. Praveen Kumar, L. MariyaSalomi, M. Veerapandian, & K. Balamurugan. *Methylene blue-fortified molybdenum trioxide nanoparticles: harnessing radical scavenging property*. **ACS applied materials & interfaces**, 10(50), 2018, 43429-43438.

21. M.E. Nedu, M. Tertis, C. Cristea, & A.V. Georgescu. *Comparative study regarding the properties of methylene blue and proflavine and their optimal concentrations for in vitro and in vivo applications*. **Diagnostics**, 10(4), 2020, 223.

22. D. Balarak, M. Bazzi, Z. Shehu, & K. Chandrika. *Application of surfactant-modified bentonite for methylene blue adsorption from aqueous solution*. **Orient J Chem**, 36(2), 2020, 293-9.

23. A.H Mijinyawa, G. Durga, & A. Mishra. *A sustainable process for adsorptive removal of methylene blue onto a food grade mucilage: kinetics, thermodynamics, and equilibrium evaluation.* **International Journal of Phytoremediation**, 21(11), 2019, 1122-1129.

24. S. Parakala, S. Moulik, & S. Sridhar. *Effective separation of methylene blue dye from aqueous solutions by integration of micellar enhanced ultrafiltration with vacuum membrane distillation.* **Chemical Engineering Journal**, 375, 2019, 122015.

25. F. Arias Arias, M. Guevara, T. Tene, P. Angamarca, R. Molina, A. Valarezo, O. Salguero, C. Vacacela Gomez, M. Arias, & L.S. Caputi. *The adsorption of methylene blue on eco-friendly reduced graphene oxide.* **Nanmaterials,** 10(4), 2020, 681.

26. M. Manimohan, S. Pugalmani, K. Ravichandran, & M.A. Sithique. *Synthesis and characterisation of novel Cu (II)-anchored biopolymer complexes as reusable materials for the photocatalytic degradation of methylene blue.* **RSC advances**, 10(31), 2020, 18259-18279.

27. P.P. Giannakopoulou, P. Petrounias, A. Rogkala, P. Lampropoulou, E. Gianni, D. Papoulis, P. Koutsovitis, B. Tsikouras, & K. Hatzipanagiotou. *Does the methylene blue test give equally satisfactory results in all studied igneous rocks relative to the identification of swelling clay minerals*. **Minerals**, 10(3), 2020, 283.

28. R.C. Dante, J. Trakulmututa, S. Meejoo-Smith, P. Martín-Ramos, P. Chamorro-Posada, D. Rutto & F.M. Sánchez-Arévalo. *Methylene blue-carbon nitride system as a reusable air-sensor*. **Materials Chemistry and Physics**, 231, 2019, 351-356.

29. Y. Zhang, Y. An, L. Wu, H. Chen, Z. Li, H. Dou,V. Murugadoss, J. Fan, X. Zhang, X. Mai, & Z. Guo. *Metal-free energy storage systems: combining batteries with capacitors based on a methylene blue functionalized graphene cathode*. **Journal of Materials Chemistry A**, 7(34), 2019, 19668-19675.

30. G. López-Carballo, V. Muriel-Galet, P. Hernández-Muñoz, & R. Gavara. *Chromatic sensor to determine oxygen presence for applications in intelligent packaging*. **Sensors**, 19(21), 2019, 4684.

31. Y. Pang, Z.H. Tong, L. Tang, Y.N. Liu, & K. Luo. *Effect of humic acid on the degradation of methylene blue by peroxymonosulfate.* **Open Chemistry**, 16(1), 2018, 401-406.

32. L. Sun, D. Hu, Z. Zhang, & X. Deng. *Oxidative degradation of methylene blue via PDS-based advanced oxidation process using natural pyrite.* **International Journal of Environmental Research and Public Health,** 16(23), 2019, 4773.

33. M. Contreras, C.D. Grande-Tovar, W. Vallejo, & C. Chaves-López. *Bio-removal of methylene blue from aqueous solution by Galactomycesgeotrichum KL20A*. **Water,** 11(2), 2019, 282.

34. E.A. Abdelrahman, R.M. Hegazey, & R.E. El-Azabawy. *Efficient removal of methylene blue dye from aqueous media using Fe/Si, Cr/Si, Ni/Si, and Zn/Si amorphous novel adsorbents.* **Journal of Materials Research and Technology**, 8(6), 2019, 5301-5313.

35. E. Santoso, R. Ediati, Y. Kusumawati, H. Bahruji, D.O. Sulistiono, & D. Prasetyoko. *Review on recent advances of carbon based adsorbent for methylene blue removal from waste water.* **Materials Today Chemistry**, 16, 2020, 100233.

36. A.H. Jawad, M. Bardhan, M.A. Islam, S.S.A. Syed-Hassan, S.N. Surip, Z.A. ALOthman, & M.R. Khan. *Insights into the modeling, characterization and adsorption performance of mesoporous activated carbon from corn cob residue via microwave-assisted H_3PO_4 activation.* **Surfaces and Interfaces**, 21, 2020, 100688.

37. L.F. Cusioli, H.B. Quesada, A.T. Baptista, R.G. Gomes, & R. Bergamasco. *Soybean hulls as a low-cost biosorbent for removal of methylene blue contaminant*. **Environmental Progress & Sustainable Energy**, 39(2), 2020, 13328.

38. Z. Wang, M. Gao, X. Li, J. Ning, Z. Zhou, & G. Li. *Efficient adsorption of methylene blue from aqueous solution by graphene oxide modified persimmon tannins.* **Materials Science and Engineering**, 108, 2020, 110196.

39. O.E. Ebi, A.F. Taiwo, & A.T. Folorunsho. *Kinetic Modelling of the Biosorption of Methylene Blue onto Wild Melon (Lagenariasphaerica)*. **American Journal of Chemical Engineering**, 6(6), 2018, 126-134.

40. S. Zhou, Z. Du, X. Li, Y. Zhang, Y. He, & Y. Zhang. *Degradation of methylene blue by natural manganese oxides: kinetics and transformation products.* **Royal Society open science,** 6(7), 2019, 90351.

41. C.P. Lawagon, R.E.C. Amon, C.P. Lawagon, & R.E.C Amon. *Magnetic rice husk ash'cleanser'as efficient methylene blue adsorbent.* **Environmental Engineering Research**, 25(5), 2019, 685-692.

42. G. Crini, E. Lichtfouse, L. D. Wilson, & N. Morin-Crini. *Conventional and non-conventional adsorbents for wastewater treatment.* **Environmental Chemistry Letters**, 17, 2019, 195–213.

43. P. Srivatsav, B. S. Bhargav, V. Shanmugasundaram, J. Arun, K. P. Gopinath, & A. Bhatnagar. *Biochar as an eco-friendly and economical adsorbent for the removal of colorants (Dyes) from aqueous environment: A review*. **Water (Switzerland),** 12, 2020: 1–27.

44. M. A. Al-Ghouti, D. Da'ana, M. Abu-Dieyeh, & M. Khraisheh. *Adsorptive removal of mercury from water by adsorbents derived from date pits.* **Scientific Reports**, 9, 2019 1–15.

45. J. Saleem, U. Bin Shahid, M. Hijab, H. Mackey, & G. McKay. *Production and applications of activated carbons as adsorbents from olive stones.* **Biomass Conversion and Biorefinery**, 9, 2019, 775–802.

46. B. Luo, G. Huang, Y. Yao, C. An, P. Zhang, & K. Zhao. *Investigation into the influencing factors and adsorption characteristics in the removal of sulfonamide antibiotics by carbonaceous materials*. **Journal of Cleaner Production**, 2021, 319-128692.

47. N. M. Aljamali, R. A. B. Aldujaili, & I. O. Alfatlawi. *Physical and chemical adsorption and its applications*. **International Journal of Thermodynamics and Chemical Kinetics**, 7, 2021, 1–8.

48. E. Torres. *Biosorption: A review of the latest advances*. **Processes**, 8, 2020, 1–23.

49. A. M. Elgarahy, K. Z. Elwakeel, S. H. Mohammad, & G. A. Elshoubaky. *A critical review of biosorption of dyes, heavy metals and metalloids from wastewater as an efficient and green process.* **Cleaner Engineering and Technology,** 4, 2021, 100209.

50. M. K. Al Mesfer, M. Danish, M. I. Khan, I. H. Ali, M. Hasan, & A. El Jery. *Continuous fixed bed co2 adsorption: breakthrough, column efficiency, mass transfer zone.* **Processes**, 8, 2020, 1233.

51. T. Selmi, M. Seffen, A. Celzard, & V. Fierro. *Effect of the adsorption pH and temperature on the parameters of the Brouers–Sotolongo models*. **Environmental Science and Pollution Research**, 27, 2020, 23437–23446.

52. G. Gopal, S. A. Alex, N. Chandrasekaran, & A. Mukherjee. *A review on tetracycline removal from aqueous systems by advanced treatment techniques*. **RSC Advances,** 10, 2020, 27081–27095.

53. J. O. Eniola, R. Kumar, & M. A. Barakat. *Adsorptive removal of antibiotics from water over natural and modified adsorbents.* **Environmental Science and Pollution Research**, 26, 2019, 34775–34788.

54. P. Hess. *Bonding, structure, and mechanical stability of 2D materials: the predictive power of the periodic table.* **Nanoscale Horizons**, 6, 2021, 856–892.

55. H. N. Hamad, & S. Idrus. *Recent developments in the application of bio-waste-derived adsorbents for the removal of methylene blue from wastewater: a review*. **Polymers**, 14, 2022.

56. J. Jjagwe, P. W. Olupot, E. Menya, & H. M. Kalibbala. *Synthesis and application of granular activated carbon from biomass waste materials for water treatment: a review.* **Journal of Bioresources and Bioproducts**, 6, 2021, 292–322.

57. P. González-García. *Activated carbon from lignocellulosics precursors: A review of the synthesis methods, characterization techniques and applications*. **Renewable and Sustainable Energy Reviews**, 82, 2018, 1393–1414.

58. Y. Wang, Y. Zhou, G. Jiang, P. Chen, & Z. Chen. *One-step fabrication of carbonaceous adsorbent from corncob for enhancing adsorption capability of methylene blue removal.* **Scientific Reports**, 10, 2020, 1–9.

59. M. Mallek, M. Chtourou, M. Portillo, H. Monclús, K. Walha, A. ben Salah, & V. Salvadó. *Granulated cork as biosorbent for the removal of phenol derivatives and emerging contaminants.* **Journal of Environmental Management**, 223, 2018, 576–585.

60. N. S. Alharbi, B. Hu, T. Hayat, S. O. Rabah, A. Alsaedi, L. Zhuang, & X. Wang. *Efficient elimination of environmental pollutants through sorption-reduction and photocatalytic degradation using nanomaterials.* **Frontiers of Chemical Science and Engineering,** 14, 2020, 1124–1135.

61. Y. Dai, M. Liu, J. Li, S. Yang, Y. Sun, Q. Sun, W. Wang, L. Lu, K. Zhang, J. Xu, W. Zheng, Z. Hu, Y. Yang, Y. Gao, & Z. Liu. *A review on pollution situation and treatment methods of tetracycline in groundwater.* **Separation Science and Technology (Philadelphia)**, 55, 2020, 1005–1021.

62. D. Liu, Q. Xie, X. Huang, C. Wan, F. Deng, D. Liang, & J. Liu. *Backwashing behavior and hydrodynamic performances of granular activated carbon blends.* **Environmental Research**, 2020, 184 109302.

63. G. Sharma, S. Sharma, A. Kumar, C. W. Lai, M. Naushad, Shehnaz, J. Iqbal, & F. J. Stadler. *Activated carbon as superadsorbent and sustainable material for diverse applications.* **Adsorption Science & Technology,** 2022, 1–21.

64. J. Lee, & R. Patel. *Wastewater treatment by polymeric microspheres: a review.* **Polymers**, 14, 2022, 1–37.

65. S.A. Ambika, & P. P. Singh. *Natural polymer-based hydrogels for adsorption applications.* **Nat. Polym. Green Adsorbents Water Treat. Elsevier,** 2021, 267–306.

66. S. Mallakpour, & F. Azimi. *Polymer nanocomposites based on alginate and their blends for remediation of pollutants from wastewater*. **Nat. Polym. Green Adsorbents Water Treat. Elsevier,** 2021, 307–332.

67. M. Cantarella, S. C. Carroccio, S. Dattilo, R. Avolio, R. Castaldo, C. Puglisi, & V. Privitera. *Molecularly imprinted polymer for selective adsorption of diclofenac from contaminated water.* **Chemical Engineering Journal**, 367, 2019, 180–188.

68. N. Morin-crini, E. Lichtfouse, M. Fourmentin, A. Ribeiro, C. Noutsopoulos, F. Mapelli, É. Fenyvesi, M. Vieira, L. Picos-corrales, J. Moreno-piraján, N. Morin-crini, E. Lichtfouse, M. Fourmentin, A. Ribeiro, C. Noutsopoulos, E. Lichtfouse, J. Schwarzbauer, D. R. Emerg-, N. Morin-crini, E. Lichtfouse, & M. Fourmentin. *Remediation of emerging contaminants.* **Environ. Chem. a Sustain. World,** 2022, 1–106.

69. J. J. Belbruno. *Molecularly imprinted polymers*. **Chemical Reviews**, 119, 2019, 94–119.

70. Z. Feng, K. Odelius, & M. Hakkarainen. *Tunable chitosan hydrogels for adsorption: Property control by biobased modifiers.* **Carbohydrate Polymers**, 196, 2018, 135–145.

71. B. Gao, P. Li, R. Yang, A. Li, & H. Yang. *Investigation of multiple adsorption mechanisms for efficient removal of ofloxacin from water using lignin-based adsorbents*. **Scientific Reports**, 9, 2019, 1–13.

72. E. N. Zare, Z. Fallah, V. T. Le, V.-D.Doan, A. Mudhoo, S.-W.Joo, Y. Vasseghian, M. Tajbakhsh, O. Moradi, M. Sillanpää, & R. S. Varma. *Remediation of pharmaceuticals from contaminated water by molecularly imprinted polymers: a review* **Springer International Publishing**. 2022.

73. W. Duan, N. Wang, W. Xiao, Y. Zhao, & Y. Zheng. *Ciprofloxacin adsorption onto different micro-structured tourmaline, halloysite and biotite.* **Journal of Molecular Liquids**, 269, 2018, 874–881.

74. A. O. Adeola, O. Fapohunda, A. T. Jimoh, T. T. Isaiah, A. O. Ige, & A. C. Ogunyele, 2019. *Scientific applications and prospects of nanomaterials: A multidisciplinary review.* **African Journal of Biotechnology**, 2019, 946–961.

75. S. M. Abdelbasir, & A. E. Shalan. *An overview of nanomaterials for industrial wastewater treatment.* **Korean Journal of Chemical Engineering**, 2019, 1209–1225.

76. V. N. Popok, & O. Kylián. *Gas-phase synthesis of functional nanomaterials.* **Applied Nano**, 2020, 25–58.

77. A. Cartwright, K. Jackson, C. Morgan, A. Anderson, & D. W. Britt. *A review of metal and metal-oxide nanoparticle coating technologies to inhibit agglomeration and increase bioactivity for agricultural applications.* **Agronomy,** 2020, 1–20.

78. A. A. Kokorina, A. V. Ermakov, A. M. Abramova, I. Y. Goryacheva, & G. B. Sukhorukov. *Carbon nanoparticles and materials on their basis.* **Colloids and Interfaces**, 2020, 4-42.

79. J. Jeevanandam, A. Barhoum, Y. S. Chan, A. Dufresne, & M. K. Danquah. *Review on nanoparticles and nanostructured materials: History, sources, toxicity and regulations.* **Beilstein Journal of Nanotechnology**, 2018, 1050–1074.

80. S. Saha, S. Bansal, & M. Khanuja. *Classification of nanomaterials and their physical and chemical nature.* **Nano-enabled Agrochem. Agric. (Elsevier, 2022)**, 2022, 7–34.

81. X. Bouju, É. Duguet, F. Gauffre, C. R. Henry, M. L. Kahn, P. Mélinon, & S. Ravaine. *Nonisotropic self-assembly of nanoparticles: from compact packing to functional aggregates.* **Advanced Materials**, 2018, 30.

82. G. Fytianos, A. Rahdar, & G. Z. Kyzas. *Nanomaterials in cosmetics: Recent updates*. **Nanomaterials**, 10, 2020, 1–16.

83. H. Moulahoum, F. Ghorbanizamani, E. G. Celik, & S. Timur. *Nano-scaled materials and polymer integration in biosensing tools*. **Biosensors,** 12, 2022.

84. D. Mustapha, D. T. Shuaib, M. M. Ndamitso, M. B. Etsuyankpa, A. Sumaila, U. M. Mohammed, & M. B. Nasirudeen. *Adsorption isotherm, kinetic and thermodynamic studies for the removal of Pb(II), Cd(II), Zn(II) and Cu(II) ions from aqueous solutions using Albizialebbeck pods.* **Applied Water Science**, 9, 2019, 1–11.

85. A. Borhan, S. Yusup, J. W. Lim, & P. L. Show. *Characterization and modelling studies of activated carbon produced from rubber-seed shell using KOH for CO_2 adsorption*. **Processes**, 7, 2019.

86. J. Fito, S. Abrham, & K. Angassa. *Adsorption of methylene blue from textile industrial wastewater onto activated carbon of Partheniumhysterophorus.* **International Journal of Environmental Research**, 14(5), 2020, 501-511.

87. J. Fito, H. Said, S. Feleke, & A. Worku. *Fluoride removal from aqueous solution onto activated carbon of Catha edulis through the adsorption treatment technology.* **Environ Syst Res** 8, 2019, 1–10

88. D. Zamel, A.H. Hassanin, R. Ellethy, G. Singer, & A. Abdelmoneim. *Novel bacteria-immobilized cellulose acetate/poly (ethylene oxide) nanofibrous membrane for wastewater treatment.* **Scientific reports**, 9(1), 2019, 1-11.

89. P.M. Thabede, N.D. Shooto, & E.B. Naidoo. *Removal of methylene blue dye and lead ions from aqueous solution using activated carbon from black cumin seeds*. **South African Journal of chemical engineering,** 33(1), 2020, 39-50.

90. L. Liu, D. He, F. Pan, R. Huang, H. Lin, & X. Zhang. *Comparative study on treatment of methylene blue dye wastewater by different internal electrolysis systems and COD removal kinetics, thermodynamics and mechanism.* **Chemosphere,** 238, 2020, 124671.

91. G. Crini, & E. Lichtfouse. *Advantages and disadvantages of techniques used for wastewater treatment.* **Environmental Chemistry Letters,** 17(1), 2019, 145-155.

92. H. Dzinun, Y. Ichikawa, M. Honda, & Q. Zhang. *Efficient immobilised tio2 in polyvinylidene fluoride (pvdf) membrane for photocatalytic degradation of methylene*. **J. Membr. Sci. Res**., 6, 2020, 188–195.

93. J.J. Samuel, & F.K. Yam. *Photocatalytic degradation of methylene blue under visible light by dye sensitized titania*. **Materials Research Express**, 7(1), 2020, 015051.

94. J. Xiong, S. Guo, T. Zhao, Y. Liang, J. Liang, S. Wang, H. Zhu, L. Zhang, J.R. Zhao, & G. Chen. *Degradation of methylene blue by intimate coupling photocatalysis and biodegradation with bagasse cellulose composite carrier.* **Cellulose,** 27, 2020, 3391–3404.

95. K.O. Iwuozor, J. O. Ighalo, L. A. Ogunfowora, A. G. Adeniyi, & C.A. Igwegbe. *An empirical literature analysis of adsorbent performance for methylene blue uptake from aqueous media*. **Journal of Environmental Chemical Engineering**, 9(4), 2021, 105-658.

96. V. Subha, K. Divya, S. Gayathri, E. Jagan Mohan, N. Keerthanaa, M. Vinitha, S. Kirubanandan, & S. Renganathan. *Applications of iron oxide nanocomposite in waste water.* **Water, Air, and Soil Pollution,** 2018, 21-22.

97. E. Zabłocka-Godlewska, W. Przystaś, & E. Grabińska-Sota. *Possibilities of obtaining from highly polluted environments: new bacterial strains with a significant decolorization potential of different synthetic dyes*. **Water, Air, and Soil Pollution,** 2019, 229.

98. K. Samal, S. Mahapatra, & M. Hibzur Ali. *Pharmaceutical wastewater as emerging contaminants: Treatment technologies, impact on environment and human health.* **Energy Nexus**, 2022, 6 100076.

99. F. Mashkoor, & A. Nasar. *Magsorbents: Potential candidates in wastewater treatment technology–A review on the removal of methylene blue dye.* **Journal of magnetism and magnetic materials,** 500, 2020, 166408.

100. S. Inamuddin. *Xanthan gum/titanium dioxide nanocomposite for photocatalytic degradation of methyl orange dye*. **International Journal of Biological Macromolecules**, 121, 2019, 1046-1053.

101. K. Qamruzzaman, & A. Nasar. *Degradative treatment of bispyribac sodium herbicide from syntheticall r treatment–dye decolourisation and anti–microbial activity*. **MOJ Drug Des. Dev. Ther,** 2019.

102. M.K. Uddin, & Z. Rehman. *Application of nanomaterials in the remediation of textile effluents from aqueous solutions in Nanomaterials in the Wet Processing of Textiles.* **Hoboken, NJ, USA: John Wiley & Sons, Inc.** 2018, 135-161.

103. M. Ahmed, F. Mashkoor, & A. Nasar. *Development, characterization, and utilization of magnetized orange peel waste as a novel adsorbent for the confiscation of crystal violet dye from aqueous solution.* **Groundwater for sustainable development,** 10, 2020, 100322.

104. S. Shakoor, & A. Nasar. *Adsorptive treatment of hazardous methylene blue dye from artificially contaminated water using cucumissativus peel waste as a low-cost adsorbent.* **Groundwater for Sustainable Development**, 5, 2017, 152-159.

105. G.K Sarma, S. Sen Gupta, & K.G. Bhattacharyya. *Removal of hazardous basic dyes from aqueous solution by adsorption onto kaolinite and acid-treated kaolinite: kinetics, isotherm and mechanistic study.* **SN Applied Sciences**, 1(3), 2019, 1-15.

106. F. Mashkoor, & A. Nasar. *Magsorbents: Potential candidates in wastewater treatment technology–A review on the removal of methylene blue dye.* **Journal of magnetism and magnetic materials,** 500, 2020, 166408.

107. Z.P. Hu, Z.M. Gao, X. Liu, & Z.Y. Yuan. *High-surface-area activated red mud for efficient removal of methylene blue from wastewater.* **Adsorption Science & Technology,** 36(1-2), 2018, 62-79.

108. L. Sheng, Y. Zhang, F. Tang, & S. Liu. *Mesoporous/microporous silica materials: preparation from natural sands and highly efficient fixed-bed adsorption of methylene blue in wastewater.* **Microporous and Mesoporous Materials**, 257, 2018, 9-18.

109. A. Pohl. *Removal of heavy metal ions from water and wastewaters by sulfur-containing precipitation agents.* **Water, Air, and Soil Pollution**, 2020, 231.

110. S. Ida, & T. Eva. *Removal of heavy metals during primary treatment of municipal wastewater and possibilities of enhanced removal: A review.* **Water (Switzerland),** 2021, 13.

111. W. Polińska, U. Kotowska, D. Kiejza, & J. Karpińska. *Insights into the use of phytoremediation processes for the removal of organic micropollutants from water and wastewater; a review.* **Water (Switzerland),** 2021, 13.

112. C. R. Delgado-González, A. Madariaga-Navarrete, J. M. Fernández-Cortés, M. Islas-Pelcastre, G. Oza, H. M. N. Iqbal, & A. Sharma. *Advances and applications of water phytoremediation: A potential biotechnological approach for the treatment of heavy metals from contaminated water.* **International Journal of Environmental Research and Public Health,** 2021, 18.

113. N. A. A. Qasem, R. H. Mohammed, & D. U. Lawal. *Removal of heavy metal ions from wastewater: a comprehensive and critical review.* **npj Clean Water**, 2021.

114. J. B. Huo, K. Gupta, C. Lu, H. C. Bruun Hansen, & M. L. Fu. *Recyclable high-affinity arsenate sorbents based on porous Fe2O3/La2O2CO3 composites derived from Fe-La-C frameworks. Colloids and Surfaces A:* **Physicochemical and Engineering Aspects,** 585, 2020, 124018.

115. Y. Chao, B. Tang, J. Luo, P. Wu, D. Tao, H. Chang, X. Chu, Y. Huang, H. Li, & W. Zhu. *Hierarchical porous boron nitride with boron vacancies for improved adsorption performance to antibiotics.* **Journal of Colloid and Interface Science,** 584, 2021, 154–163.

116. S. Gupta, Y. Mittal, R. Panja, K. B. Prajapati, & A. K. Yadav. *Conventional wastewater treatment technologies.* **Curr. Dev. Biotechnol. Bioeng.** 2021, 47–75.

117. G. Gangaraju, R. Uma, & K. J. Shah. *Introduction to conventional wastewater treatment technologies: limitations and recent advances. adv. wastewater treat.* **I (Materials Research Foundations LLC**, 2021, pp. 1–36.

118. H. Su, W. Li, Y. Han, & N. Liu. *Magnetic carboxyl functional nanoporous polymer: Synthesis, characterization and its application for methylene blue adsorption.* **Scientific Reports**, 2018, 1–8.

119. G. Jalloul, I. Keniar, A. Tehrani, & C. Boyadjian. *Antibiotics contaminated irrigation water: an overview on its impact on edible crops and visible light active titania as potential photocatalysts for irrigation water treatment.* **Frontiers in Environmental Science**, 2021, 1–29.

120. M. M. Sabzehmeidani, S. Mahnaee, M. Ghaedi, H. Heidari, & V. A. L. Roy. *Carbon based materials: a review of adsorbents for inorganic and organic compounds.* **Materials Advances,** 2, 2021, 598–627.

121. L. Xu, M. Zhang, Y. Wang, & F. Wei. *Highly effective adsorption of antibiotics from water by hierarchically porous carbon: Effect of nanoporous geometry.* **Environmental Pollution,** 274, 2021, 116591.

122. M. Allsopp, A. Walters, & D. Santillo. *Nanotechnologies and nanomaterials in electrical and electronic goods: a review of uses and health concerns.* **Greenpeace Research Laboratories**, 2007, 1–22.

123. G. Fytianos, A. Rahdar, & G. Z. Kyzas. *Nanomaterials in cosmetics: Recent updates.* **Nanomaterials,** 10, 2020, 1–16.

124. H. Moulahoum, F. Ghorbanizamani, E. G. Celik, & S. Timur. *Nano-scaled materials and polymer integration in biosensing tools*. **Biosensors,** 12, 2022.

125. N. Ayawei, A. N. Ebelegi, & D. Wankasi. *Modelling and Interpretation of Adsorption Isotherms.* **Journal of Chemistry,** 2017.

126. S. Mustapha, D. T. Shuaib, M. M. Ndamitso, M. B. Etsuyankpa, A. Sumaila, U. M. Mohammed, & M. B. Nasirudeen. *Adsorption isotherm, kinetic and thermodynamic studies for the removal of Pb(II), Cd(II), Zn(II) and Cu(II) ions from aqueous solutions using Albizia lebbeck pods.* **Applied Water Science,** 9, 2019: 1–11.

127. I. A. W. Tan, A. L. Ahmad, & B. H. Hameed. *Adsorption isotherms, kinetics, thermodynamics and desorption studies of 2,4,6-trichlorophenol on oil palm empty fruit bunch-based activated carbon.* **Journal of Hazardous Materials**, 164, 2009, 473–482.

128. Y. Gao, Y. Li, L. Zhang, H. Huang, J. Hu, S. M. Shah, & X. Su. *Adsorption and removal of tetracycline antibiotics from aqueous solution by graphene oxide.* **Journal of Colloid and Interface Science,** 368, 2012, 540–546.

129. T.Y. Suman, S.Y. Kim, D.H. Yeom, & J. Jeon. *Transformation products of emerging pollutants explored using non-target screening: perspective in the transformation pathway and toxicity mechanism—a review.* **Toxics, 10**, 2022, 54.

130. X. Zhang, J. Li, W. Y. Fan, M. C. Yao, L. Yuan, & G. P. Sheng. *Enhanced photodegradation of extracellular antibiotic resistance genes by dissolved organic matter photosensitization.* **Environmental Science and Technology,** 53, 2019, 10732–10740.

131. J. Yang, G. Lv, C. Zhang, Z. Wang, & X. Sun. *Indirect photodegradation of sulfamethoxazole and trimethoprim by hydroxyl radicals in aquatic environment: Mechanisms, transformation products and eco-toxicity evaluation.* **International Journal of Molecular Sciences,** 21, 2020, 1–14.

132. K. H. Wammer, A. R. Korte, R. A. Lundeen, J. E. Sundberg, K. McNeill, & W. A. Arnold. *Direct photochemistry of three fluoroquinolone antibacterials: Norfloxacin, ofloxacin, and enrofloxacin.* **Water Research,** 47, 2013, 439–448.

133. Y. Tian, J. Zou, L. Feng, L. Zhang, & Y. Liu. *Chlorella vulgaris enhance the photodegradation of chlortetracycline in aqueous solution via extracellular organic matters (EOMs): Role of triplet state EOMs.* **Water Research,** 149, 2019, 35–41.

134. S. Li & J. Hu. *Photolytic and photocatalytic degradation of tetracycline: Effect of humic acid on degradation kinetics and mechanisms.* **Journal of Hazardous Materials,** 318, 2016, 134–144.

135. L. Wei, H. Li, & J. Lu. *Algae-induced photodegradation of antibiotics: a review*. **Environmental Pollution,** 272, 2021, 115589.

136. F. Qu, H. Liang, J. He, J. Ma, Z. Wang, H. Yu, & G. Li. *Characterization of dissolved extracellular organic matter (dEOM) and bound extracellular organic matter (bEOM)*

of Microcystis aeruginosa and their impacts on UF membrane fouling. **Water Research, 46** 46, 2012, 2881–2890.

137. R. Tenorio, A. C. Fedders, T. J. Strathmann, & J. S. Guest. *Impact of growth phases on photochemically produced reactive species in the extracellular matrix of algal cultivation systems.* **Environmental Science: Water Research and Technology,** 3, 2017, 1095–1108.

138. Y. Li, J. Zhao, G. Zhang, L. Zhang, S. Ding, E. Shang, & X. Xia. *Visible-light-driven photocatalytic disinfection mechanism of Pb-BiFeO3/rGO photocatalyst.* **Water Research,** 161, 2019, 251–261.

139. Q. Zhao, J. Wang, Z. Li, Y. Guo, J. Wang, B. Tang, A. Abudula, & G. Guan. *Heterostructured graphitic-carbon-nitride-nanosheets/copper(I) oxide composite as an enhanced visible light photocatalyst for decomposition of tetracycline antibiotics.* **Separation and Purification Technology**, 250, 2020, 117238.

140. W. Kong, Y. Gao, Q. Yue, Q. Li, B. Gao, Y. Kong, X. Wang, P. Zhang, & Y. Wang. *Performance optimization of CdS precipitated graphene oxide/polyacrylic acid composite for efficient photodegradation of chlortetracycline.* **Journal of Hazardous Materials, 388** 388, 2020, 121780.

141. L. Wang, X. Huang, M. Han, L. Lyu, T. Li, Y. Gao, Q. Zeng, & C. Hu. *Efficient inhibition of photogenerated electron-hole recombination through persulfate activation and dual-pathway degradation of micropollutants over iron molybdate.* **Applied Catalysis B: Environmental,** 257, 2019, 117904.

142. M. Malakootian, A. Nasiri, A. Asadipour, & E. Kargar. *Facile and green synthesis of ZnFe2O4@CMC as a new magnetic nanophotocatalyst for ciprofloxacin degradation from aqueous media.* **Process Safety and Environmental Protection,** 129, 2019, 138–151.

143. N. Javid, Z. Honarmandrad, & M. Malakootian. *Ciprofloxacin removal from aqueous solutions by ozonation with calcium peroxide.* **Desalination and Water Treatment,** 174, 2020, 178–185.

144. A. Hom-Diaz, Z. N. Norvill, P. Blánquez, T. Vicent, & B. Guieysse. *Ciprofloxacin removal during secondary domestic wastewater treatment in high rate algal ponds.* **Chemosphere,** 180, 2017, 33–41.

145. M. Malakootian & M. Ahmadian. *Ciprofloxacin removal by electro-activated persulfate in aqueous solution using iron electrodes.* **Applied Water Science,** 9, 2019, 1–10.

146. A. L. Tasca, D. Clematis, E. Stefanelli, M. Panizza, & M. Puccini. *Ciprofloxacin removal: BDD anode coupled with solid polymer electrolyte and ultrasound irradiation.*

Journal of Water Process Engineering, 33, 2020, 101074.

147. T. Ahamad, M. Naushad, & S. M. Alshehri. *Analysis of degradation pathways and intermediates products for ciprofloxacin using a highly porous photocatalyst.* **Chemical Engineering Journal,** 417, 2021, 127969.

Chapter Three

Methodology

3.1 Chemical Reagents

In this research, chemicals, apparatus and instruments used are listed below;

Sodium hydroxide, powdered methylene blue, Distilled water, Aluminum chloride hydrated, Ferric chloride, Polyethylene glycol, Volumetric flask, Beakers, Measuring cylinder, Micropipettes, Electronic balance, Shaker, pH. Meter, Ultra violet spectrophotometer, Magnetic stirrer, SEM, XRD, FTIR spectroscopy, Hot plate, Oven, Muffle furnace and Desiccator

3.2 Adsorbent Preparation

The snail shell was purchased in a neighborhood market in Nigeria's Ibadan Oyo state. The snail shell was thoroughly cleaned with tap water to remove debris, and then it was washed with distilled water to further eliminate contaminants and undesired materials. The snail shell was then partially broken into fragments. Then, to get rid of all the moisture, the snail shell was dried in an oven for 12 hours at 100 ^{0}C. The dried, cleaned snail shell was finely ground into a powder and sieved. The adsorbent was then activated by calcining the powdered snail shell for two hours at 800 ^{o}C in a muffled furnace. After calcination, the adsorbent was kept in a desiccator to keep it out of the air to prepare the second adsorbent, Powdered 0.15g Ferric chloride and 0.15g Aluminum chloride hydrated were then slowly added to distill water to create the solution using the wet impregnation process .70 g of Snail shell powder was then added to the solution, which was then stirred with a magnetic stirrer at a speed of 500 rpm for 2 hours at 60 ^{o}C before being left for 24 hours to allow for evaporation. It was then further dried for 3 hours in an oven at 120 ^{0}C and then calcined at 800 ^{0}C for two hours to activate the doped adsorbent. The dry product was placed in a dessiccator to keep moisture out. The PEGylated adsorbent was prepared by gradually mixing the calcined 15% Fe_2O_3 and 15% Al_2O_3-CaO with polyethylene glycol, mixed

with a magnetic stirrer at 500 rpm for one hour, and then left for 24 hours to allow evaporation.. It was then further dried for another hour in an oven at 120 ^{0}Cand then calcined at 800 °C for two hours to activate the doped adsorbent. The dry product was placed in a dessiccator to keep moisture out.

3.3 Determination of pH. Zero Point Charge

The point of zero charge of the catalyst is very important for us to understand the adsorption mechanism. The point of zero charge shows us the net surface of the adsorbent in solution.[1]The pH point of zero charge attributes the pH in which the adsorbent surface has net electrical neutrality and gives us information on electrostatic interactions between adsorbent and adsorbate[1,2]. The pH at the point of zero charge of the adsorbent was measured using the solid addition method. According to this method, distilled water (20 mL each) was prepared in series of beakers; the pH of each beaker was adjusted from 2 to 12 using 0.1M of HCl and NaOH. And then 0.1g of the adsorbents was added into each beaker and immediately covered with foil paper. The suspension was shaken in an oven for 2 hours and then left at rest for 24 hours for pH stabilization. And then the final pH was measured.

3.4 Preparation of standard Stock Solution of Methylene blue.

3.4.1 Preparation of 1000ppm of Methylene blue stock Solution.

Standard stock solution was prepared by adding 100 mg of Methylene blue in a 100 mL volumetric flask, and then few mL of distilled water was added and shake well. Then volume was made up to 100 mL with distilled water to get the concentration of 1 mg/mL (1000 ppm) solution[3,4].

3.4.2 Preparation of Working Standard Solution

The standard working solution of Methylene blue was prepared by further diluting the prepared stock solution with distilled water. Working standard solution of 5, 10, 15, 20, and 25 ppm was prepared[5,6].

3.5 Preparation of Reagents

All chemicals used are of grade

3.5.1 Preparation of 0.1 M NaOH and 0.1 M HCl

0.4 g of NaOH was weighed and transferred into 100 mL volumetric flask and dissolved with distilled water and diluted up to the standard mark. 0.69 mL concentrated HCl acid was taken and transferred into 250 mL volumetric flask and diluted with distilled water up to the standard mark. The concentration of the above prepared solution was 0.1 M.

3.5.2 Buffer Solution

Buffer solution of pH 4.0 and 7.0 were prepared by dissolving buffer tablet of pH 4.0 and 7.0 in 100 mL volumetric flasks with tripled distilled water and used for the calibration of pH meter.

3.6 Preparation of Calibration Curve

Firstly, the maximum absorbance was obtained by finding the λmax for the preparation of calibration curve. It was done by preparing 25 mg/L solution of methylene blue. The absorbance was measured against wavelength ranging from 600 to 700 nm using UV spectrophotometer at Lead City University Chemistry Laboratory. The maximum absorbance was obtained at 668 nm. After that, the absorbance of all the working solution of methylene blue was taken at 668 nm

wavelength. Then a plot of absorbance versus concentration gave us a calibration curve for methylene blue solution.

3.7 Adsorption Studies of Methylene blue

3.7.1 Effect of pH

For the pH of methylene blue adsorption, the initial concentration and volume of solution were taken 25 mg/L and 10 mL respectively. The solutions were taken in a 100 mL beaker and the pH of the solution were adjusted to 3, 5, 7, 9, and 11 using 0.1 M HCl and 0.1 M NaOH solutions as per requirement with the help of pH meter. In each beaker 10 mg of each adsorbents was added and then shaken in a mechanical shaker for 2 hours at speed 200 rpm at 25 ^{0}C. After shaking, each suspension was filtered immediately using filter paper. The concentration of the filtrate is determined with the help of an ultra violet spectrophotometer.

3.7.2 Adsorption Isotherm Studies

For the study of isotherm of the three adsorbent, the effect of the concentration on the adsorption was studied under optimum pH. The adsorption isotherm was carried out with different initial concentrations ranging from 25, 50, 100, 200, 250, and 300 ppm, with 10mg adsorbent. The suspension was shaken in a mechanical shaker for 2 hours, at speed 200 rpm. After shaking each suspension was filtered immediately using filter paper. The equilibrium concentrations of the snail shell after adsorption were analyzed using the ultra violet spectrophotometer. Four models: Langmuir-Freudlich, Sips, Temkinand Elovich were widely used to fit the data obtained[7].

3.7.3 Kinetics Studies

For the kinetic studies of the adsorbents, the adsorption kinetics experiments were performed at corresponding optimum pH for snail shell. For the study of kinetic behavior, different initial

concentrations ranging from 25, 50, 100, 200, 250, and 300 ppm, with 10 mg adsorbent were prepared in different beakers. The suspension was shaken in a mechanical shaker for different length of time ranging from 1, 5, 10, 20, 30, 40 minutes, 60, and 120 minutes at speed 200 rpm. After shaking each suspension was filtered immediately using filter paper. The concentration of the filtrate is determined with the help of UV-Visible spectrophotometer. The kinetics was investigated by testing the data obtained with pseudo-first order, pseudo-second order, BS Fractal and Lagergren kinetics models[8].

3.7.4 Adsorbent Dosage

The variation of adsorbent dosage experiment was carried out to study the adsorption efficiency of the adsorbents, different dosage ranges, from 10, 20, 50, & 100 mg, were added in a 25 ppm concentration of methylene blue, The suspension was shaken in a mechanical shaker for 1 hour, After shaking each suspension was filtered immediately using filter paper. The concentration of the filtrate is determined with the help of ultra violet spectrophotometer.

3.8 Characterization of Adsorbent Material

The structure and morphology of the calcined Snail Shell, doped metals nanocatalysts, and PEGylated nanocatalyst were assessed using FTIR, XRD and SEM

3.8.1 Fourier Transform Infrared (FTIR) Analysis

The sample structures were characterized by FTIR spectroscopy (Thermo Nicolet 6700 FT-IR spectrophotometer, United States)[9].

3.8.2 X-Ray Diffraction (XRD) Analysis

Using a Cu Ka radiation source (= 1.542) and a nickel filter in the 2 range of 3°-80°, the XRD patterns of all the precursor and calcined samples were captured on a Riganu Ultima IV, Kuraray Co. ltd. Japan (40 kV, 30 mA) X-ray diffractometer[9].

3.8.3 EDX and SEM Analysis

Using a JSM-6619LV, Scanning Electron Microscope, JEOL, United States device operating at 15 kV, EDX and SEM investigations were carried out to examine the morphology, size, and elemental makeup of the produced catalyst samples. The range of magnification was 5000–70,000. Carbon glue was used to evenly distribute the catalyst powder on an aluminum sample holder prior to examination. To prevent the induction of electric current, the sample was subsequently coated with gold using a sputter coater[9].

Endnotes

1. X. Wei, Y. Wang, Y. Feng, X. Xie, X. Li, & S. Yang. *Different adsorption-degradation behavior of methylene blue and Congo red in nanoceria/H_2O_2 system under alkaline conditions.* **Scientific reports,** 9(1), 2019, 1-10.

2. M. S. Tizo, L. A. V. Blanco, A. C. Cagas, B. R. Dela, B. Cruz, J. C. Encoy, J. V. Gunting, R. O. Arazo, & V. I. F. Mabayo. *Efficiency of calcium carbonate from eggshells as an adsorbent for cadmium removal in aqueous solution.* **Sustain. Environ. Res.** 28, 2018, 326–332.

3. Z. Helwani, M. Ramli, E. Saputra, B. Bahruddin, D. Yolanda, W. Fatra, G. M. Idroes, M. Muslem, T. M. I. Mahlia, & R. Idroes. *Impregnation of CaO from eggshell waste with magnetite as a solid catalyst (Fe_3O_4/CaO) for transesterification of palm oil off-grade.* **Catalysts,** 10, 2020, 164.

4. F. Mashkoor, & A. Nasar. *Magsorbents: Potential candidates in wastewater treatment technology–A review on the removal of methylene blue dye.* **Journal of magnetism and magnetic materials,** 500, 2020, 166408.

5. Z.P. Hu, Z.M. Gao, X. Liu, & Z.Y. Yuan. *High-surface-area activated red mud for efficient removal of methylene blue from wastewater.* **Adsorption Science & Technology,** 36(1-2), 2018, 62-79.

6. L. Sheng, Y. Zhang, F. Tang, & S. Liu. *Mesoporous/microporous silica materials: preparation from natural sands and highly efficient fixed-bed adsorption of methylene blue in wastewater.* **Microporous and Mesoporous Materials**, 257, 2018, 9-18.

7. A. Pohl. *Removal of heavy metal ions from water and wastewaters by sulfur-containing precipitation agents.* **Water, Air, and Soil Pollution**, 2020, 231.

8. S. Ida, & T. Eva. *Removal of heavy metals during primary treatment of municipal wastewater and possibilities of enhanced removal: A review.* **Water (Switzerland),** 2021, 13.

9. W. Polińska, U. Kotowska, D. Kiejza, & J. Karpińska. *Insights into the use of phytoremediation processes for the removal of organic micropollutants from water and wastewater; a review.* **Water (Switzerland),** 2021, 13.

Chapter Four

Results and Discussion of Findings

4.1 Synthesis and Physical Examination of Snail Shell-Based Catalyst

From **Figure 4.1**, the physical appearance shows dark brown colour after impregnating $FeCl_3.H_2O$ into the snail shell. After calcination at 800 °C, the appearance turns to light dark brown as presented in **Figure 4.4** (I). **Figure 4.2** shows the synthesis of snail shell doped with Al_2O_3 by wet impregnation. A whitish colour appears after synthesizing and calcination.

Figure 4.1: Preparation of snail shell doped with ferric chloride by wet impregnation

Source: Field work, 2022.

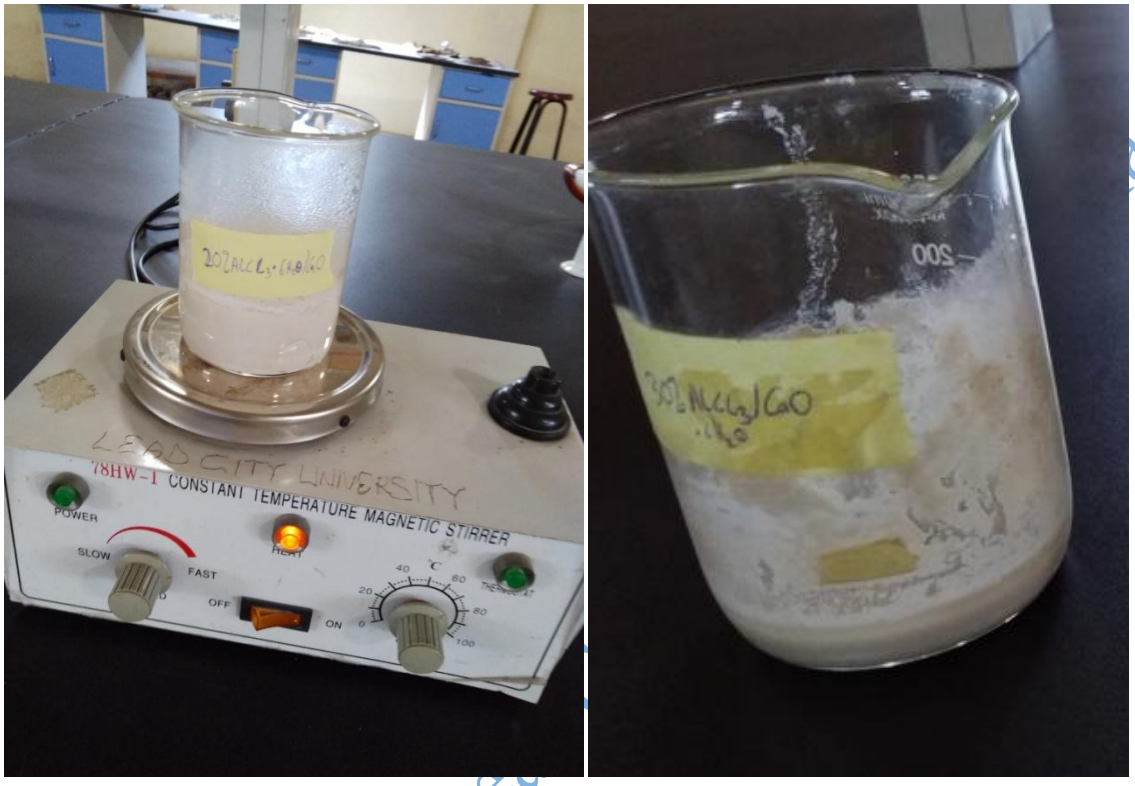

Figure 4.2: Preparation of snail shell doped with Aluminum chloride hydrated by wet impregnation.

Source: Field work, 2022.

Figure 4.3: Nanocatalyst samples: (A) snail shell (B) snail shell powder (C) calcined snail shell (D) snail shell doped with Al_2O_3 and Fe_2O_3 (E) snail shell doped with Al_2O_3

Source: Field work, 2022.

Figure 4.4: Different nanocatalysts after calcination at 800 °C; (A, D and E are bimetallic PEGylated nanocatalysts), (B and J are calcinedSS-Al_2O_3), (C and H are calcined SS), (F and G are SS-15% Al_2O_3-15% Fe_2O_3) and (I is SS-Fe_2O_3).

Source: Field work, 2022.

4.2 Surface Chemistry of Nanocatalysts

4.2.1 FTIR Analysis

Table 4.1: The FTIR absorption value of the catalysts and their assignments

Wave number (cm^{-1})	Calcined CaO	15% Al_2O_3/ 15%Fe_2O_3/CaO	PEGylated	Functional group
3630-3600	3639	3644	3648	O-H (stretch)
3500-3100	-	3415	-	N-H (stretch)
3000-2850	2978	2976 & 2893	2977 & 2892	C-H (stretch)
2250-2100	-	-	-	C=C
1810-1775	1793	-	1793	C=O (stretch)
1680-1600	-	1629	-	C=C
1300-1000	1249, 1161 & 1072	1251, 1073 & 1153	1251& 1074	C-O
900-690	868& 707	828	871 & 702	C-H (out of plane bend)

Source: Field work, 2022.

Table 4.2: Calcined SS and 15%Al_2O_3/15%Fe_2O_3/CaO

Wave number range (cm^{-1})	Calcined SS	15%Al_2O_3/ 15%Fe_2O_3/CaO	Differences	Functional group
3650-3600	3639.20	3644.35	-5.15	O-H (stretch)
3500-3100	-	3415.06	-	N-H (stretch)
3000-2850	2978.70	2976.13	2.57	C-H (stretch)
1810-1775	1793.83	-	-	C=O (stretch)
1680-1600	-	1629.95	-	C=C
1300-1000	1249.71, 1161.58 & 1072.58	1251.35, 1153.70 & 1073.31	-1.64, 7.88 & -0.73	C-O
900-690	868.90 & 707.02	828.14	38.76	C-H (out of plane bend)

Source: Field work, 2022.

Table 4.3: Calcined SS and PEGylated bimetallic nanocatalyst

Wave number range (cm^{-1})	Calcined CaO	PEGylated	Differences	Functional group
3650-3600	3639.20	3648.43	-9.23	O-H (stretch)
3000-2850	2978.70	2977.04	1.66	C-H (stretch)
1810-1775	1793.83	1793.07	0.76	C=O (stretch)
1300-1000	1249.71, 1161.58 & 1072.58	1251.94, 1074.55 & 1074.55	-2.23, 87.03 & -1.97	C-O
900-690	868.90 & 707.02	871.52 & 702.25	-2.62 & 4.77	C-H (out of plane bend)

Source: Field work, 2022.

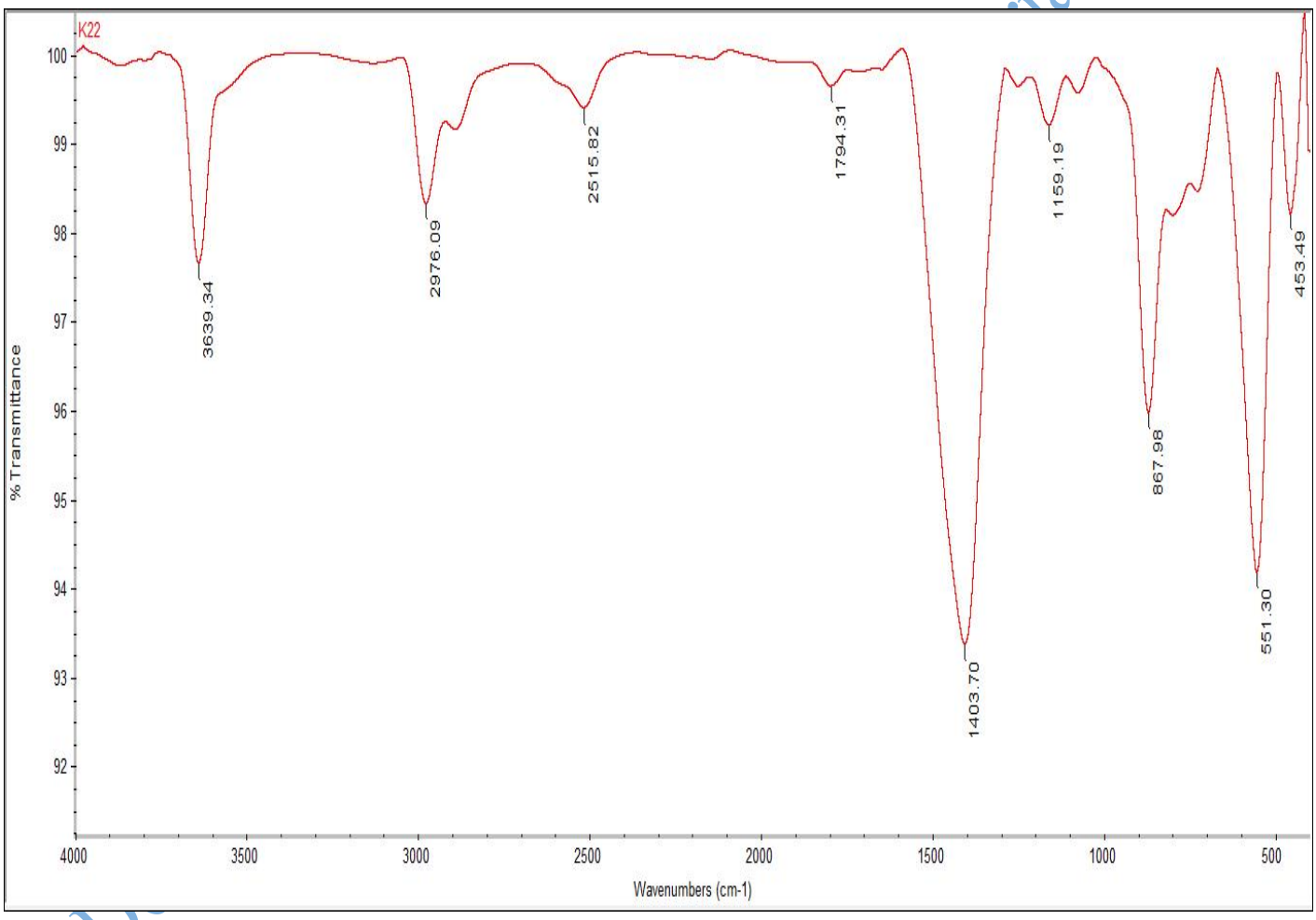

Figure 4.5: FT-IR spectrum of calcined snail shell

Source: Field work, 2022.

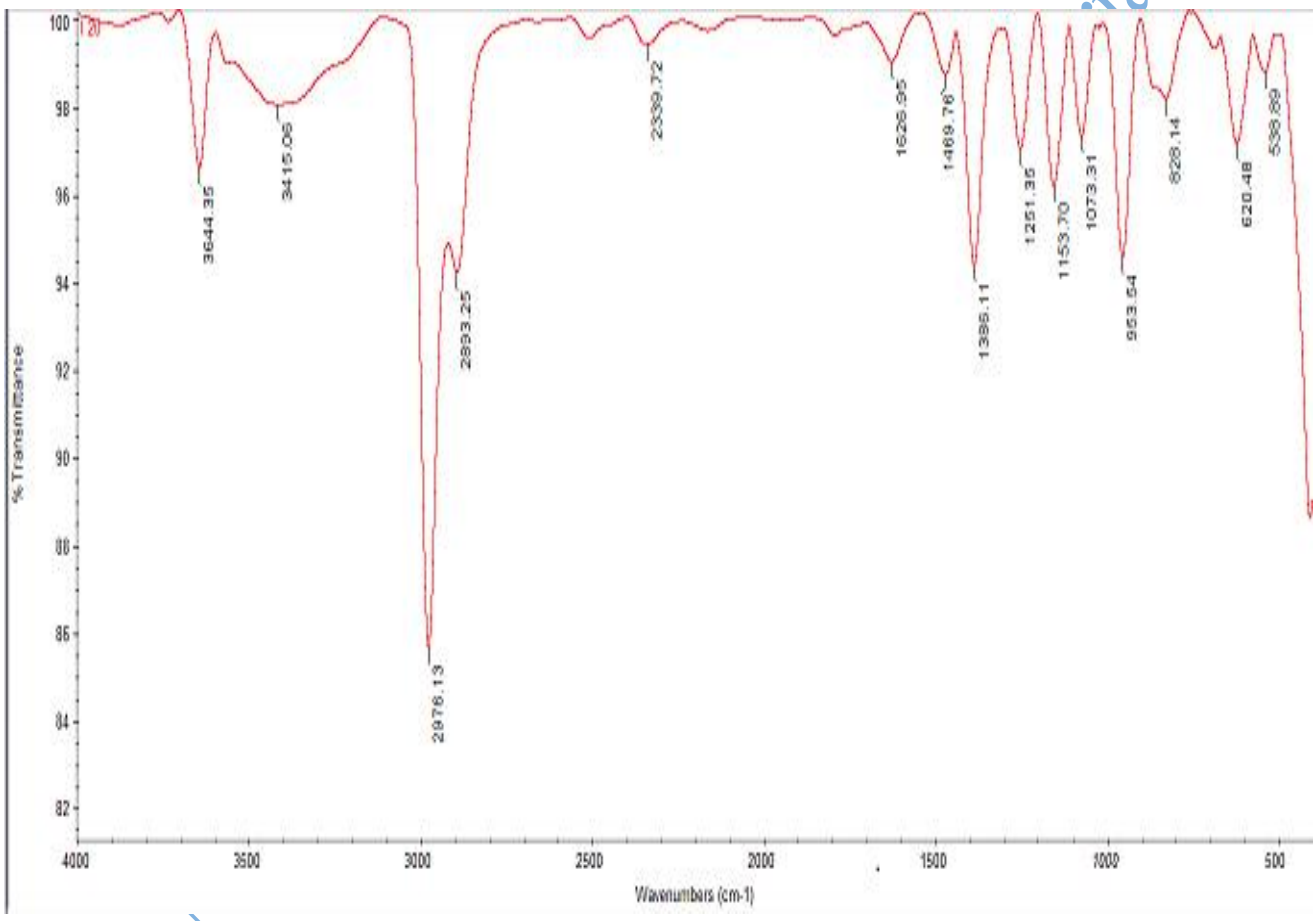

Figure 4.6: FT-IR spectrum of 15%Al_2O_3/15%Fe_2O_3/CaO

Source: Field work, 2022.

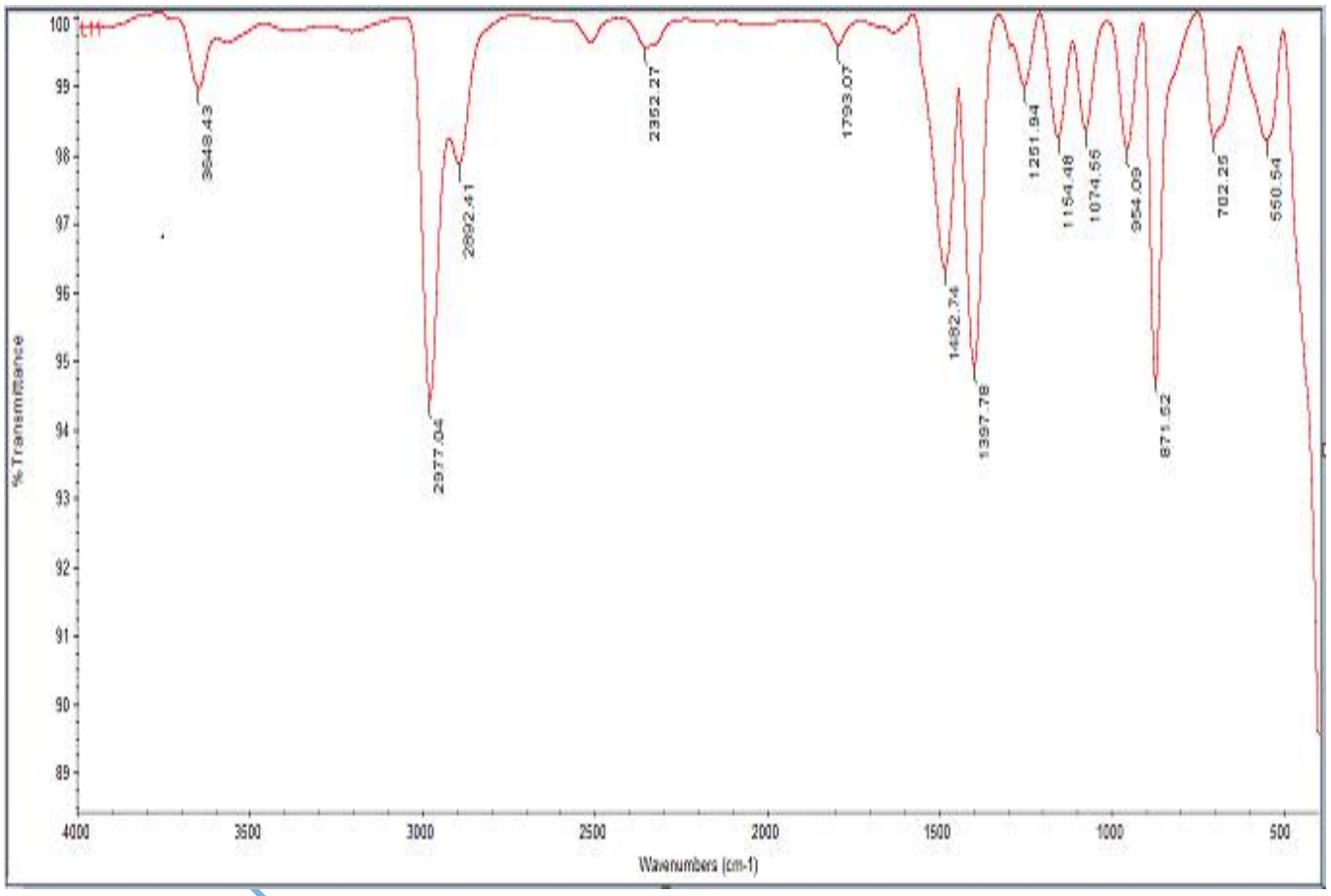

Figure 4.7: ATR-FTIR spectra of PEGylated nanocatalysts.

Source: Field work, 2022.

FTIR spectroscopy was used to determine the functional groups in the surface of the catalysts. The wave number values and the characteristic of absorption of all the catalysts are presented in Table 4.1-4.3 while Figures 4.5-4.7 shows the FTIR spectra of CaO, 15%Fe_2O_3/15Al_2O_3/CaO and PEGylated nanocatalysts accordingly. CaO is hygroscopic in nature. After calcining SS, the emergence of $Ca(OH)_2$ spectrum is therefore confirmed and supports the conversion of $CaCO_3$ to CaO. Sharp peaks were observed in the absorption range value of 3600 – 3620 cm^{-1} which is a characteristic absorption of O-H. These could be observed in the catalyst analyzed as presented in Table 4.1

Characteristic absorption range value of 3000 – 2850 cm^{-1} is attributed of alkyl C-H stretch due to organic matter of the of the catalyst. While the characteristic Fe-O vibration bond absorption bands were seen at approximately 537, 538, and 550 cm^{-1} from 15%Fe_2O_3/15Al_2O_3/CaO, and PEGylated bimetallic nanocatalyst, respectively[1,2]. The appearance and disappearance of wave numbers of the catalysts when compared with the calcined snail shell as well as absorption band as recorded in Table 4.2 and 4.3 suggest surface modification[3].

Furthermore, the doping of CaO with Al_2O_3-Fe_2O_3 to yield Al_2O_3/Fe_2O_3/CaO catalyst complex are recorded in Figure 4.6 while the comparative study of SS with Al_2O_3/Fe_2O_3/CaO complex modified with PEG 400 resulting to the formation of PEGylated Al_2O_3/Fe_2O_3/CaO catalyst complex presented in Figure 4.7 is in accordance with the other prepared studies in which surface restructuring of the SS was noted due to the reaction with the oxides of Fe and Al at constant ration of 15% respectively. Studies have shown that the introduction of PEG known as PEGylation is to improve the surface of the catalyst through size reduction of the PEGylated material[4,5]. This phenomenon was observed in and thus was confirmed in the shift in the

absorption band and disappearance of certain peaks when SS is compared to $Al_2O_3/Fe_2O_3/CaO$ and PEG $Al_2O_3/Fe_2O_3/CaO$ respectively as shown in Figures 4.7.

4.2.2 Crystallinity Study of the Catalysts

The crystalline nature of the catalysts was examined using XRD. Figures 4.8 - 4.10 depicts the XRD patterns of the calcined SS, $15\%Al_2O_3/15\%Fe_2O_3/CaO$ and PEGylated nanocatalysts. The primary components of quicklime, $Ca(OH)_2$ and $CaCO_3$, were entirely converted to CaO (JCPDS #371497) after being calcined at 800 °C for 2 hours[6,7]. The sharpness of the peaks and intensity are the parameters that are used to determine the crystallinity or amophoric nature of any material. The reported data suggested that the ideal temperature to convert $CaCO_3$ and $Ca(OH)_2$ from snail shells, quicklime, and egg shells to CaO is 800 °C[4]. However, the calcined SS (CaO) mainly consist of CaO as shown by several peaks at 2Θ about 17.83°, 22.19°, 29.26°, 35.82°, 37.20°, and 39.27° indexed as 111, 210, 220, 222, 320, and 321 planes respectively, which was in good agreement with previous studies[3]. From Figure 4.9, $15\%Al_2O_3/15\%Fe_2O_3/CaO$, the diffraction peaks identified at 2Θ = 13.13°, 18.28°, 29.67°, and 33.33° correspond to the (200), (220), (332), and (333). A shift in the 2θ values of SS when compared with $15\%Al_2O_3/15\%Fe_2O_3/CaO$ is as a result of modification of SS with Al_2O_3 and Fe_2O_3, suggesting an effective impregnation with improved crystallinity as shown by Figure 4.9. The XRD results are in good agreement with a related prior report on calcium oxide powder made from eggshell that was synthesized[5]. The recorded XRD data for PEGylated nanocatalyst with 2θ values of 12.66°, 17.70°, 22.82°, and 29.17° corresponds to the 211, 222, 420 and 440 planes, respectively. A shift in the 2θ values of SS when compared with PEGylated nanocatalyst is as a result of modification of SS with Al_2O_3, Fe_2O_3 and PEG. As depicted in Figure 4.10, this suggests an effective impregnation with improved crystallinity[8,9].

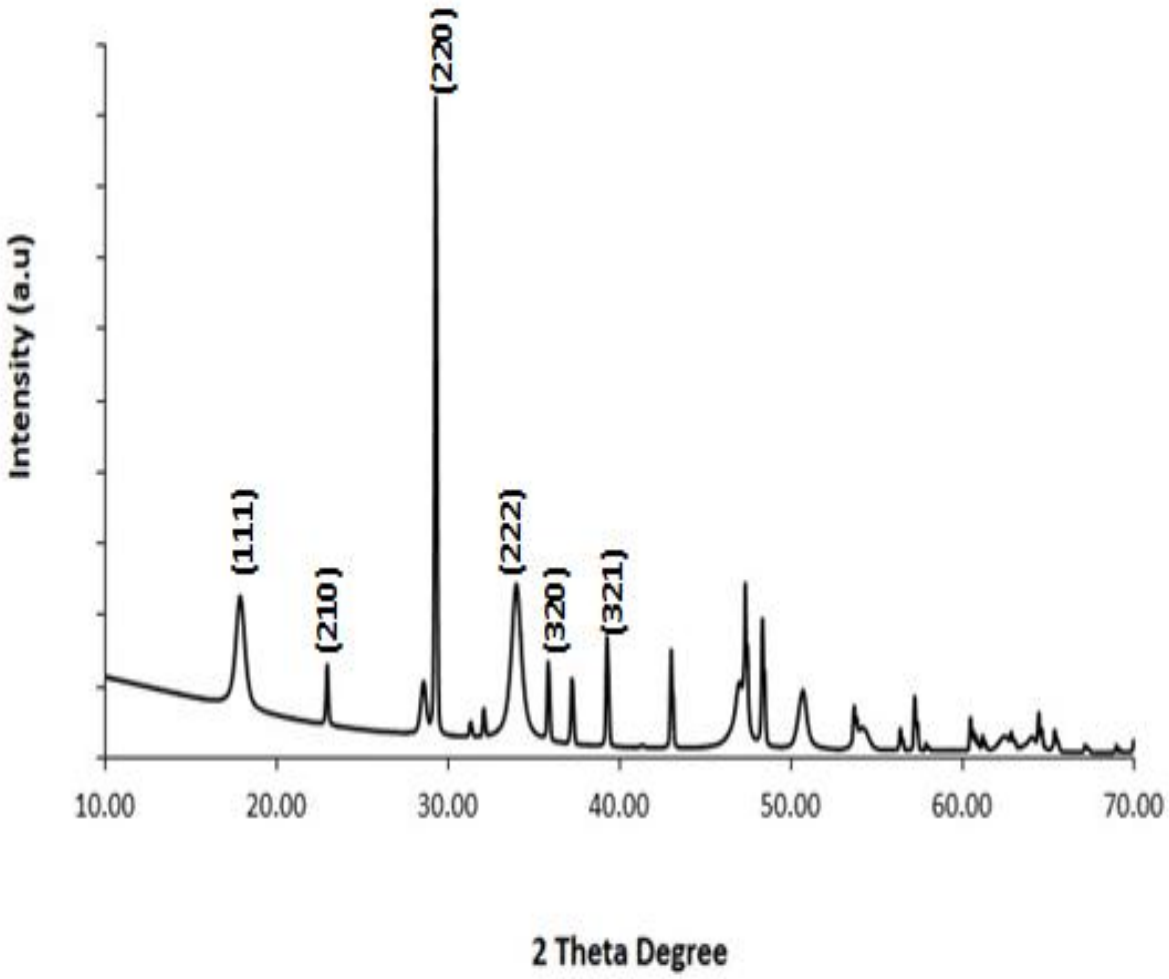

Figure 4.8: Crystallogram of calcined snail shell nanocatalyst.

Source: Field work, 2022.

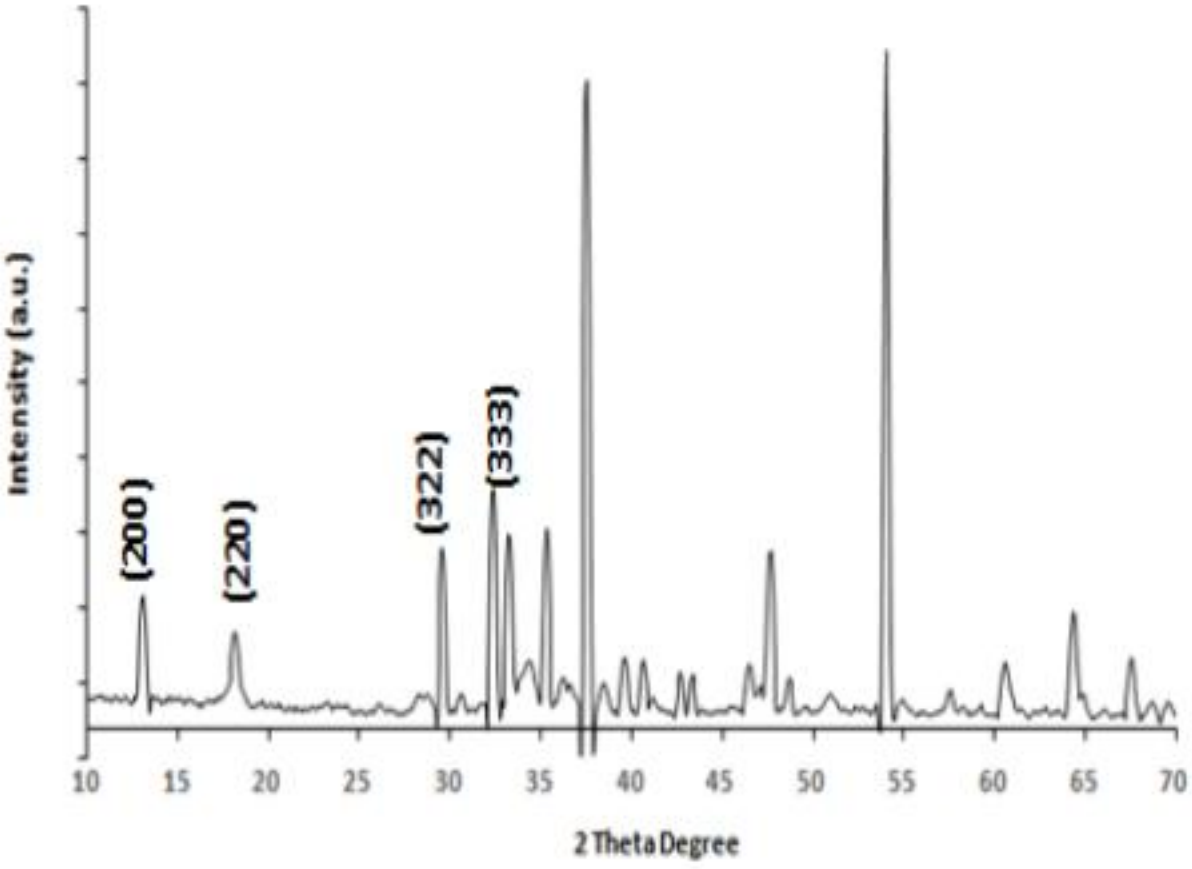

Figure 4.9: Crystallogram of 15%Al_2O_3/15% Fe_2O_3/CaO nanocatalyst.

Source: Field work, 2022.

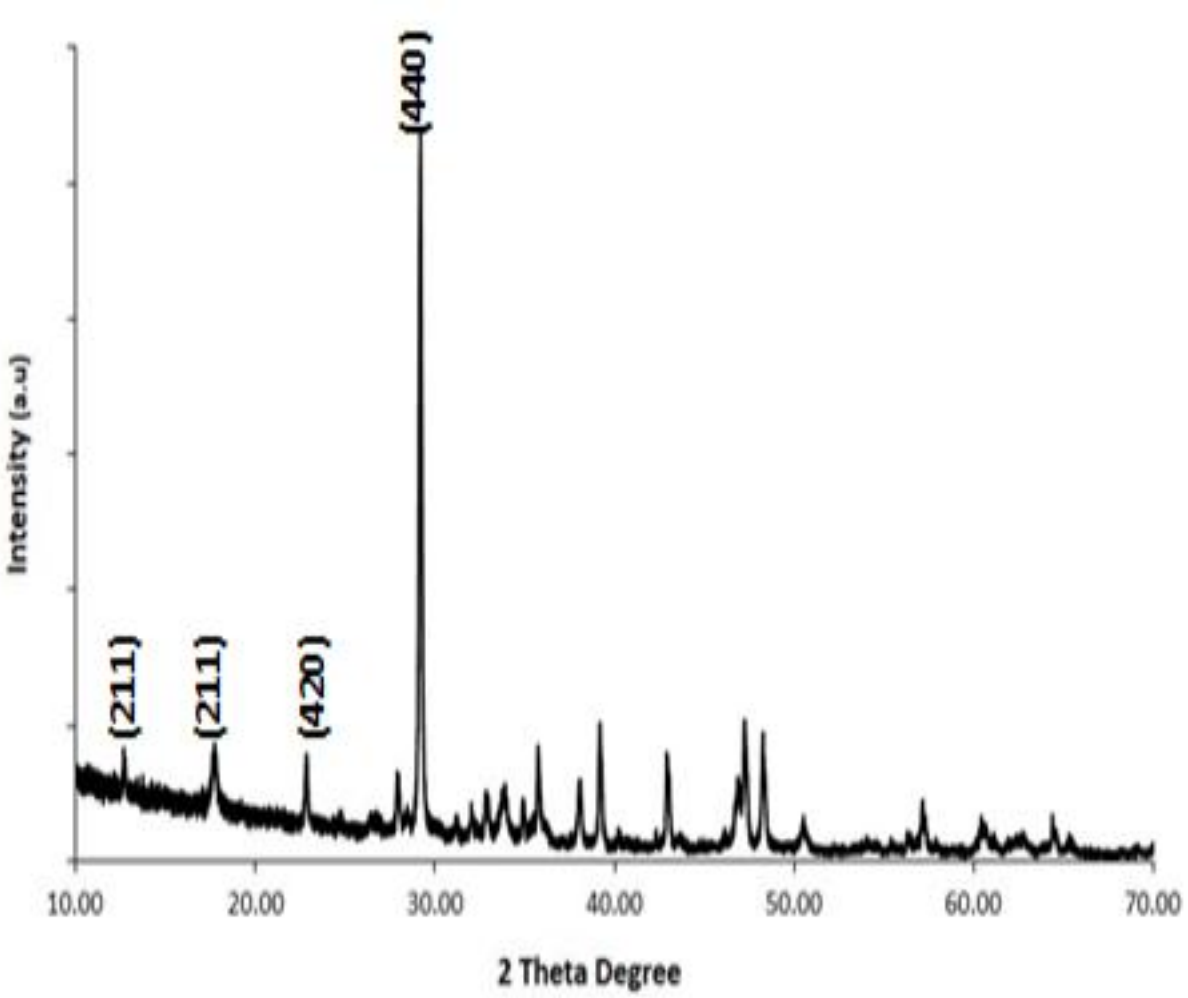

Figure 4.10: Crystallogram of PEGylated nanocatalyst.

Source: Field work, 2022.

4.2.3 Morphological Characterization and Mapping of Nanocatalysts

The morphology of the catalysts which include SS (CaO), 15%Al_2O_3-15%Fe_2O_3-CaO and PEGylated 15%Al_2O_3-15%Fe_2O_3-CaO were determined using SEM. While EDX examined the existence of the metal(s) utilized as a dopant and its percentage composition (mapping) in each of the components[10,11]. The SEM micrograph of SS is shown in Figure 4.11a and b thus revealing a well-organized crystalline aggregate. The crystallite surface might offer the catalyst's accessible active sites, while the EDX shows the percentage composition of the metals that make up the catalyst[12,13]. This therefore confirms the formation of Ca-O which is the major composition with higher calcium concentration than oxygen expected for calcined snail shell shown Figure 4.12.

Research has shown that PEGylation enhances the surface characteristics of particles which necessitated the modification of the bimetallic oxides of SS comprising ratio 1:1 of Al_2O_3 and Fe_2O_3 with PEG 400. The micrograph presented in Figure 4.13a and b shows aggregates particles comprising of rod-like and spherical particles compared with the cubic crystal structure of calcium oxide. Decreased Al and Fe concentrations compared to CaO was observed. High PEG particle dispersion may be the cause of the irregular size distribution of sphere and rod-like formations. Figure 4.14 shows that PEGylated nanocatalyst has a higher Ca content than oxygen, aluminum, and iron[14,15].

The morphological restructuring observed in the doped catalyst when compared with the CaO (SS) is attributed to the presence of the dopants which in alignment with the disappearance, appearance and shift in the absorption bands of the catalyst recorded in the FTIR vis-à-vis XRD crystallographic studies of the catalyst. The results of this study suggests the confirmation of the

morphological restructuring and transformation of the catalyst due to modification of SS with the dopants. The finding is in agreement with earlier reported studies[16,17].

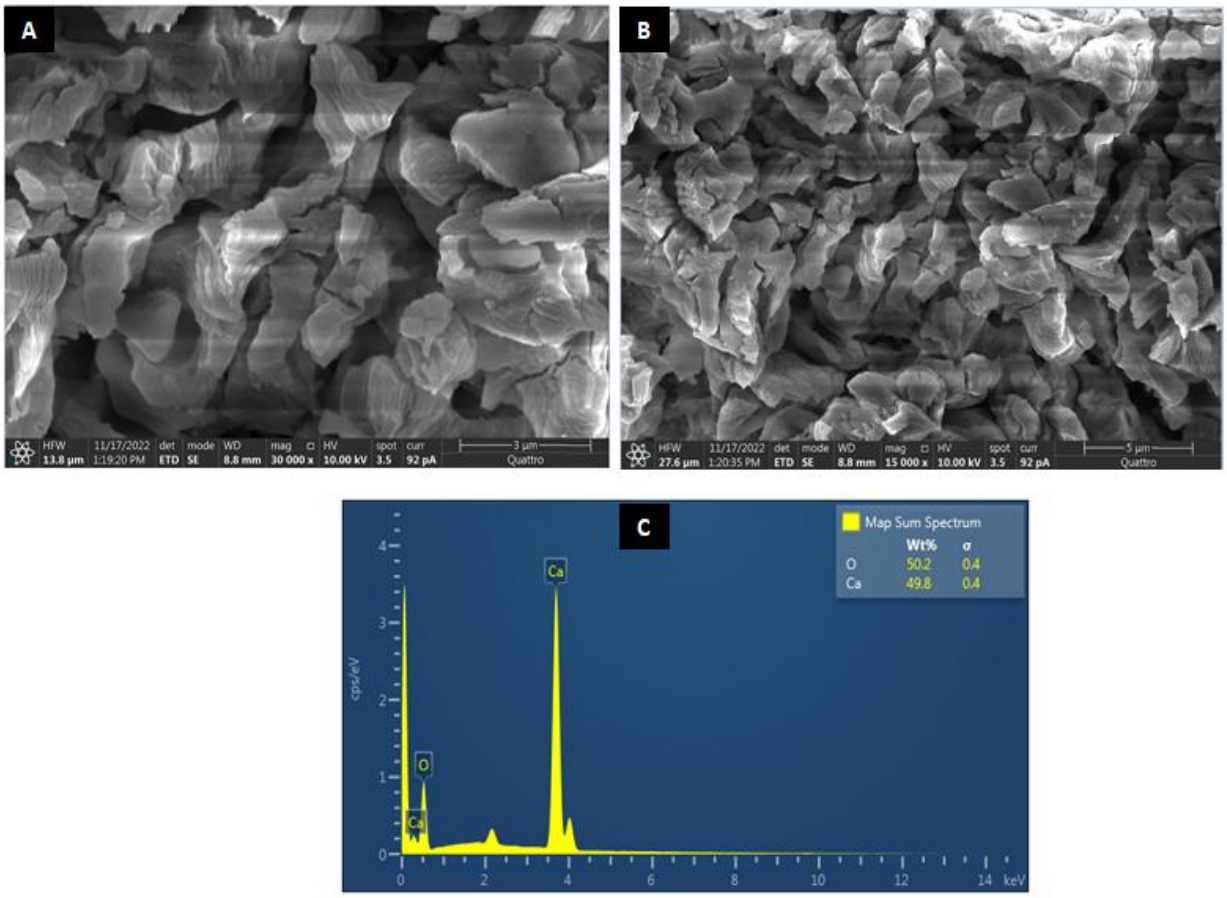

Figure 4.11: SEM micrographs of CaO at (a) 30,000x (b) 15,000x and (c) EDX chart the elemental composition of catalyst.

Source: Field work, 2022.

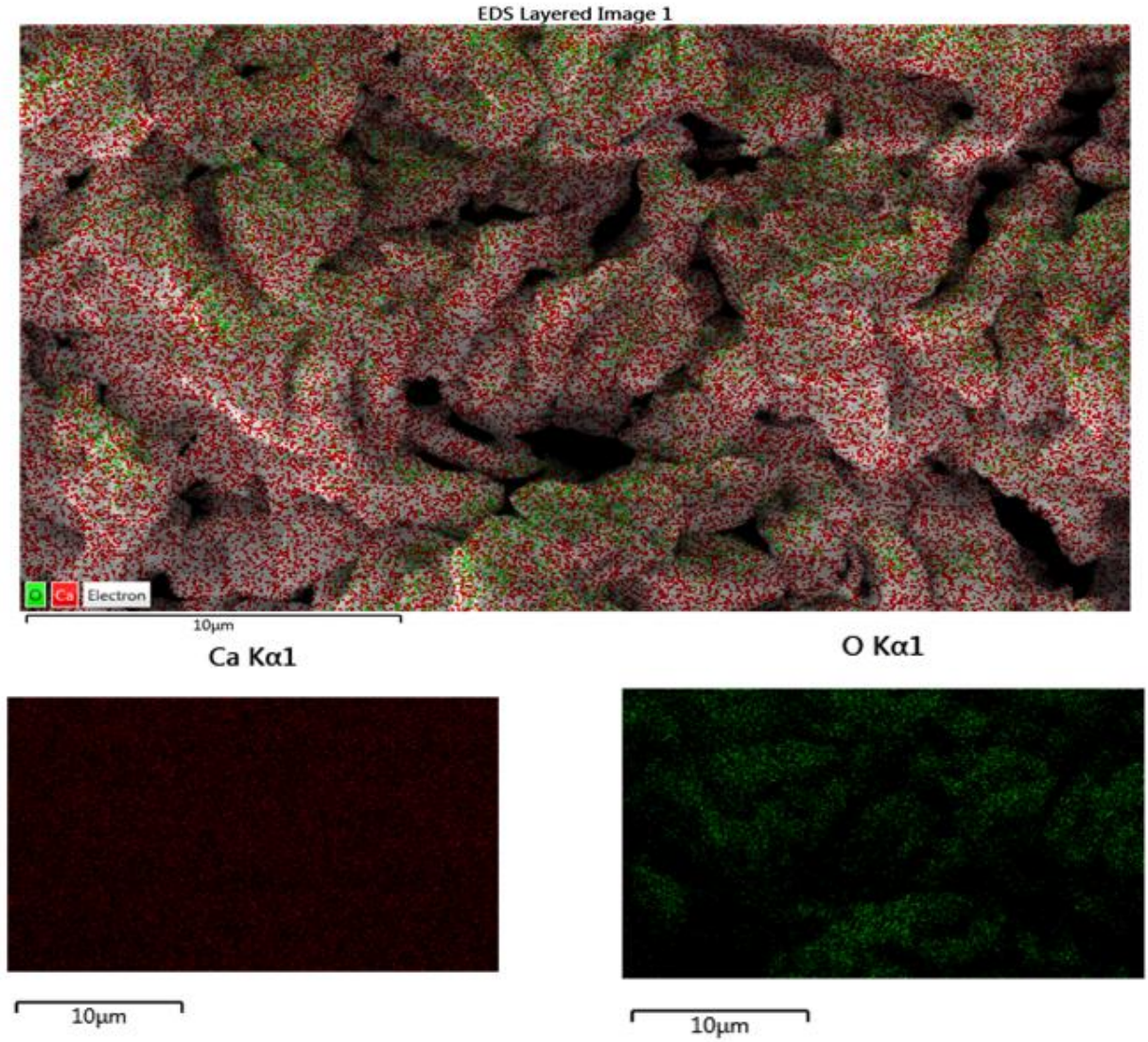

Figure 4.12: Chemical mapping of CaO nanocatalysts.

Source: Field work, 2022.

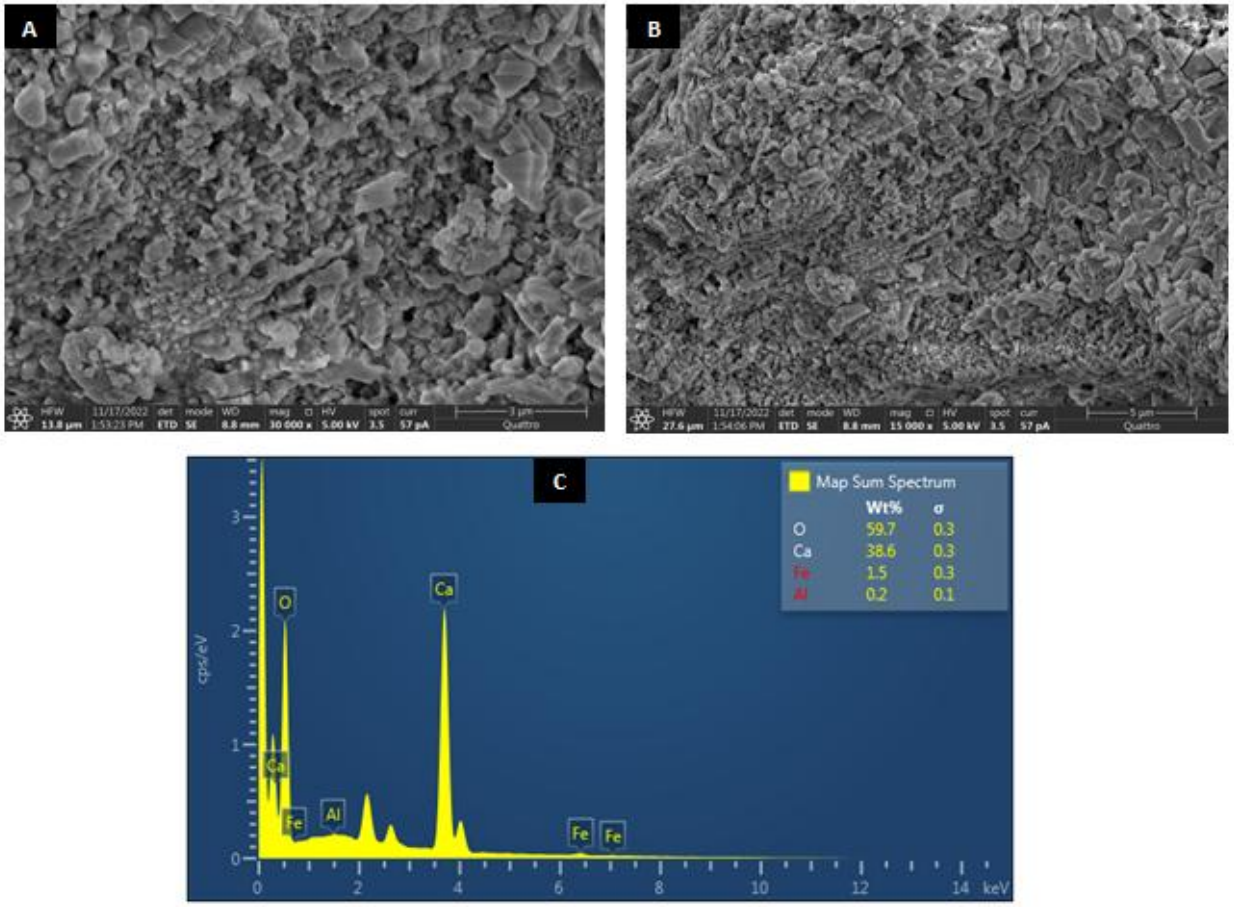

Figure 4.13: SEM micrographs of PEGylated nanocatalyst at (a) 30,000x (b) 15,000x and (c) EDX chart the elemental composition of catalyst.

Source: Field work, 2022.

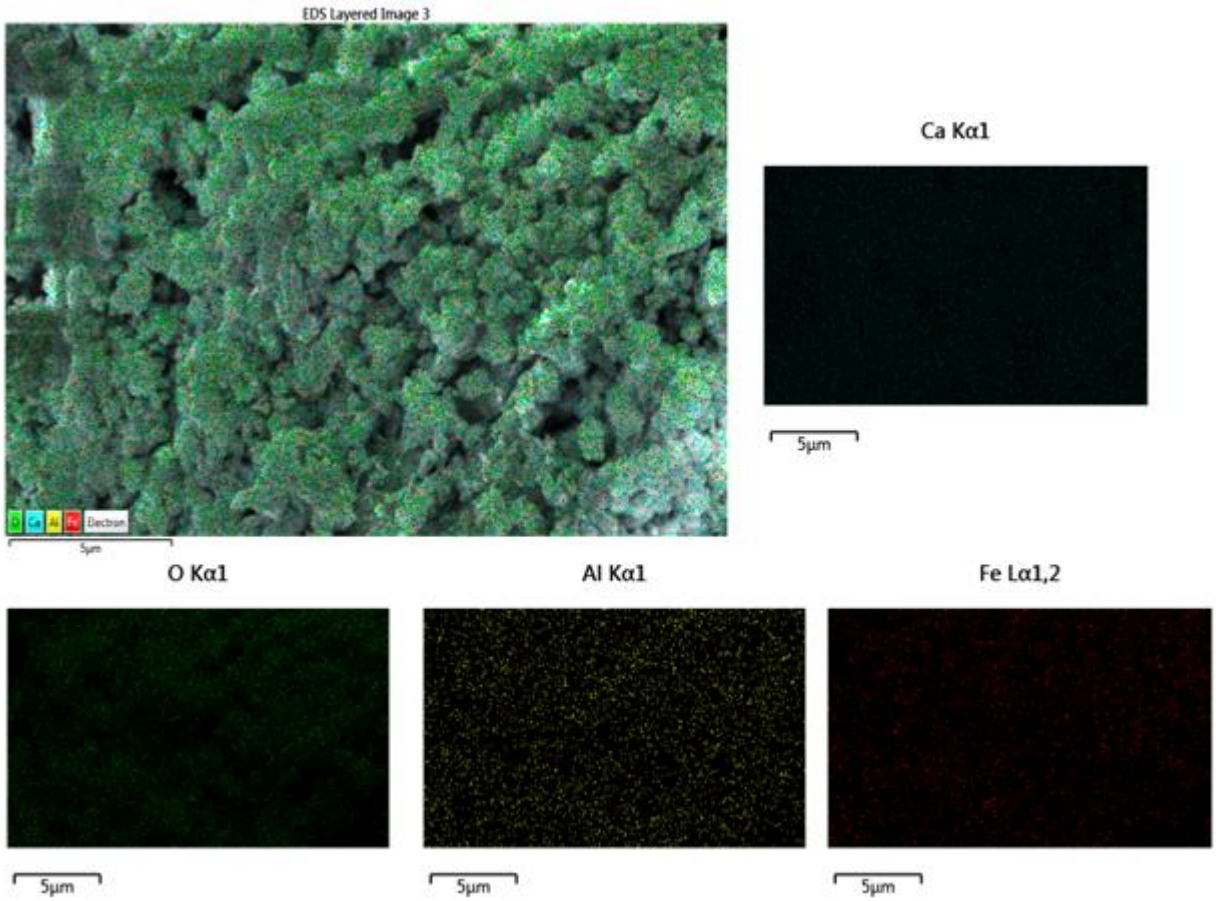

Figure 4.14: Chemical mapping of PEGylated nanocatalyst.

Source: Field work, 2022.

4.3 pH. Zero Point Charge (pH_{ZPC}) of Adsorbents

Zero point charge determination of the adsorbent is very important in determining the adsorption mechanism. In this study, pHzpc of the snail shell according to section 3.4 was found to be about 11.5 for CaO, 13.4 for snail shell doped in aluminum and iron oxides, and 9.2 for PEGylated snail shell. The graph is obtained by plotting change in pH versus initial pH and shown in Figure 4.15a, b and c below.

The pH at ZPC, the surface charge of adsorbents is expected to be neutral and the electrostatic force between methylene blue and surface of adsorbents were balanced which can be disturbed when pH is deviated from Zero Point Charge[18,19]. At pH less than Zero Point Charge, the adsorbent surface is positively charge which results in an electrostatic attraction with anions and causes high anions adsorption. Similarly, at pH greater than Zero Point Charge, the surface charge of the adsorbent becomes negatively charge and anions in solution are expected to be repulsed to its surface. It can be concluded that maximum adsorption is likely to occur at pH values less than Zero Point Charge when adsorbents have a net positive charge. Therefore, anion adsorption will be more favorable at pH value lower than pH_{ZPC} if electrostatic force of attraction is suggested to be main mechanism of adsorption[20,21,22].

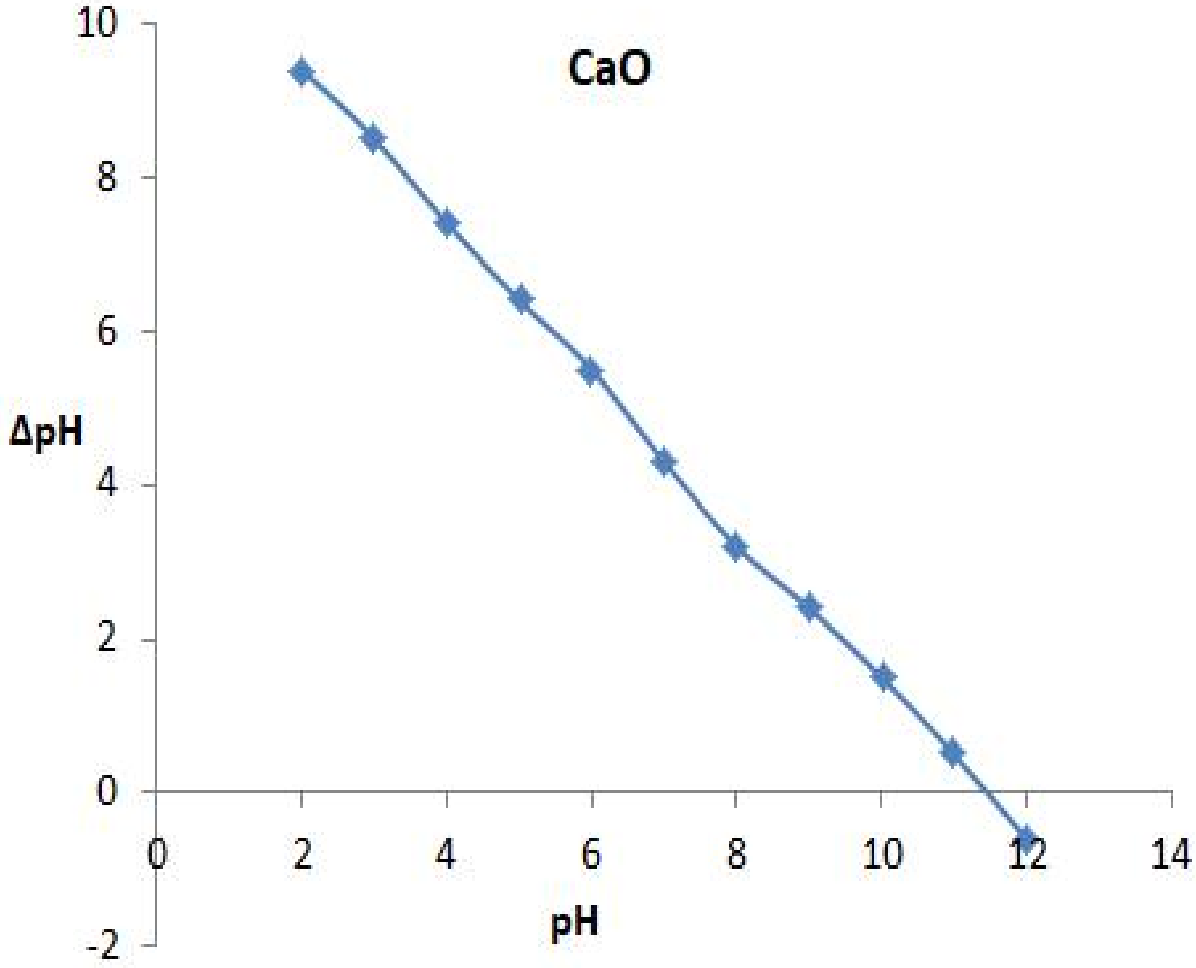

Figure 4.15a: pH_{ZPC} plot of calcined snail shell

Source: Field work, 2022.

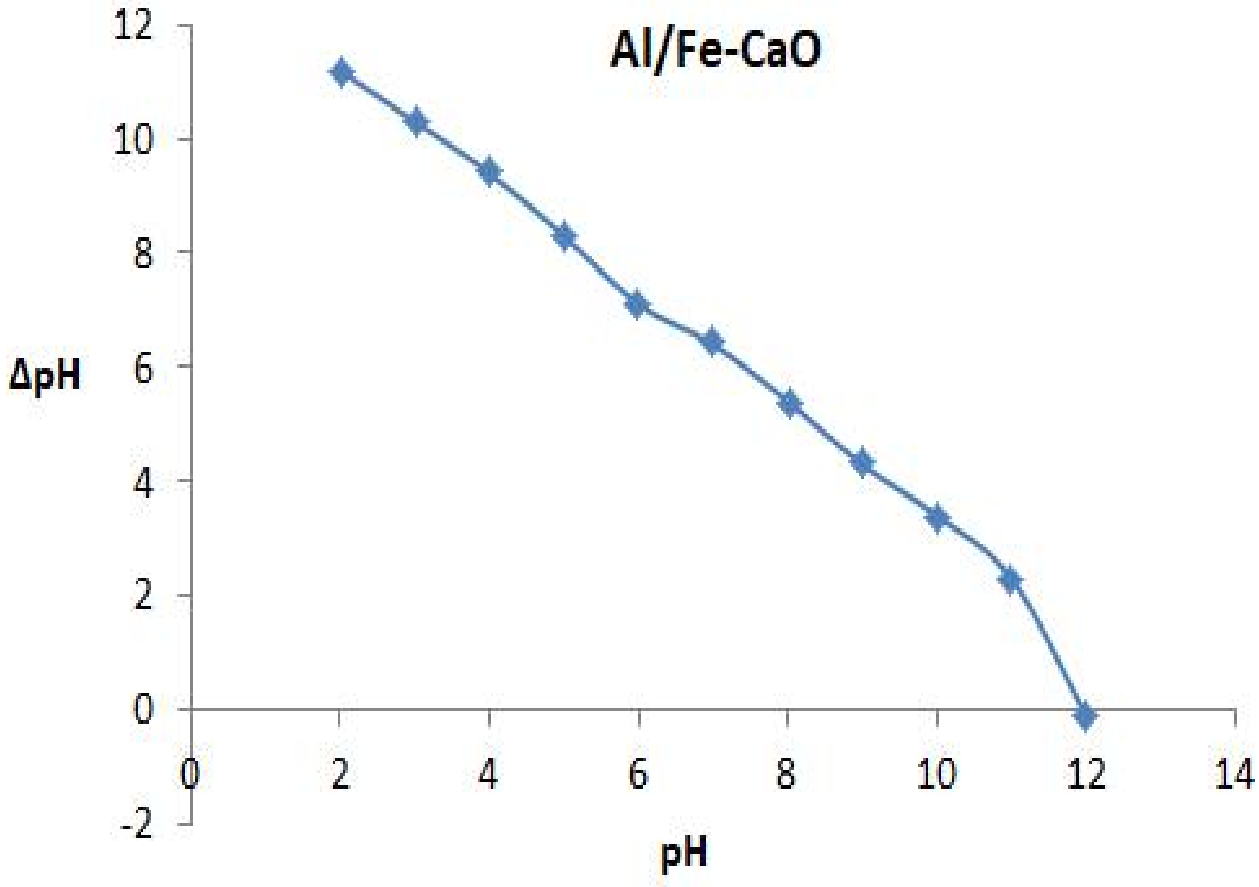

Figure 4.15b: pH_{ZPC} plot ofAl_2O_3/Fe_2O_3-CaO

Source: Field work, 2022.

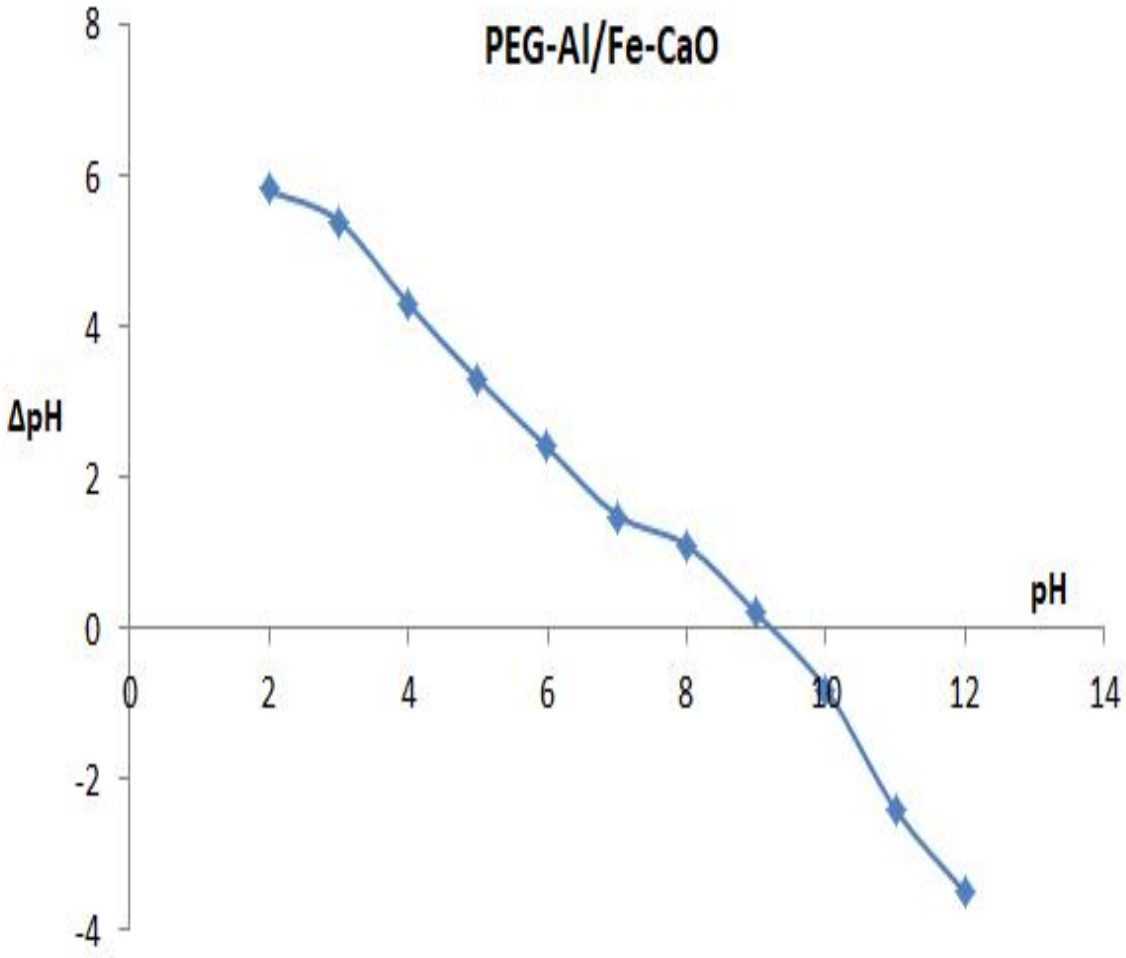

Figure 4.15c: pH_{ZPC} plot of PEGylated

Source: Field work, 2022.

4.4 Determination of λmax for Methylene Blue Solution.

The absorbance of methylene blue with the variation of wavelength is shown in figure. As shown in figure, the maximum absorbance was obtained at 668 nm which is in trend with previous reported datas[23,24,25].

4.5 Calibration Curve for Methylene Blue Solution

The calibration curve of methylene blue solution is shown in Figure 4.16, it shows the relationship between the absorbance and the concentration up to 15 ppm and thus the follows the Beer-Lambert's law. For the higher concentrations of the methylene blue solution further dilution is entailed.

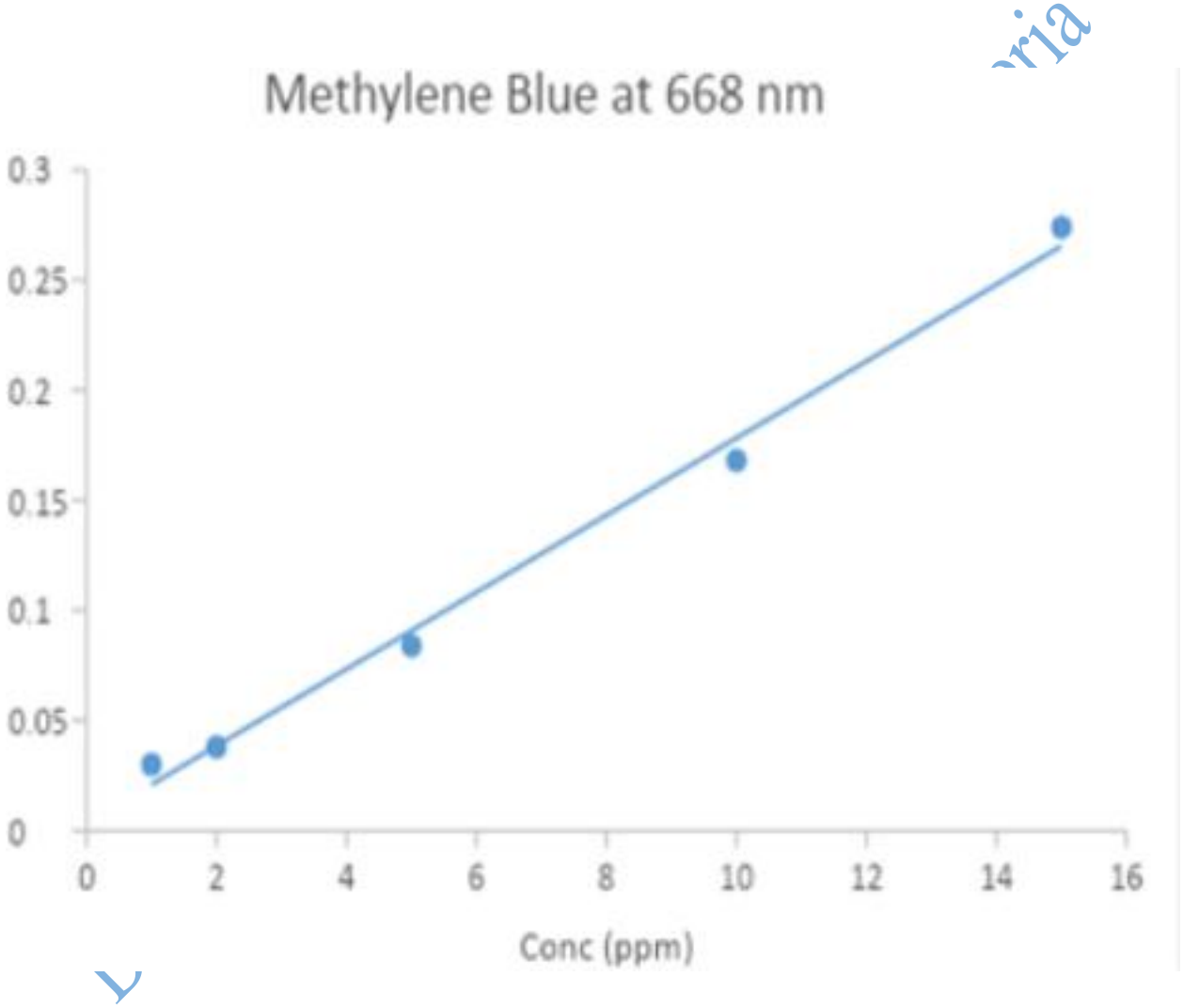

Figure 4.16: Calibration Curve for Methylene Blue Solution

Source: Field work, 2022.

4.6 Batch Adsorption Study

The results of the batch adsorption study are discussed below.

4.6.1 Effect of pH for the Adsorption of methylene blue

In the adsorption process, the pH was significant. However, for all three of the utilized adsorbents in our investigation, the dye removal percentages at varied pH values were marginally different at acidic condition than at alkaline condition. At an acidic situation, it has a high rate of dye removal[26,27]. Figure 4.17a, b, and c illustrate dye removal under various pH circumstances, with acid condition (pH 3) showing the greatest results. The removal of methylene blue dye significantly declines between pH values of 3 and 5, with pH 3 removing 93.5 %, 94.19 %, and 91.91 % of the dye for each adsorbent, and pH 5 removing 87.34 %, 88.94 %, and 85.97% for each. At basic conditions (pH 9 and 11), the dye removal of methylene blue gradually lowers once more in comparison to pH 7, but is still lower than at acid conditions (pH 3 and 5). Because H^+ ions competed with MB in the adsorption process at lower pH levels, this resulted to an increase in the amount of methylene blue that was adsorbed onto the adsorbents. However, after the acid treatment, the positive charge of H^+ balanced out the negative charge on the adsorbent surface. Furthermore, the acid site of the adsorbents was increased by adding HCl to the dilution of powdered methylene blue. As a result, the MB may become more basic under acidic conditions, making it simpler for the adsorbents to connect to the acid site[28,29].

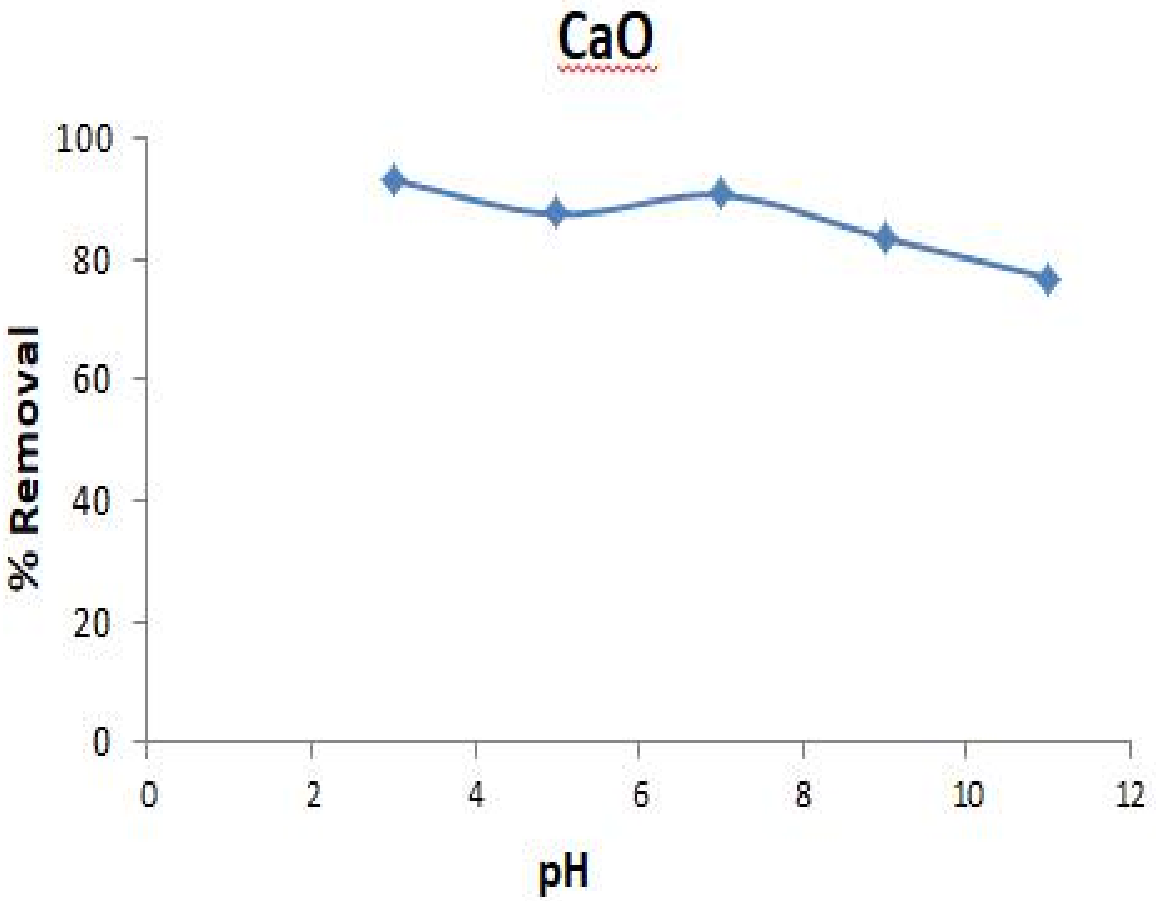

Figure 4.17a: Effect of pH on the adsorption CaO

Source: Field work, 2022.

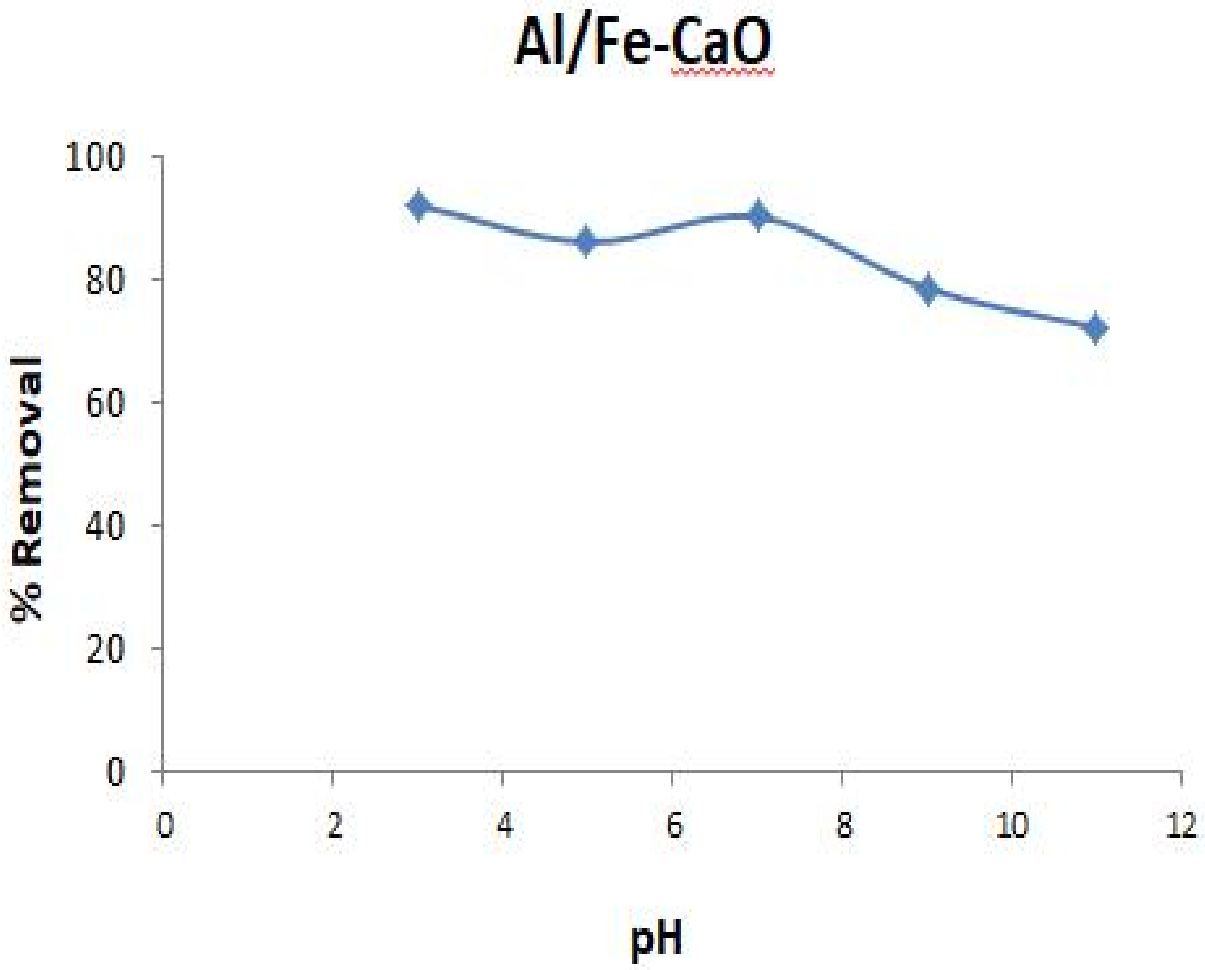

Figure 4.17b: Effect of pH on the adsorption Al_2O_3/Fe_2O_3-CaO

Source: Field work, 2022.

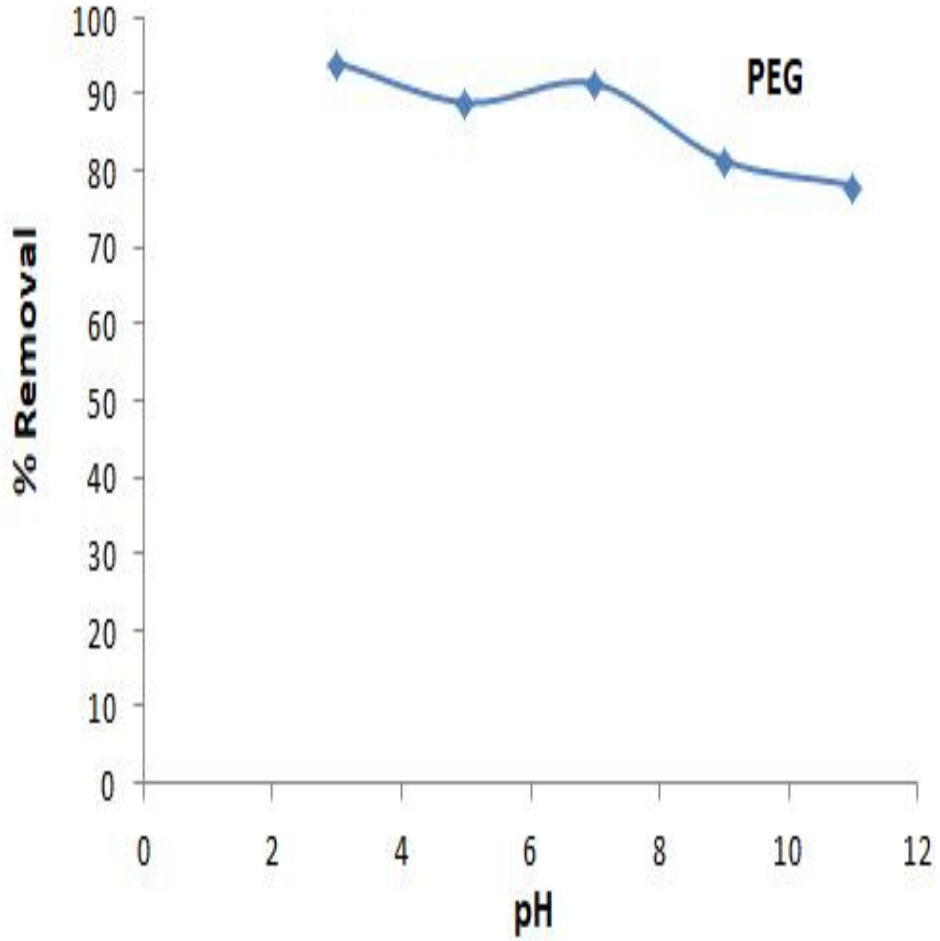

Figure 4.17c: Effect of pH on the adsorption PEGylated

Source: Field work, 2022.

4.6.2 Effect of Contact Time

Contact time is an important factor in adsorption mechanism. The purpose of the experiment is to determine the contact time required to obtain the equilibrium between the adsorbents and the adsorbate[30,31]. In this research, the effect of contact time was investigated at 25 mg/L of MB solution, 0.1 g of adsorbent dosage and an initial pH3 of MB solution. The quantity adsorbed onto the surface of the activated carbons increased as the contact time progresses. The reaction reached equilibrium at 60 minutes for all the adsorbents respectively after which there was no significant increase in the quantity adsorbed[32,33]. The rapidness of adsorption to reach equilibrium within a short period can be attributed to its wider surface area. It has been reported that during adsorption of dyes, initially, the dye molecules have to diffuse into the adsorbent surface and then diffuse slowly into the porous structure of the adsorbent[34]. The effect of the contact time on the batch adsorption was performed at pH3, with the adsorbent dosage of 10 mg, at 25 ^{0}C. Shown in Figure 4.18 below

The curve shows that the adsorption of methylene blue increases with time up to 60 minutes and then it becomes almost constant till the end of the experiment. It can be concluded that the rate of methylene blue binding with the adsorbent is more predominantly during initial stages and remains constant after 60 minutes[35,36].

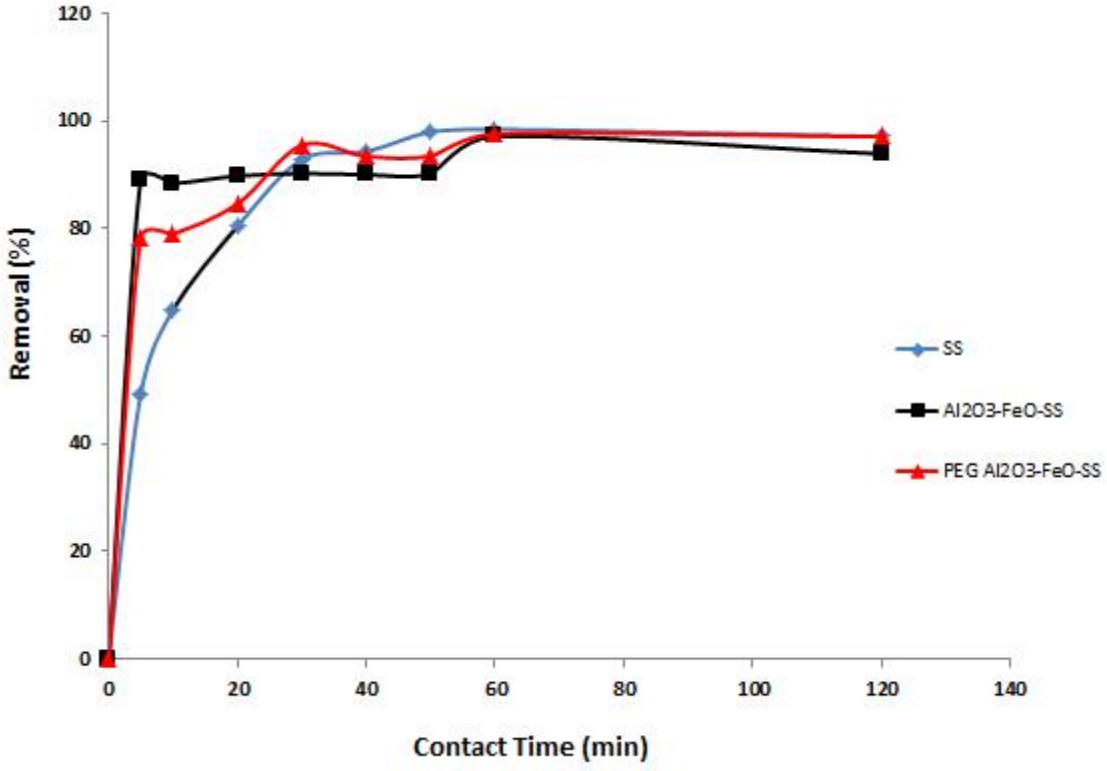

Figure 4.18: Effect of contact time on percentage removal of methylene blue by snail shell based absorbents.

Source: Field work, 2022.

4.6.3 Effect of Adsorbent Dosage

The effect of variation of adsorbent dosage on the adsorption efficiency of snail shell based absorbents is shown in Figure 4.19. The percentage removal of all the adsorbents used in this experiment decreases with increasing adsorbent dosage. It was reported that the removal of methylene blue decreases on increasing the adsorbent dosage[37]. The overlapping of the adsorption sites on the material caused this reduction in adsorption capability of the adsorbent, lengthening the diffusion route in the process[38].

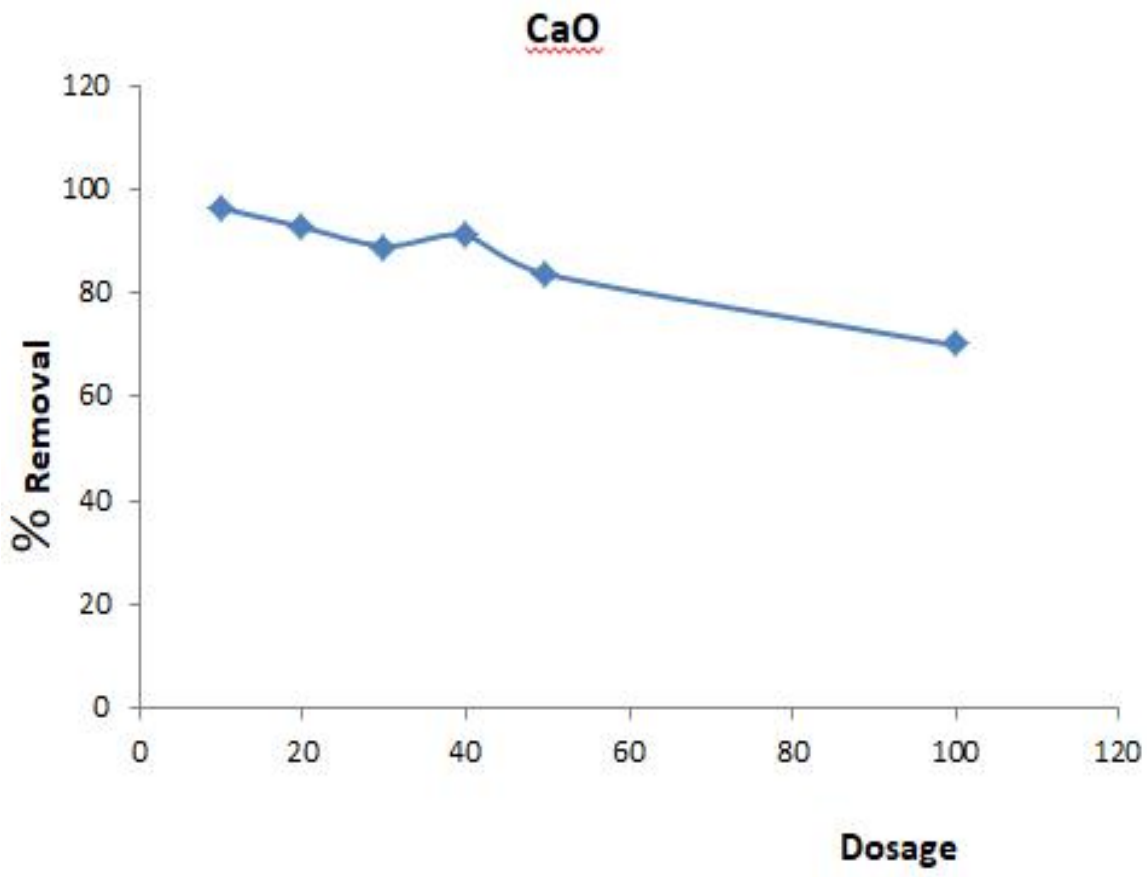

Figure 4.19a: Effect of adsorbent dosage on percentage removal of MB using Calcined SS

Source: Field work, 2022.

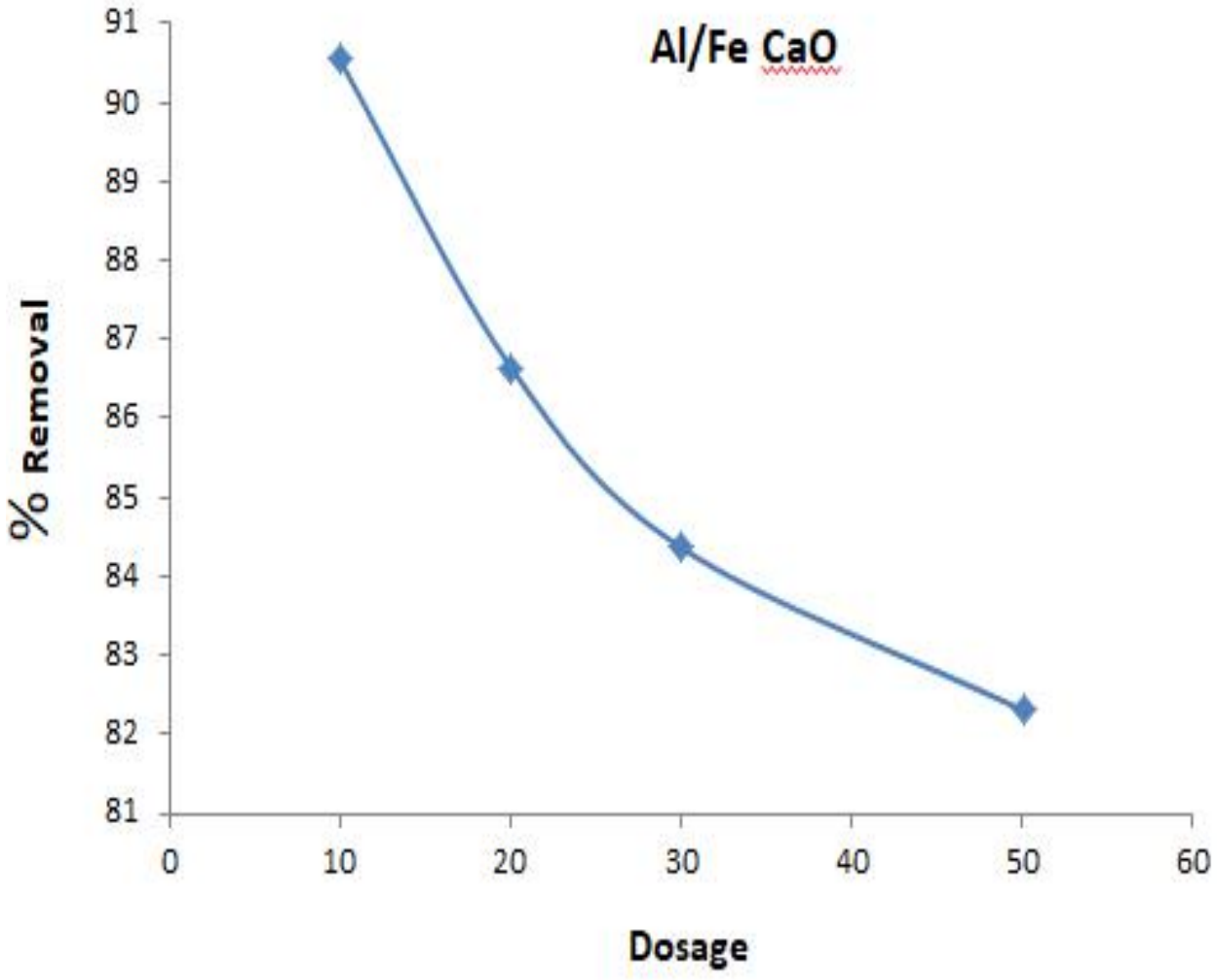

Figure 4.19b: Effect of adsorbent dosage on percentage removal using Al_2O_3/Fe_2O_3-CaO

Source: Field work, 2022.

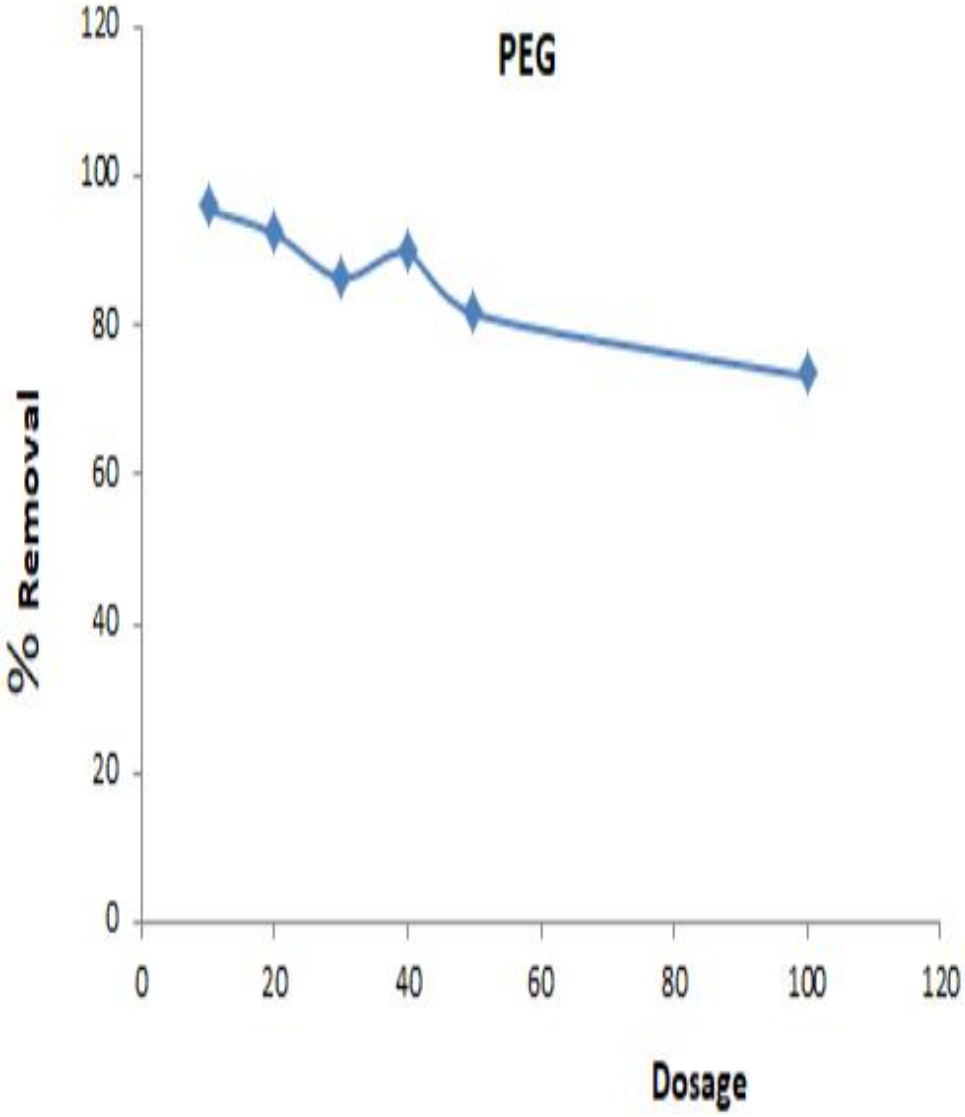

Figure 4.19c: Effect of adsorbent dosage on percentage removal using PEGylated Al_2O_3/Fe_2O_3-CaO

Source: Field work, 2022.

4.7 Adsorption Isotherm

The adsorption isotherm is an equation that shows the transmission of adsorbate from solution phase to the adsorbent phase at equilibrium condition. Langmuir-Freundlich, Sips, Elovich and Temkin isotherms were used to evaluate the experimental results.

Langmuir-Freundlich isotherm is in the following form

$$q_e = \frac{q_{MLF}\,(K_{LF}C_e)^{MLF}}{1 + (K_{LF}C_e)^{MLF}},$$

Where; q_{MLF} is Langmuir-Freundlich maximum adsorption capacity (mg g^{-1}), K_{LF} is equilibrium constant for heterogeneous solid, and MLF is heterogeneous parameter.

Sips isotherm is in the following form

$$= \frac{K_s C_e^{\beta s}}{1 - a_s C_e^{\beta s}},$$

where K_S is Sips isotherm model constant (Lg−1), β_s is Sips isotherm exponent, and a_s is Sips isotherm model constant (Lg−1).

Elovich isotherm is in the following form

$$\frac{q_e}{q_m} = K_E C_e e^{\frac{q_e}{q_m}},$$

where K_E is Elovich isotherm model constant and

Temkin isotherm is in the following form

$$q_e = \frac{Rt}{b} \ln K_T + \frac{RT}{b} \ln C_e,$$

where b is Temkin constant which is related to the heat of adsorption and K_T is Temkin isotherm constant

4.7.1 Adsorption Study of methylene blue on calcined snail shell (CaO)

The experimental data were tested using the Langmuir-Freundlich, Sips, Temkin, and Elovich models in their non-linear forms.The isotherm plots and parameters are shown in Figure 4.20, and Table 4.4 respectively. It may be inferred that the adsorption of methylene blue onto snail shell adsorbent is best matched to the Langmuir-Freundlich (R^2 = 0.9941, Error = 76.60) and Sips (R^2 = 0.9759, Error = 314.08) isotherm models based on a close comparison of coefficient of determination R^2 error values, and other characteristics for all the isotherms models with a slight variation in the characteristics anticipated by the two models[39]. The Q_{max} adsorption capacity of snail shell for methylene blue is estimated by Langmuir-Freundlich to be approximately 350 mg/g. This isotherm suggests that the multilayer adsorption of methylene blue on the snail shell was carried out via heterogeneous active surfaces. With an R^2 value of 0.9941, the theoretical Q_{max} value of 349.37 mg/g found for Langmuir-Freudlich demonstrated satisfactory fit. While Sips demonstrated an adsorption capability with a Q_{max} value of 11.19 mg/g and the lowest R^2 value of 0.9759 in comparison to the other isotherms shown in Table 4.4. A crucial Langmuir-Freudlich measure indicates favorability is the separation factor (K_{LF}). To assess the adsorption process, the (favorable $0<R_L< 1$) equation was utilized. The measured K_{LF}=0.041 in the investigated concentration range (25-300 mg/L) points to a successful adsorption in the methylene blue adsorption on snail shell system[37].

More specifically, the degree of adsorption favorability can be determined using the heterogeneity factor (n) of the Langmuir-Freundlich model. The highly beneficial adsorption of the methylene blue dye on the surface of the snail shell is shown by n = 0.78 in Table 4.4.

Similar study for methylene blue was reported[40]. The Langmuir-freudlich model assumes the presence of heterogeneous active sites on surface of snail shell adsorbent with different energy responsible for uptake of methylene blue.

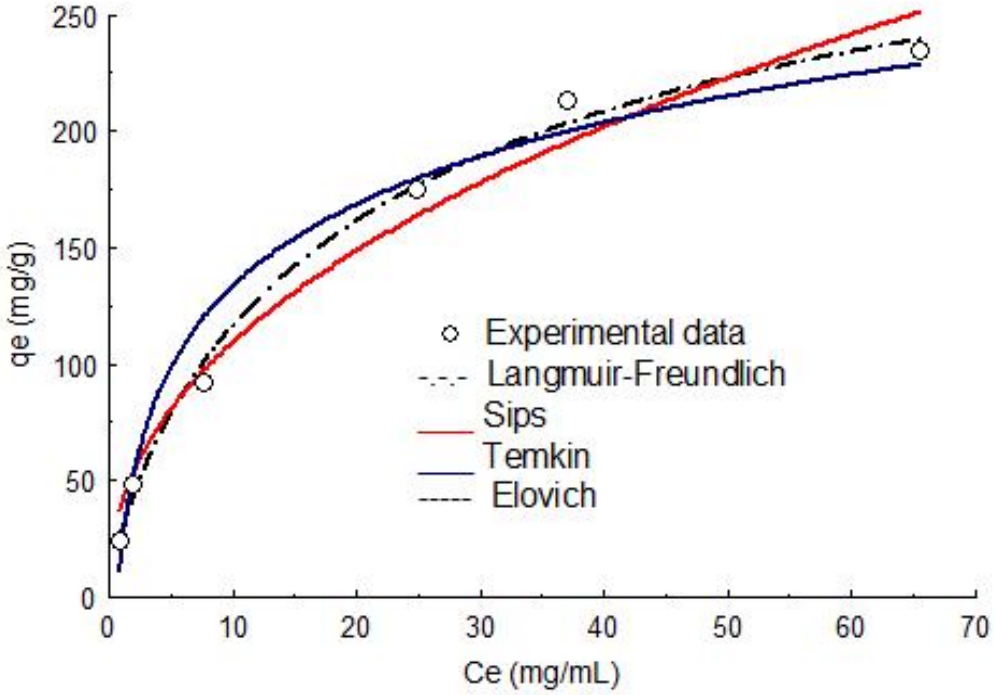

Figure 4.20: Isothermal plots of methylene blue on calcined snail shell (CaO)

Source: Field work, 2022.

Table 4.4: Adsorption study of methylene blue on calcined snail shell (CaO)

Isotherms	R^2	S.E	Parameters
Langmuir-Freundlich	0.994	76.60	Q_m=349.37mg/g: K_{LF}=0.041 n= 0.78
Sips	0.975	314.08	Q^0= 11.19, K=14.44, N= 0.44
Temkin	0.970	285.55	β= 50.5 J.mol-1, K_T= 1.41
Elovich	0.970	285.55	Q_m=0.19, K_E= 71.27.

Source: Field work, 2022.

4.7.2 Adsorption Study of Methylene blue using a Bimetallic Oxide (Al_2O_3/Fe_2O_3) Doped Snail Shell (CaO) Nanocatalyst

The following models; Langmuir-Freudlich, Sips, Temkin, and Elovich models in their non-linear forms were used to determine the adsorption potential of the biomass based bimetallic nanocatalysts. The isotherm plots and the corresponding parameters are presented in Figure 4.21, and Table 4.5 respectively. It can be concluded that the Langmuir-Freudlich model fits the adsorption of methylene blue onto snail shell adsorbent the best (R^2 = 0.9857, Error = 202.49) and Elovich and (R^2 = 0.9230, Error = 826.68) isotherm models based on a close comparison of coefficient of determination (R^2), error values, and other characteristics for all the isotherms models with a slight variation in the characteristics anticipated by the two models. The adsorption capacity of snail shell for methylene blue is estimated by Langmuir-Freudlich to be approximately 200 mg/g. This isotherm suggests that the multilayer adsorption of methylene blue on the snail shell was carried out via heterogeneous active surfaces. With an R^2 value of 0.9857, the theoretical Q_m value of 218.5 mg/g found for Langmuir-Freudlich demonstrated satisfactory fit. While Elovich demonstrated a snail shell's adsorption capability with a Q_M value of 0.015 mg/g and the R^2 value of 0.923 in comparison to the other isotherms shown in Table 4.5. A crucial Langmuir-Freudlich measure that indicates favorability is the separation factor (K_{LF}). To assess the adsorption process, the (favorable $0 < RL < 1$) equation was utilized. The measured K_{LF}=0.112 in the investigated concentration range (25-300 mg/L) points to a successful adsorption in the methylene blue adsorption on calcined snail shell doped Al_2O_3/Fe_2O_3.

The heterogeneity factor (n) of the Langmuir-Freudlich model can be used to more precisely determine the level of adsorption favorability. The highly advantageous adsorption of the methylene blue dye on the snail shell surface is demonstrated by n = 2.73 in Table 4.5.

The Langmuir-Freundlich model posits the presence of heterogeneous active sites on the surface of snail shell adsorbent with variable energy responsible for uptake of methylene blue. A similar studies for methylene blue was conducted by[41,42].

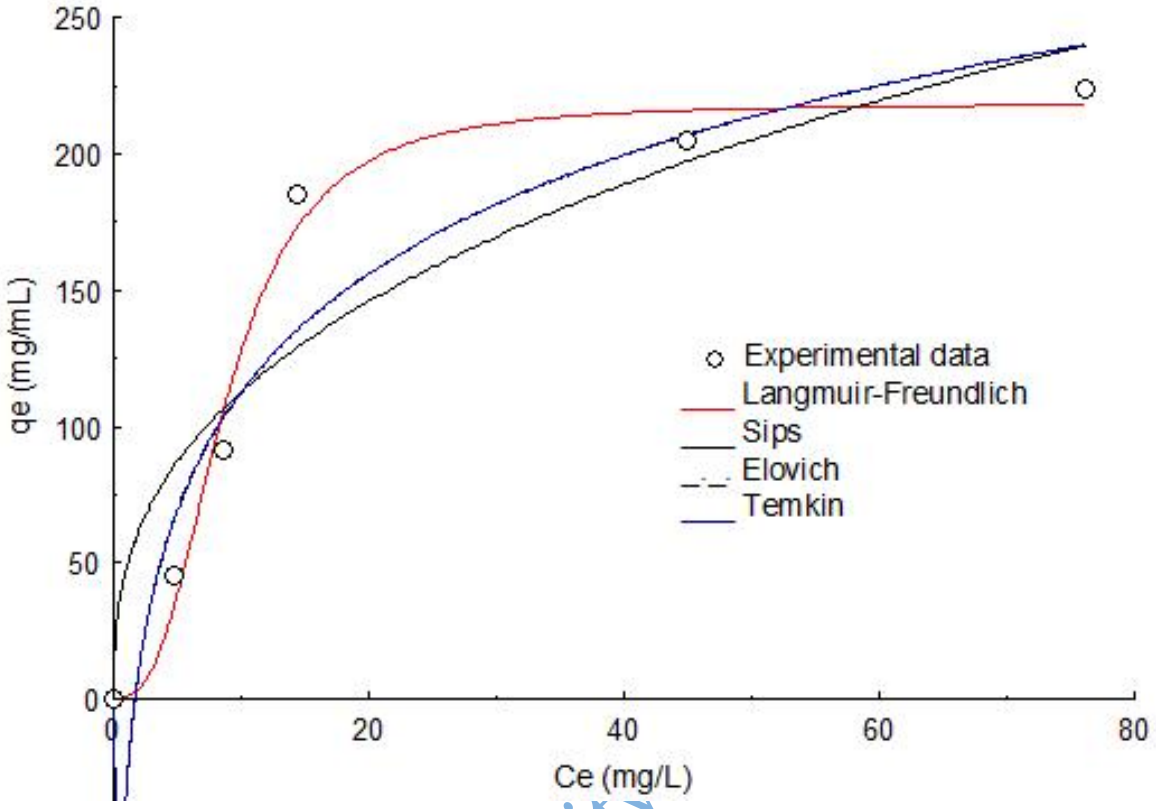

Figure 4.21: Isothermal plots of methylene blue using a bimetallic oxide (Al_2O_3/Fe_2O_3) doped snail shell (CaO) nanocatalyst

Source: Field work, 2022.

Table 4.5: Adsorption study of methylene blue using a bimetallic oxide (Al_2O_3/Fe_2O_3) doped snail shell (CaO) nanocatalyst

Isotherms	R^2	S.E	Parameters
Langmuir-Freundlich	0.985	202.49	Q_M=218.5 mg/g: K_{LF}=0.112 n= 2.73
Sips	0.875	1777.9	Q^0= 18.07, K=11.63, N= 0.37
Temkin	0.923	826.68	β= 62.86J.mol-1, K_T= 0.59
Elovich	0.923	826.6	Q_m=0.015 , K_E= 37.56

Source: Field work, 2022.

4.7.3 Adsorption Study of Methylene Blue using PEGylated Bimetallic Oxide (Al_2O_3/Fe_2O_3) Doped Snail Shell (Cao) Nanocatalyst

The non-linear versions of the Langmuir-Freudlich, Sips, Temkin, and Elovich models were used to test the experimental isotherm data. Figure 4.22 depicts the isotherm plots for the methylene

blue dye on snail shell. Table 4.6 lists the matching isotherm parameters for each plot. Based on a close comparison of coefficient of determination (R^2), error values, and other characteristics for all the isotherm models with a slight variation in the characteristics anticipated by the two models, it can be concluded that the adsorption of methylene blue onto snail shell adsorbent is best matched to the Langmuir-Freundlich (R^2 = 0.9845, Error = 69.95) and Elovich (R^2 = 0.9689, Error = 112.5).

Langmuir-Freundlich calculated that the adsorption capacity of snail shell for methylene blue was about 160 mg/g of methylene blue in mg/g of snail shell. This isotherm implies that heterogeneous active surfaces were involved in the multilayer adsorption of methylene blue on the snail shell. The theoretical Q_M value of 157.0 mg/g discovered for Langmuir-Freundlich showed excellent fit with an R^2 value of 0.9845. When compared to the other isotherms in Table 4.6, Elovich's snail shell isotherm had an R^2 value of 0.9689 and a Q_M value of 0.047 mg/g, proving that it was capable of adsorption. The separation factor is a significant Langmuir-Freundlich statistic that shows favorability (K_{LF}). Using the equation (favorable RL 1), the adsorption process was evaluated. The methylene blue adsorption on snail shell system appears to have achieved satisfactory adsorption as indicated by the measured KLF= 0.07 in the examined concentration range (25-300 mg/L).

More specifically, the heterogeneity factor (n) of the Langmuir-Freundlich model can be used to calculate the level of adsorption favorability. N = 0.71 in Table 4.6 illustrates the methylene blue dye's highly advantageous adsorption on the surface of the snail shell. The Langmuir-Freudlich model posits the presence of heterogeneous active sites on the surface of snail shell adsorbent with variable energy responsible for uptake of methylene blue. A similar study for methylene blue was published[43,44].

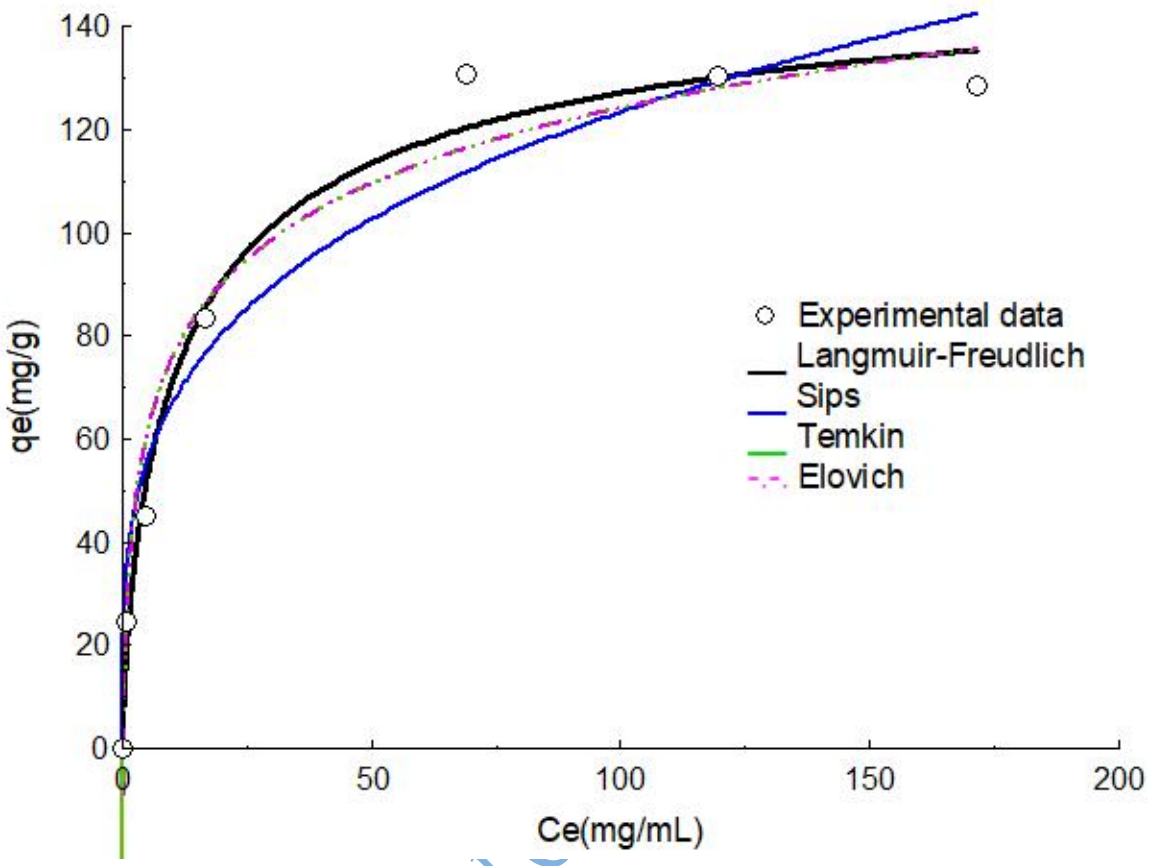

Figure 4.22: Isothermal plots of methylene blue adsorption using PEGylated bimetallic oxide (Al_2O_3/Fe_2O_3) doped snail shell (CaO) nanocatalyst

Source: Field work, 2022.

Table 4.6: Adsorption isotherm data of methylene blue using PEGylated bimetallic oxide (Al_2O_3/Fe_2O_3) doped snail shell (CaO) nanocatalyst

Isotherms	R^2	S.E	Parameters
Langmuir-Freundlich	0.984	69.95	Q_M= 157.0 mg/g: K_{LF}= 0.07 n= 0.71
Sips	0.958	188.9	Q^0= 32.48 , K=1.35 , N= 0.26
Temkin	0.968	112.5	β= 21.05 J.mol-1, K_T= 3.64
Elovich	0.968	112.5	Q_m= 0.04 , K_E= 76.81

Source: Field work, 2022.

4.8 Kinetics Studies

The study of kinetics helps to know the solute uptake and the time required for the adsorbate uptake at the solid-solution interface[14]. For kinetics studies, the effect of contact time and four

models: pseudo-first order, pseudo-second order, BS Fractals, and Largergren were employed to the experimental kinetics data[45].

4.8.1 Kinetics Study of Adsorption of Methylene Blue Using Calcined Snail Shell (CaO)

The kinetic plots and parameters for each model adopted in this study are presented in Table 4.7 and Figure 4.23. The uptake of the methylene blue onto the surface of the biosorbent was observed to be rapid, until adsorption equilibrium was attained, as shown in Figure 4.23. This is thought to be the result of a bigger concentration gradient and a higher availability of unoccupied pores on the adsorbent, which speeds up the adsorption. PFOM, PSOM, BS fractal, and Lagergren are the four kinetic models that were used to determine the kinetics of this process. The recorded R^2 values of all the models were recorded to be near to unity. However, BS fractal was observed to record the lowest error value of 0.79. This suggests that the adsorption process is best fitted into BS fractal model at $R^2 = 0.991$. This suggests that the rate-limiting phase is the exchange or sharing of electrons between the adsorbent and the adsorbate, which suggests chemisorption.

It is considered that methylene blue dye is most likely transported through an intra-particle diffusion mechanism from the bulk solution into the solid phase[46].

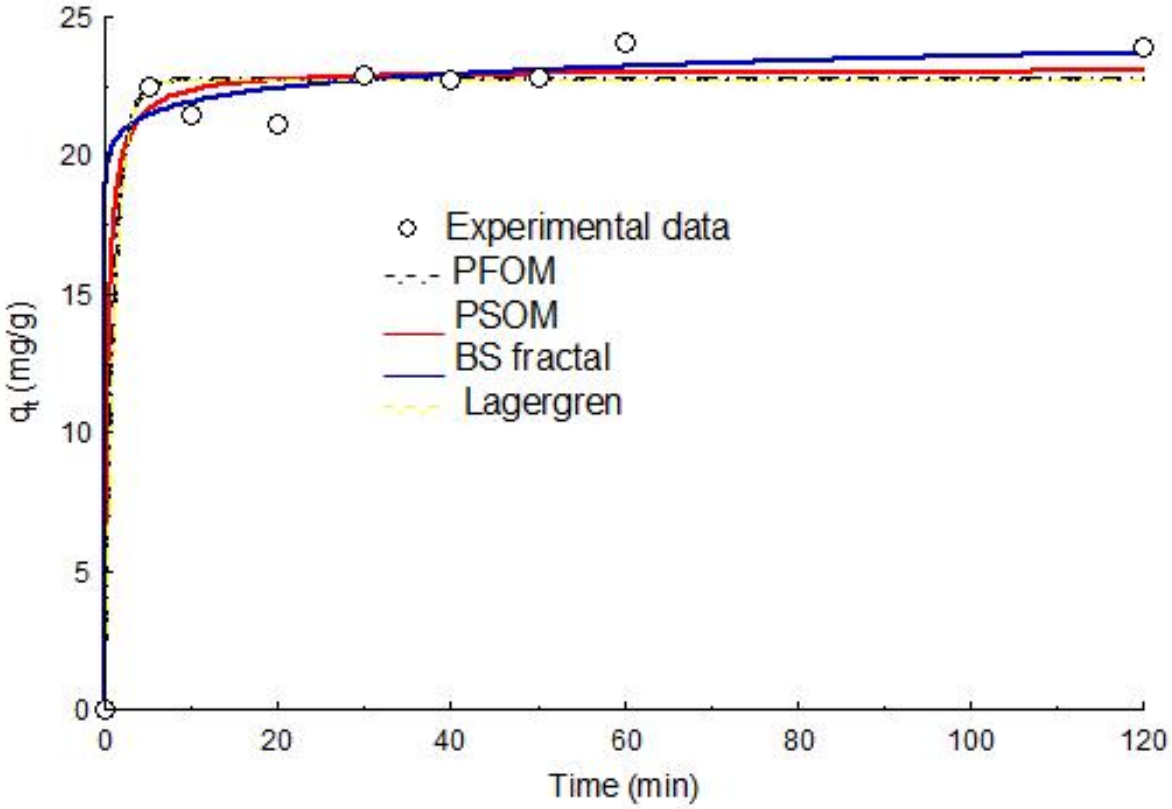

Figure 4.23: Kinetic study of methylene blue using calcined snail shell (CaO)

Source: Field work, 2022.

Table 4.7: Kinetics parameter of methylene blue using calcined snail shell (CaO)

Kinetics	R^2	S.E	Parameters
PFOM	0.983	1.07	Qe =22.71 K_1 = 0.87
PSOM	0.986	0.87	Qe=0.13 K_2= 23.09
BS fractals	0.991	0.79	Qe = 78.91 mg/g, n = 1.18 t = 3.84 °C α = 3.84 cm
Lagergren	0.983	1.07	Qe = 22.71 K = 0.87

Source: Field work, 2022.

4.8.2 Kinetics Study of Methylene Blue using A Bimetallic Oxide (Al_2O_3/Fe_2O_3) Doped Snail Shell (CaO) Nanocatalyst

The numerous kinetic parameters for each model used on this adsorbent are displayed in Table 4.8, and the kinetic model plots used to examine the adsorption-time connection of the adsorption process are displayed in Figure 4.24. Intake of the methylene blue dye greatly rose at first, changing gradually over time until adsorption equilibrium was attained, as shown in Figure 4.24. (5-120mins). This is thought to be the result of a bigger concentration gradient and a higher availability of unoccupied pores on the adsorbent, which speeds up adsorption. PFOM, PSOM, BS fractal, and Lagergrn are the four kinetic models that have correlation coefficients (R^2) obtained for all of them. All of the models' R^2 values were found to be near to 1, but the BS fractal had the lowest error value of them all, at 0.38. This suggests that the removal might match the BS fractal model with $R^2 = 0.995$ the best. This demonstrates that the rate-limiting phase is the exchange or sharing of electrons between the adsorbent and the adsorbate, which suggests chemisorption[47].

It is considered that methylene blue dye is most likely transported through an intra-particle diffusion mechanism from the bulk solution into the solid phase.

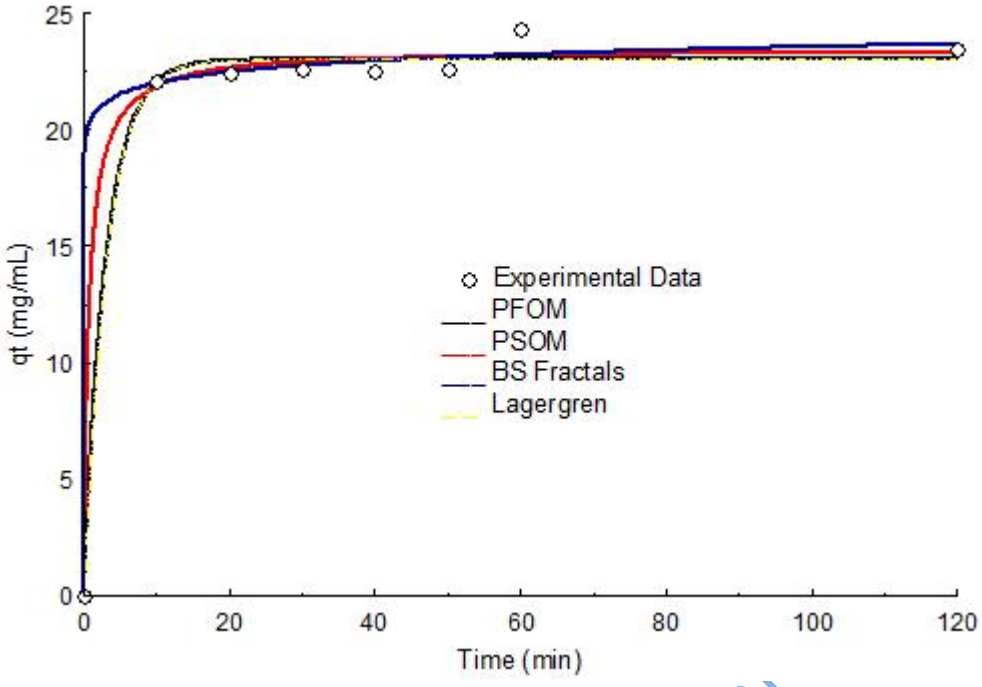

Figure 4.24: Kinetic plot of methylene blue using a bimetallic oxide (Al_2O_3/Fe_2O_3) doped snail shell (CaO) nanocatalyst

Source: Field work, 2022.

Table 4.8: Kinetics parameters of methylene blue using a bimetallic oxide (Al_2O_3/Fe_2O_3) doped snail shell (CaO) nanocatalyst

Kinetics	R^2	S.E	Parameters
PFOM	0.992	0.48	Qe = 22.87 mg/g K1 = 0.72
PSOM	0.994	0.38	Qe= 0.158 mg/g K2= 23.13
BS fractals	0.995	0.38	Qe =52.10 mg/g , n = 1.24 t = 0.0001 α = 0.034
Lagergren	0.992	0.48	Qe = 22.87 mg/g K = 0.72

Source: Field work, 2022.

4.8.3 Kinetics Study of Methylene Blue Adsorption using PEGylated Bimetallic Oxide (Al_2O_3/Fe_2O_3) Doped Snail Shell (CaO) Nanocatalyst

Table 4.9 lists the many kinetic parameters for each model applied to this adsorbent, and Figure 4.25 shows the kinetic model plots used to analyze the adsorption-time relationship of the adsorption process. As shown in Figure 4.25, intake of the methylene blue dye initially increased significantly before gradually changing over time until adsorption equilibrium was reached (5-120 mins). This is believed to be the outcome of a greater concentration gradient and a greater availability of open pores on the adsorbent, which accelerates adsorption[48]. The four kinetic models with obtained correlation coefficients (R^2) are PFOM, PSOM, BS fractal, and Lagergrn.

The R^2 values for all of the models were close to 1, but the BS fractal had the lowest error of them all, at 0.729. This suggests that the removal may have the best R2 = 0.992 BS fractal model match. This demonstrates that the exchange or sharing of electrons between the adsorbent and the adsorbate is the rate-limiting phase, which points to chemisorption. It is hypothesized that methylene blue dye is most likely transferred from the bulk solution into the solid phase by an intra-particle diffusion mechanism[49].

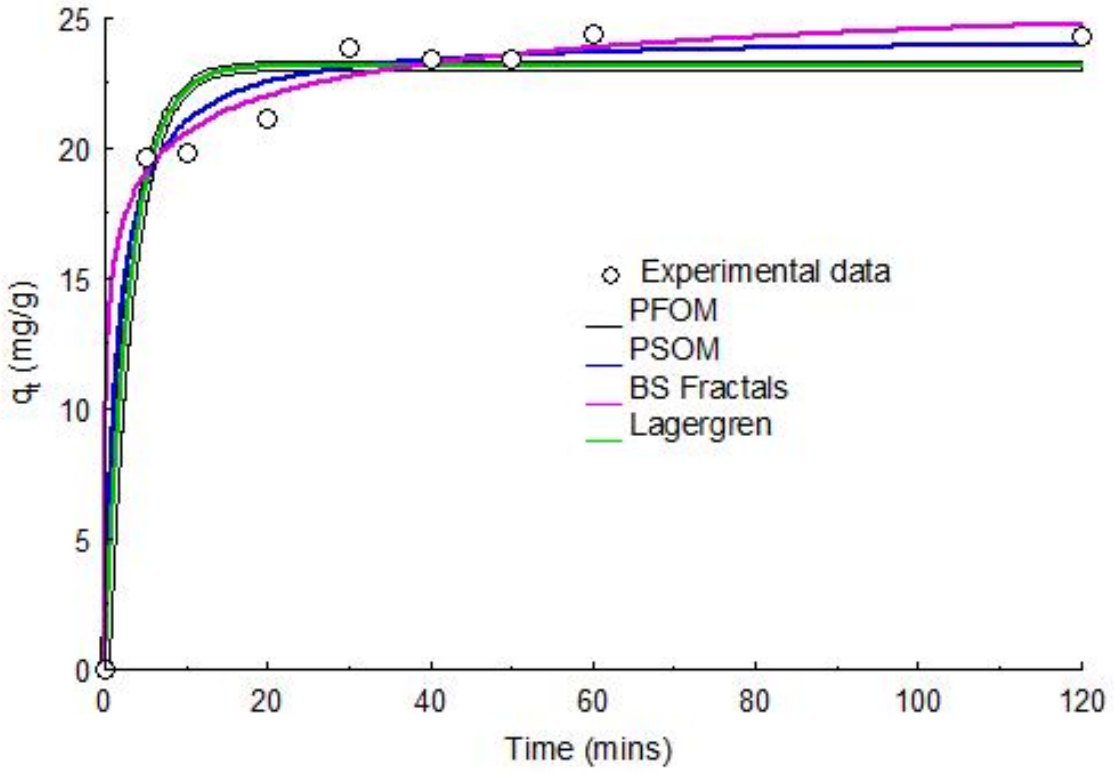

Figure 4.25: Kinetic plots of methylene blue adsorption using PEGylated bimetallic oxide (Al_2O_3/Fe_2O_3) doped snail shell (CaO) nanocatalyst

Source: Field work, 2022.

Table 4.9: Kinetics parameters of Isothermal plots of methylene blue adsorption using PEGylated bimetallic oxide (Al_2O_3/Fe_2O_3) doped snail shell (CaO) nanocatalyst

Kinetics	R^2	S.E	Parameters
PFOM	0.969	2.078	Qe = 23.16 mg/g K1 = 0.323
PSOM	0.987	0.847	Qe= 0.026 mg/g K2= 24.28
BS fractals	0.992	0.729	Qe =27.69 mg/g ,n =1.120 t = 0.009 α = 0.310
Lagergren	0.969	2.078	Qe = 23.16 mg/g K = 0.323

Source: Field work, 2022.

Endnotes

1. P.P. Giannakopoulou, P. Petrounias, A. Rogkala, P. Lampropoulou, E. Gianni, D. Papoulis, P. Koutsovitis, B. Tsikouras, & K. Hatzipanagiotou. *Does the methylene blue test give equally satisfactory results in all studied igneous rocks relative to the identification of swelling clay minerals*. **Minerals**, 10(3), 2020, 283.

2. R.C. Dante, J. Trakulmututa, S. Meejoo-Smith, P. Martín-Ramos, P. Chamorro-Posada, D. Rutto, & F.M. Sánchez-Arévalo. *Methylene blue-carbon nitride system as a reusable air-sensor*. **Materials Chemistry and Physics**, 231, 2019, 351-356.

3. Y. Zhang, Y. An, L. Wu, H. Chen, Z. Li, H. Dou,V. Murugadoss, J. Fan, X. Zhang, X. Mai, & Z. Guo. *Metal-free energy storage systems: combining batteries with capacitors based on a methylene blue functionalized graphene cathode*. **Journal of Materials Chemistry A**, 7(34), 2019, 19668-19675.

4. G. López-Carballo, V. Muriel-Galet, P. Hernández-Muñoz, & R. Gavara. *Chromatic sensor to determine oxygen presence for applications in intelligent packaging*. **Sensors**, 19(21), 2019, 4684.

5. Y. Pang, Z.H. Tong, L. Tang, Y.N. Liu, & K. Luo. *Effect of humic acid on the degradation of methylene blue by peroxymonosulfate.* **Open Chemistry**, 16(1), 2018, 401-406.

6. L. Sun, D. Hu, Z. Zhang, & X. Deng. *Oxidative degradation of methylene blue via PDS-based advanced oxidation process using natural pyrite.* **International Journal of Environmental Research and Public Health,** 16(23), 2019, 4773.

7. M. Contreras, C.D. Grande-Tovar, W. Vallejo, & C. Chaves-López. *Bio-removal of methylene blue from aqueous solution by Galactomycesgeotrichum KL20A*. **Water,** 11(2), 2019, 282.

8. E.A. Abdelrahman, R.M. Hegazey, & R.E. El-Azabawy. *Efficient removal of methylene blue dye from aqueous media using Fe/Si, Cr/Si, Ni/Si, and Zn/Si amorphous novel adsorbents.* **Journal of Materials Research and Technology**, 8(6), 2019, 5301-5313.

9. E. Santoso, R. Ediati, Y. Kusumawati, H. Bahruji, D.O. Sulistion, & D. Prasetyoko. *Review on recent advances of carbon based adsorbent for methylene blue removal from waste water.* **Materials Today Chemistry**, 16, 2020, 100233.

10. A.H. Jawad, M. Bardhan, M.A. Islam, S.S.A. Syed-Hassan, S.N. Surip, Z.A. ALOthman, & M.R. Khan. *Insights into the modeling, characterization and adsorption performance of mesoporous activated carbon from corn cob residue via microwave-assisted H3PO4 activation.* **Surfaces and Interfaces**, 21, 2020, 100688.

11. L.F. Cusioli, H.B. Quesada, A.T. Baptista, R.G. Gomes, & R. Bergamasco. *Soybean hulls as a low-cost biosorbent for removal of methylene blue contaminant*. **Environmental Progress & Sustainable Energy**, 39(2), 2020, 13328.

12. Z. Wang, M. Gao, X. Li, J. Ning, Z. Zhou, & G. Li. *Efficient adsorption of methylene blue from aqueous solution by graphene oxide modified persimmon tannins.* **Materials Science and Engineering**, 108, 2020, 110196.

13. O.E. Ebi, A.F. Taiwo, & A.T. Folorunsho. *Kinetic modelling of the biosorption of methylene blue onto wild melon (lagenariasphaerica)*. **American Journal of Chemical Engineering**, 6(6), 2018, 126-134.

14. S. Zhou, Z. Du, X. Li, Y. Zhang, Y. He, & Y. Zhang. *Degradation of methylene blue by natural manganese oxides: kinetics and transformation products.* **Royal Society open science,** 6(7), 2019, 190351.

15. C.P. Lawagon, R.E.C. Amon, C.P. Lawagon, & R.E.C. Amon. *Magnetic rice husk ash'cleanser'as efficient methylene blue adsorbent.* **Environmental Engineering Research**, 25(5), 2019, 685-692.

16. G. Crini, E. Lichtfouse, L. D. Wilson, & N. Morin-Crini. *Conventional and non-conventional adsorbents for wastewater treatment.* **Environmental Chemistry Letters**, 17, 2019, 195–213.

17. P. Srivatsav, B. S. Bhargav, V. Shanmugasundaram, J. Arun, K. P. Gopinath, & A. Bhatnagar. *Biochar as an eco-friendly and economical adsorbent for the removal of colorants (Dyes) from aqueous environment: A review*. **Water (Switzerland),** 12, 2020, 1–27.

18. M. A. Al-Ghouti, D. Da'ana, M. Abu-Dieyeh, & M. Khraisheh. *Adsorptive removal of mercury from water by adsorbents derived from date pits.* **Scientific Reports**, 9, 2019, 1–15.

19. J. Saleem, U. Bin Shahid, M. Hijab, H. Mackey, & G. McKay. *Production and applications of activated carbons as adsorbents from olive stones.* **Biomass Conversion and Biorefinery**, 9, 2019, 775–802.

20. B. Luo, G. Huang, Y. Yao, C. An, P. Zhang, & K. Zhao. *Investigation into the influencing factors and adsorption characteristics in the removal of sulfonamide antibiotics by carbonaceous materials*. **Journal of Cleaner Production**, 2021, 319-128692.

21. N. M. Aljamali, R. A. B. Aldujaili, & I. O. Alfatlawi. *Physical and chemical adsorption and its applications*. **International Journal of Thermodynamics and Chemical Kinetics**, 2021, 7 1–8.

22. A. M. Elgarahy, K. Z. Elwakeel, S. H. Mohammad, & G. A. Elshoubaky. *A critical review of biosorption of dyes, heavy metals and metalloids from wastewater as an efficient and green process.* **Cleaner Engineering and Technology,** 4, 2021, 100209.

23. M. K. Al Mesfer, M. Danish, M. I. Khan, I. H. Ali, M. Hasan, & A. El Jery. *Continuous fixed Bed CO2 adsorption: breakthrough, column efficiency, mass transfer zone.* **Processes**, 2020, 8, 1233.

24. T. Selmi, M. Seffen, A. Celzard, & V. Fierro. *Effect of the adsorption pH and temperature on the parameters of the Brouers–Sotolongo models*. **Environmental Science and Pollution Research**, 27, 2020, 23437–23446.

25. G. Gopal, S. A. Alex, N. Chandrasekaran, & A. Mukherjee. *A review on tetracycline removal from aqueous systems by advanced treatment techniques*. **RSC Advances,** 10, 2020, 27081–27095.

26. J. O. Eniola, R. Kumar, & M. A. Barakat. *Adsorptive removal of antibiotics from water over natural and modified adsorbents.* **Environmental Science and Pollution Research**, 26, 2019, 34775–34788.

27. P. Hess. *Bonding, structure, and mechanical stability of 2D materials: The predictive power of the periodic table.* **Nanoscale Horizons**, 6, 2021, 856–892.

28. H. N. Hamad, & S. Idrus. *Recent developments in the application of bio-waste-derived adsorbents for the removal of methylene blue from wastewater: a review*. **Polymers**, 14, 2022.

29. J. Jjagwe, P. W. Olupot, E. Menya, & H. M. Kalibbala. *Synthesis and application of granular activated carbon from biomass waste materials for water treatment: a review.* **Journal of Bioresources and Bioproducts**, 6, 2021, 292–322.

30. P. González-García. *Activated carbon from lignocellulosics precursors: A review of the synthesis methods, characterization techniques and applications*. **Renewable and Sustainable Energy Reviews**, 82, 2018, 1393–1414.

31. Y. Wang, Y. Zhou, G. Jiang, P. Chen, & Z. Chen. *One-step fabrication of carbonaceous adsorbent from corncob for enhancing adsorption capability of methylene blue removal.* **Scientific Reports**, 10, 2020, 1–9.

32. M. Mallek, M. Chtourou, M. Portillo, H. Monclús, K. Walha, A. ben Salah, & V. Salvadó. *Granulated cork as biosorbent for the removal of phenol derivatives and emerging contaminants.* **Journal of Environmental Management**, 223, 2018, 576–585.

33. N. S. Alharbi, B. Hu, T. Hayat, S. O. Rabah, A. Alsaedi, L. Zhuang, & X. Wang. *Efficient elimination of environmental pollutants through sorption-reduction and photocatalytic degradation using nanomaterials.* **Frontiers of Chemical Science and Engineering,** 14, 2020, 1124–1135.

34. Y. Dai, M. Liu, J. Li, S. Yang, Y. Sun, Q. Sun, W. Wang, L. Lu, K. Zhang, J. Xu, W. Zheng, Z. Hu, Y. Yang, Y. Gao, & Z. Liu. *A review on pollution situation and treatment methods of tetracycline in groundwater.* **Separation Science and Technology (Philadelphia)**, 55, 2020, 1005–1021.

35. D. Liu, Q. Xie, X. Huang, C. Wan, F. Deng, D. Liang, & J. Liu. *Backwashing behavior and hydrodynamic performances of granular activated carbon blends.* **Environmental Research**, 2020, 184 109302.

36. G. Sharma, S. Sharma, A. Kumar, C. W. Lai, M. Naushad, Shehnaz, J. Iqbal, & F. J. Stadler. *Activated carbon as superadsorbent and sustainable material for diverse applications.* **Adsorption Science & Technology,** 2022, 1–21.

37. J. Lee, & R. Patel. *Wastewater treatment by polymeric microspheres: a review.* **Polymers**, 14, 2022, 1–37.

38. S.A. Ambika, & P. P. Singh. *Natural polymer-based hydrogels for adsorption applications.* **Nat. Polym. Green Adsorbents Water Treat. Elsevier,** 2021, 267–306.

39. S. Mallakpour, & F. Azimi. *Polymer nanocomposites based on alginate and their blends for remediation of pollutants from wastewater*. **Nat. Polym. Green Adsorbents Water Treat. Elsevier,** 2021, 307–332.

40. M. Cantarella, S. C. Carroccio, S. Dattilo, R. Avolio, R. Castaldo, C. Puglisi, & V. Privitera. *Molecularly imprinted polymer for selective adsorption of diclofenac from contaminated water*. **Chemical Engineering Journal**, 367, 2019, 180–188.

41. N. Morin-crini, E. Lichtfouse, M. Fourmentin, A. Ribeiro, C. Noutsopoulos, F. Mapelli, É. Fenyvesi, M. Vieira, L. Picos-corrales, J. Moreno-piraján, N. Morin-crini, E. Lichtfouse, M. Fourmentin, A. Ribeiro, C. Noutsopoulos, E. Lichtfouse, J. Schwarzbauer, D. R. Emerg-, N. Morin-crini, E. Lichtfouse, & M. Fourmentin. *Remediation of emerging contaminants.* **Environ. Chem. a Sustain. World,** 2022, 1–106.

42. J. J. Belbruno. *Molecularly Imprinted Polymers*. **Chemical Reviews**, 119, 2019, 94–119.

43. Z. Feng, K. Odelius, & M. Hakkarainen. *Tunable chitosan hydrogels for adsorption: Property control by biobased modifiers.* **Carbohydrate Polymers**, 196, 2018, 135–145.

44. B. Gao, P. Li, R. Yang, A. Li, & H. Yang. *Investigation of multiple adsorption mechanisms for efficient removal of ofloxacin from water using lignin-based adsorbents*. **Scientific Reports**, 9, 2019, 1–13.

45. E. N. Zare, Z. Fallah, V. T. Le, V.-D.Doan, A. Mudhoo, S.-W.Joo, Y. Vasseghian, M. Tajbakhsh, O. Moradi, M. Sillanpää, & R. S. Varma. *Remediation of pharmaceuticals from contaminated water by molecularly imprinted polymers: a review* **Springer International Publishing**. 2022.

46. W. Duan, N. Wang, W. Xiao, Y. Zhao, & Y. Zheng. *Ciprofloxacin adsorption onto different micro-structured tourmaline, halloysite and biotite.* **Journal of Molecular Liquids**, 269, 2018, 874–881.

47. A. O. Adeola, O. Fapohunda, A. T. Jimoh, T. T. Isaiah, A. O. Ige, & A. C. Ogunyele, 2019. *Scientific applications and prospects of nanomaterials: A multidisciplinary review.* **African Journal of Biotechnology**, 2019, 946–961.

48. S. M. Abdelbasir, & A. E. Shalan. *An overview of nanomaterials for industrial wastewater treatment.* **Korean Journal of Chemical Engineering**, 2019, 1209–1225.

Chapter Five

Conclusion

5.1 Summary of Findings

The synthesized bio-sorbents showed excellent adsorption properties for the removal of MB from wastewater. The FTIR spectra obtained and the analysis showed a marked difference between the calcined snail shells (CaO) and the modified (Al_2O_3/Fe_2O_3-CaO and PEGylated Al_2O_3/Fe_2O_3-CaO) which was corroborated with the SEM and EDX micrographs of the samples. This study shows that the adsorption of MB depends on the following parameters; initial concentrations, solution pH, and contact time.

The optimum pH for this study was found at pH 3 with dosage of 10 mg, at 25 °C uptake of MB at 93.5% (CaO), 94.19% (Al_2O_3/Fe_2O_3-CaO) and 91.91% (PEGylated Al_2O_3/Fe_2O_3-CaO). SEM images of the catalysts showed a well-organized rod-like and cubic aggregates, while XRD showed a highly crystalline bio-sorbent material. The EDX confirms an effective impregnation of the biomass material with the metal oxide while FTIR spectra showed the presence of O-H, N-H, C=O and C-O moiety available for the efficient adsorption of methylene blue.

Langmuir-Freundlich isotherm model best described the adsorption data for all the catalysts; CaO with R^2 value-0.994 and Q_{max}= 34937mg/g, Al_2O_3/Fe_2O_3-CaO; with R^2 value=0.986 and Q_{max}= 218.5 mg/g and PEGylated Al_2O_3/Fe_2O_3-CaO; with R^2 value 0.984 and Q_{max}= 157.0 mg/g Furthermore, the experimental data is best fitted into Brouers Sotolongo sractals kinetics at a recorded R^2 = 0.991 and Q_{max}= 78.91 mg/g (CaO), R^2 = 0.995 and Q_{max}= 52.10 mg/g (Al_2O_3/Fe_2O_3-CaO), and R^2 = 0.992 and Q_{max}= 27.69 mg/g (PEGylated Al_2O_3/Fe_2O_3-CaO).

This shows that the synthesized biomass-based catalysts has the potential to effectively adsorb MB.

5.2 Conclusion

This study reveals that both Al_2O_3/Fe_2O_3-CaO and PEGylated Al_2O_3/Fe_2O_3-CaO have a promising capacity for the adsorption of methylene blue, which can serve as a good and cost effective alternative for the remediation of methylene blue-laden wastewater.

5.3 Recommendations

Despite the high adsorption capacity and selectivity for methylene blue dye shown by the metallic oxide and PEGylated biomass based catalysts. It is therefore recommended to determine the recyclability of the catalyst in order to ascertain their durability.

5.4 Contribution to Knowledge

This research serves as a baseline for further work on the eradication of MB-contaminated waste water in Ibadan, Nigeria. It has necessitated public sensitization and awareness of the importance of remediating MB-contaminated waste water and measures to reduce pollution so as to curb the human health and ecological risks associated with consuming polluted water. Solving these challenges involves close coordination between researchers at universities and government agencies, as well as the industry and decision makers at all levels.

5.5 Suggested Areas for Further Studies

Proper characterization of adsorbent materials was not done completely due to the limitation of instrumental facilities such as Transmission electron microscope (TEM) and Thermogravimetric analysis (TGA). Further works on characterization of adsorbent materials can be done.

Bibliography

Books

Gangaraju, G., Uma, R., & Shah, K. J. *Introduction to conventional wastewater treatment technologies: limitations and recent advances. adv. wastewater treat.* **I (Materials Research Foundations LLC**, 2021, 1–36.

Uddin, M. K., & Rehman, Z. *Application of nanomaterials in the remediation of textile effluents from aqueous solutions in Nanomaterials in the Wet Processing of Textiles*. **Hoboken, NJ, USA: John Wiley & Sons, Inc.** 2018, 135-161.

Qamruzzaman, K., & Nasar, A. *Degradative treatment of bispyribac sodium herbicide from syntheticall r treatment–dye decolourisation and anti–microbial activity*. **MOJ Drug Des. Dev. Ther,** 2019.

Qasem, N. A. A., Mohammed, R. H., & Lawal, D. U. *Removal of heavy metal ions from wastewater: a comprehensive and critical review.* **npj Clean Water**, 2021.

Conference Proceeding

Crini, G., & Lichtfouse, E. *Advantages and disadvantages of techniques used for wastewater treatment.* **Environmental Chemistry Letters,** 17(1), 2019, 145-155.

Crini, G., Lichtfouse, E., Wilson, L. D., & Morin-Crini, L. *Conventional and non-conventional adsorbents for wastewater treatment.* **Environmental Chemistry Letters**, 17, 2019, 195–213.

Cusioli, L. F., Quesada, H. B., Baptista, A.T., Gomes, R.G., & Bergamasco, R. *Soybean hulls as a low-cost biosorbent for removal of methylene blue contaminant*. **Environmental Progress & Sustainable Energy**, 39(2), 2020, 13328.

Pang, Y., Tong, Z. H., Tang, L., Liu, Y. N. & Luo, O. *Effect of humic acid on the degradation of methylene blue by peroxymonosulfate.* **Open Chemistry**, 16(1), 2018, 401-406.

Zhou, S., Du, Z., Li, X., Zhang, Y., He, Y., & Zhang, Y. *Degradation of methylene blue by natural manganese oxides: kinetics and transformation products.* **Royal Society open science,** 6(7), 2019, 190351.

Journals

Abdelbasir, S. M., & Shalan, A. E. *An overview of nanomaterials for industrial wastewater treatment.* **Korean Journal of Chemical Engineering**, 2019, 1209–1225.

Abd-Elhamid, A. I., Emran, M., El-Sadek, M. H., El-Shanshory, A. A., Soliman, H., Akl, M. A., & Rashad, M. *Enhanced removal of cationic dye by eco-friendly activated biochar derived from rice straw.* **Applied Water Science**, 10(1), 2020, 1-11.

Abdelrahman, E. A., Hegazey, R. M., & El-Azabawy, R. H. *Efficient removal of methylene blue dye from aqueous media using Fe/Si, Cr/Si, Ni/Si, and Zn/Si amorphous novel adsorbents.* **Journal of Materials Research and Technology**, 8(6), 2019, 5301-5313.

Adeola, A. O., Fapohunda, O., Jimoh, A. J., Isaiah, T. T., Ige, A. O., & Ogunyele, A. C *Scientific applications and prospects of nanomaterials: A multidisciplinary review.* **African Journal of Biotechnology**, 2019, 946–961.

Ahamad, T., Naushad, M., & Alshehri, S.M. *Analysis of degradation pathways and intermediates products for ciprofloxacin using a highly porous photocatalyst.* **Chemical Engineering Journal,** 417, 2021, 127969.

Ahmed, M., Mashkoor, F., & Nasar, A. *Development, characterization, and utilization of magnetized orange peel waste as a novel adsorbent for the confiscation of crystal violet dye from aqueous solution.* **Groundwater for sustainable development,** 10, 2020, 100322.

Al Mesfer, M. K., Danish, M., Khan, M. I., Ali, I. H., Hasan, M., & El Jery, M. *Continuous fixed bed co2 adsorption: breakthrough, column efficiency, mass transfer zone.* **Processes**, 8, 2020, 1233.

Al-Ghouti, M. A., Da'ana, D., Abu-Dieyeh, M., & Khraisheh, M. *Adsorptive removal of mercury from water by adsorbents derived from date pits.* **Scientific Reports**, 9, 2019, 1–15.

Alharbi, N. S., Hu, B., Hayat, T., Rabah, S. O. Alsaedi, A., Zhuang, L., & Wang, L. *Efficient elimination of environmental pollutants through sorption-reduction and photocatalytic degradation using nanomaterials.* **Frontiers of Chemical Science and Engineering,** 14, 2020, 1124–1135.

Aljamali, N. M., Aldujaili, R. A. B., & Alfatlawi, I. O. *Physical and chemical adsorption and its applications*. **International Journal of Thermodynamics and Chemical Kinetics**, 7, 2021, 1–8.

Ambika, S. A., & Singh, P. P. *Natural polymer-based hydrogels for adsorption applications.* **Nat. Polym. Green Adsorbents Water Treat. Elsevier,** 2021, 267–306.

Anushree, C., & Philip, J. *Efficient removal of methylene blue dye using cellulose capped Fe3O4 nanofluids prepared using oxidation-precipitation method.* **Colloids and Surfaces A: Physicochemical and Engineering Aspects,** 567, 2019, 193-204.

Arias Arias, F., Guevara, M., Tene, T., Angamarca, P., Molina, R., Valarezo, A., Salguero, O., Vacacela Gomez, C., Arias, M., & Caputi, L.S. *The adsorption of methylene blue on eco-friendly reduced graphene oxide.* **Nanmaterials,** 10(4), 2020, 681.

Balarak, D., Bazzi, M., Shehu, Z., & Chandrika, K. *Application of surfactant-modified bentonite for methylene blue adsorption from aqueous solution*. **Orient J Chem**, 36(2), 2020, 293-9.

Belbruno, J. J. *Molecularly imprinted polymers*. **Chemical Reviews**, 119, 2019, 94–119.

Benkhaya, S., M'rabet, A., & El Harfi, A. *A review on classifications, recent synthesis and applications of textile dyes.* **Inorganic Chemistry Communications**, 115, 2020, 107891.

Borhan, A., Yusup, S., Lim, J. W., & Show, P. L. *Characterization and modelling studies of activated carbon produced from rubber-seed shell using KOH for CO_2 adsorption*. **Processes**, 7, 2019.

Bouju, X., Duguet, E., Gauffre, F., Henry, C. R., Kahn, M. L., Mélinon, P., & Ravaine, S. *Nonisotropic self-assembly of nanoparticles: from compact packing to functional aggregates.* **Advanced Materials**, 2018, 30.

Bouras, H. D., Isik, Z., Arikan, E. B., Yeddou, A. R., Bouras, N., Chergui, A., Favier, L., Amrane, A., & Dizge, N. *Biosorption characteristics of methylene blue dye by two fungal biomasses.* **International Journal of Environmental Studies**, 78(3), 2021, 365-381.

Cantarella, M., Carroccio, S. C., Dattilo, S., Avolio, R., Castaldo, R., Puglisi, C., & Privitera, V. *Molecularly imprinted polymer for selective adsorption of diclofenac from contaminated water.* **Chemical Engineering Journal**, 367, 2019, 180–188.

Cartwright, A., Jackson, K., Morgan, C., Anderson, A., & Britt, D. W. *A review of metal and metal-oxide nanoparticle coating technologies to inhibit agglomeration and increase bioactivity for agricultural applications.* **Agronomy,** 2020, 1–20.

Chao, Y., Tang, B., Luo, J., Wu, P., Tao, D., Chang, H., Chu, X., Huang, Y., Li, H., & Zhu, W. *Hierarchical porous boron nitride with boron vacancies for improved adsorption performance to antibiotics.* **Journal of Colloid and Interface Science,** 584, 2021, 154–163.

Cheng, J., Zhan, C., Wu, J., Cui, Z., Si, J., Wang, Q., Peng, X., & Turng, L. S. *Highly efficient removal of methylene blue dye from an aqueous solution using cellulose acetate nanofibrous membranes modified by polydopamine*. **ACS omega**, 5(10), 2020, 5389-5400.

Contreras, M., Grande-Tovar, C.D., Vallejo, W., & Chaves-López, C. *Bio-removal of methylene blue from aqueous solution by Galactomycesgeotrichum KL20A*. **Water,** 11(2), 2019, 282.

Dai, Y., Liu, M., Li, J., Yang, S., Sun, Y., Sun, Q., Wang, W., Lu, L., Zhang, K., Xu, J., Zheng, W., Hu, Z., Yang, Y., Gao, Y., & Liu, Z. *A review on pollution situation and treatment methods of tetracycline in groundwater.* **Separation Science and Technology (Philadelphia)**, 55, 2020, 1005–1021.

Dante, R.C., Trakulmututa, J., Meejoo-Smith, S., Martín-Ramos, P., Chamorro-Posada, P., Rutto, D., & Sánchez-Arévalo, F.M. *Methylene blue-carbon nitride system as a reusable air-sensor*. **Materials Chemistry and Physics**, 231, 2019, 351-356.

Delgado-González, C. R., Madariaga-Navarrete, A., Fernández-Cortés, J.M., Islas-Pelcastre, M., Oza, G., Iqbal, H. M. N., & Sharma, A. *Advances and applications of water phytoremediation: A potential biotechnological approach for the treatment of heavy metals from contaminated water.* **International Journal of Environmental Research and Public Health,** 2021, 18.

Din, M.I., Khalid, R., Najeeb, J., & Hussain, Z. *Fundamentals and photocatalysis of methylene blue dye using various nanocatalytic assemblies-a critical review*. **Journal of Cleaner Production**, 298, 2021, 126567.

Duan, W., Wang, N., Xiao, W., Zhao, Q., & Zheng, Y. *Ciprofloxacin adsorption onto different micro-structured tourmaline, halloysite and biotite.* **Journal of Molecular Liquids**, 269, 2018, 874–881.

Dzinun, H., Ichikawa, Y., Honda, M., & Zhang, Q. *Efficient Immobilised TiO2 in polyvinylidene fluoride membrane for photocatalytic degradation of methylene*. **J. Membr. Sci. Res**., 6, 2020, 188–195.

Ebi, O. E., Taiwo, A. F., & Folorunsho, A.T. *Kinetic modelling of the biosorption of methylene blue onto wild melon (lagenariasphaerica)*. **American Journal of Chemical Engineering**, 6(6), 2018, 126-134.

Elgarahy, A. M., Elwakeel, K. Z., Mohammad, S. H., & Elshoubaky, G. A. *A critical review of biosorption of dyes, heavy metals and metalloids from wastewater as an efficient and green process.* **Cleaner Engineering and Technology,** 4, 2021, 100209.

Eniola, J. O., Kumar, R., & Barakat, M. A. *Adsorptive removal of antibiotics from water over natural and modified adsorbents.* **Environmental Science and Pollution Research**, 26, 2019, 34775–34788.

Feng, Z., Odelius, K., & Hakkarainen, M. *Tunable chitosan hydrogels for adsorption: Property control by biobased modifiers.* **Carbohydrate Polymers**, 196, 2018, 135–145.

Fito, J. Said, H., Feleke, S., & Worku, A. *Fluoride removal from aqueous solution onto activated carbon of Catha edulis through the adsorption treatment technology.* **Environ Syst Res,** 8, 2019, 1–10

Fito, J., Abrham, S., & Angassa, K. *Adsorption of methylene blue from textile industrial wastewater onto activated carbon of Partheniumhysterophorus.* **International Journal of Environmental Research**, 14(5), 2020, 501-511.

Fytianos, G., Rahdar, A., & Kyzasg, G. N. *Nanomaterials in cosmetics: Recent updates*. **Nanomaterials**, 10, 2020, 1–16.

Gao, B., Li, P., Yang, R., Li, A., & Yang, H. *Investigation of multiple adsorption mechanisms for efficient removal of ofloxacin from water using lignin-based adsorbents*. **Scientific Reports**, 9, 2019, 1–13.

Giannakopoulou, P. P., Petrounias, P., Rogkala, A., Lampropoulou, P., Gianni, E., Papoulis, D., Koutsovitis, P., Tsikouras, B., & Hatzipanagiotou, K. *Does the methylene blue test give equally satisfactory results in all studied igneous rocks relative to the identification of swelling clay minerals*. **Minerals**, 10(3), 2020, 283.

González-García, P. *Activated carbon from lignocellulosics precursors: A review of the synthesis methods, characterization techniques and applications*. **Renewable and Sustainable Energy Reviews**, 82, 2018, 1393–1414.

Gopal, G., Alex, S.A., Chandrasekaran, N., & Mukherjee, A. *A review on tetracycline removal from aqueous systems by advanced treatment techniques*. **RSC Advances,** 10, 2020, 27081–27095.

Gupta, S., Mittal, Y., Panja, R., Prajapati, K. B., & Yadav, A. K. *Conventional wastewater treatment technologies.* **Curr. Dev. Biotechnol. Bioeng.** 2021, 47–75.

Hamad, H. N. & Idrus, S. *Recent developments in the application of bio-waste-derived adsorbents for the removal of methylene blue from wastewater: a review*. **Polymers**, 14, 2022.

Hess, P. *Bonding, structure, and mechanical stability of 2D materials: The predictive power of the periodic table.* **Nanoscale Horizons**, 6, 2021, 856–892.

Hom-Diaz, A., Norvill, Z.N., Blánquez, P., Vicent, T., & Guieysse, B. *Ciprofloxacin removal during secondary domestic wastewater treatment in high rate algal ponds.* **Chemosphere,** 180, 2017, 33–41.

Hou, C., Hu, B., & Zhu, B. *Photocatalytic degradation of methylene blue over TiO2 pretreated with varying concentrations of NaOH.* **Catalysts,** 8(12), 2018, 575.

Hu, Z. P., Gao, Z. M., Liu, X., & Yuan, Z. Y. *High-surface-area activated red mud for efficient removal of methylene blue from wastewater.* **Adsorption Science & Technology,** 36(1-2), 2018, 62-79.

Huo, J. B., Gupta, K., Lu, C., Bruun Hansen, H. C., & Fu, M. L. *Recyclable high-affinity arsenate sorbents based on porous $Fe_2O_3/La_2O_2CO_3$ composites derived from Fe-La-C frameworks. Colloids and Surfaces A:* **Physicochemical and Engineering Aspects,** 585, 2020, 124018.

Ida, S., & Eva, T. *Removal of heavy metals during primary treatment of municipal wastewater and possibilities of enhanced removal: A review.* **Water (Switzerland),** 2021, 13.

Inamuddin, S. *Xanthan gum/titanium dioxide nanocomposite for photocatalytic degradation of methyl orange dye*. **International Journal of Biological Macromolecules**, 121, 2019, 1046-1053.

Iwuozor, K. O., Ighalo, J. O., Ogunfowora, L. A., Adeniyi, A. G., & Igwegbe, C. A. *An empirical literature analysis of adsorbent performance for methylene blue uptake from aqueous media*. **Journal of Environmental Chemical Engineering**, 9(4), 2021, 105-658.

Jalloul, G., Keniar, I., Tehrani, S., & Boyadjian, C. *Antibiotics Contaminated Irrigation Water: An Overview on Its Impact on Edible Crops and Visible Light Active Titania as Potential Photocatalysts for Irrigation Water Treatment.* **Frontiers in Environmental Science**, 2021, 1–29.

Javid, N., Honarmandrad, Z., & Malakootian, M. *Ciprofloxacin removal from aqueous solutions by ozonation with calcium peroxide.* **Desalination and Water Treatment,** 174, 2020, 178–185.

Jawad, A. H., Bardhan, M., Islam, M. A., Syed-Hassan, S. S. A., Surip, S. N., ALOthman, A. Z., & Khan, A. Z. *Insights into the modeling, characterization and adsorption performance of mesoporous activated carbon from corn cob residue via microwave-assisted H_3PO_4 activation.* **Surfaces and Interfaces**, 21, 2020, 100688.

Jeevanandam, J., Barhoum, A., Chan, Y. S., Dufresne, A., & Danquah, A. M. *Review on nanoparticles and nanostructured materials: History, sources, toxicity and regulations.* **Beilstein Journal of Nanotechnology**, 2018, 1050–1074.

Jia, P., Tan, H., Liu, K., & Gao, W. *Removal of methylene blue from aqueous solution by bone char.* **Applied Sciences**, 8(10), 2018, 1903.

Jjagwe, J., Olupot, P. W., Menya, E., & Kalibbala, H. M. *Synthesis and application of granular activated carbon from biomass waste materials for water treatment: a review.* **Journal of Bioresources and Bioproducts**, 6, 2021, 292–322.

Khan, I., Saeed, K., Ali, N., Khan, I., Zhang, B., & Sadiq, M. *Heterogeneous photodegradation of industrial dyes: an insight to different mechanisms and rate affecting par*. **Current Analytical Chemistry**, 2(1), 2020, 16-70.

Khan, I., Saeed, K., Zekker, I., Zhang, B., Hendi, A. H., Ahmad, A., Ahmad, S., Zada, N., Ahmad, H., Shah, L. A., & Shah, T. *Review on methylene blue: its properties, uses, toxicity and photodegradation.* **Water,** 14(2), 2022, 242.

Kokorina, A. A., Ermakov, A. V., Abramova, A. M., Goryacheva, I. Y., & Sukhorukov, G. B. *Carbon nanoparticles and materials on their basis.* **Colloids and Interfaces**, 2020, 4-42.

Kong, W., Gao, Y., Yue, Q., Li, Q., Gao, B., Kong, Y., Wang, X., Zhang, P., & Wang, Y. *Performance optimization of CdS precipitated graphene oxide/polyacrylic acid composite for efficient photodegradation of chlortetracycline.* **Journal of Hazardous Materials, 388** 388, 2020, 121780.

Lawagon, C. P., Amon, R. E. C., Lawagon, C. P., & Amon, R. E. C. *Magnetic rice husk ash'cleanser'as efficient methylene blue adsorbent.* **Environmental Engineering Research**, 25(5), 2019, 685-692.

Lee, J., & Patel, A. *Wastewater treatment by polymeric microspheres: a review.* **Polymers**, 14, 2022, 1–37.

Li, S., & Hu, J. *Photolytic and photocatalytic degradation of tetracycline: Effect of humic acid on degradation kinetics and mechanisms.* **Journal of Hazardous Materials,** 318, 2016, 134–144.

Li, Y., Zhao, J., Zhang, G., Zhang, L., Ding, S., Shang, E., & Xia, A. *Visible-light-driven photocatalytic disinfection mechanism of Pb-BiFeO3/rGO photocatalyst.* **Water Research,** 161, 2019, 251–261.

Lin, J., Luo, Z., Liu, J., & Li, P. *Photocatalytic degradation of methylene blue in aqueous solution by using ZnO-SnO_2 nanocomposites*. **Materials Science in Semiconductor Processing,** 87, 2018, 24-31.

Liu, D., Xie, Q., Huang, X., Wan, C., Deng, F., Liang, D., & Liu, J. *Backwashing behavior and hydrodynamic performances of granular activated carbon blends.* **Environmental Research**, 184, 2020, 109302.

Liu, L. He, D., Pan, F., Huang, R., Lin, H., & Zhang, L. *Comparative study on treatment of methylene blue dye wastewater by different internal electrolysis systems and COD removal kinetics, thermodynamics and mechanism.* **Chemosphere,** 238, 2020, 124671.

López-Carballo, G., Muriel-Galet, V., Hernández-Muñoz, P., & Gavara, R. *Chromatic sensor to determine oxygen presence for applications in intelligent packaging*. **Sensors**, 19(21), 2019, 4684.

Lu, G., Nagbanshi, M., Goldau, N., Mendes Jorge, M., Meissner, P., Jahn, A., Mockenhaupt, F. P., & Mueller, O. *Efficacy and safety of methylene blue in the treatment of malaria: a systematic review.* **BMC medicine**, 16(1), 2018, 1-16.

Luo, B., Huang, G., Yao, Y., An, C., Zhang, P., & Zhao, K. *Investigation into the influencing factors and adsorption characteristics in the removal of sulfonamide antibiotics by carbonaceous materials*. **Journal of Cleaner Production**, 2021, 319-128692.

Makeswari, M., & Saraswathi, P. *Photo catalytic degradation of methylene blue and methyl orange from aqueous solution using solar light onto chitosan bi-metal oxide composite.* **SN Applied Sciences**, 2(3), 2020, 1-12.

Malakootian, M., & Ahmadian, M. *Ciprofloxacin removal by electro-activated persulfate in aqueous solution using iron electrodes.* **Applied Water Science,** 9, 2019, 1–10.

Malakootian, M., Nasiri, A., Asadipour, A., & Kargar, E. *Facile and green synthesis of ZnFe2O4@CMC as a new magnetic nanophotocatalyst for ciprofloxacin degradation from aqueous media.* **Process Safety and Environmental Protection,** 129, 2019, 138–151.

Mallakpour, S., & Azimi, F. *Polymer nanocomposites based on alginate and their blends for remediation of pollutants from wastewater*. **Nat. Polym. Green Adsorbents Water Treat. Elsevier,** 2021, 307–332.

Mallek, M., Chtourou, M., Portillo, M., Monclús, H., Walha, K., ben Salah, A., & Salvadó, V. *Granulated cork as biosorbent for the removal of phenol derivatives and emerging contaminants.* **Journal of Environmental Management**, 223, 2018, 576–585.

Manimohan, M., Pugalmani, S., Ravichandran, K., & Sithique, A. *Synthesis and characterisation of novel Cu (II)-anchored biopolymer complexes as reusable materials for the photocatalytic degradation of methylene blue.* **RSC advances**, 10(31), 2020, 18259-18279.

Marimuthu, M., Praveen Kumar, B., MariyaSalomi, L., Veerapandian, M., & Balamurugan, K. *Methylene blue-fortified molybdenum trioxide nanoparticles: harnessing radical scavenging property*. **ACS applied materials & interfaces**, 10(50), 2018, 43429-43438.

Mashkoor, F., & Nasar, A. *Magsorbents: Potential candidates in wastewater treatment technology–A review on the removal of methylene blue dye.* **Journal of magnetism and magnetic materials,** 500, 2020, 166408.

Mijinyawa, A.H., Durga, G., & Mishra, A. *A sustainable process for adsorptive removal of methylene blue onto a food grade mucilage: kinetics, thermodynamics, and equilibrium evaluation.* **International Journal of Phytoremediation**, 21(11), 2019, 1122-1129.

Morin-crini, N., Lichtfouse, E., Fourmentin, M., Ribeiro, A., Noutsopoulos, C., Mapelli, F., Fenyvesi, E., Vieira, M., Picos-corrales, L., Moreno-piraján, J., Morin-crini, N., Lichtfouse, E., Fourmentin, M., Ribeiro, A., Noutsopoulos, C., Lichtfouse, E., Schwarzbauer, J., Emerg-, D.G., Morin-crini, N., Lichtfouse, E., & Fourmentin, M. *Remediation of emerging contaminants.* **Environ. Chem. a Sustain. World,** 2022, 1–106.

Moulahoum, F. Ghorbanizamani, E. G., & S. Timur. *Nano-scaled materials and polymer integration in biosensing tools*. **Biosensors,** 12, 2022.

Mustapha, D., Shuaib, D. T., Ndamitso, M. M., Etsuyankpa, M. B., Sumaila, A., Mohammed, M. A., & Nasirudeen, M.B. *Adsorption isotherm, kinetic and thermodynamic studies for the*

removal of Pb(II), Cd(II), Zn(II) and Cu(II) ions from aqueous solutions using Albizialebbeck pods. **Applied Water Science**, 9, 2019, 1–11.

Nedu, M. E., Tertis, M., Cristea, C., & Georgescu, A. V. *Comparative study regarding the properties of methylene blue and proflavine and their optimal concentrations for in vitro and in vivo applications*. **Diagnostics**, 10(4), 2020, 223.

Parakala, S., Moulik, S., & Sridhar, S. *Effective separation of methylene blue dye from aqueous solutions by integration of micellar enhanced ultrafiltration with vacuum membrane distillation.* **Chemical Engineering Journal**, 375, 2019, 122015.

Pham,V. L., Kim, D. G., & Ko, S. O. *Mechanisms of methylene blue degradation by nano-sized β-MnO2 particles.* **KSCE Journal of Civil Engineering**, 24(5), 2020, 1385-1394

Pohl, A. *Removal of heavy metal ions from water and wastewaters by sulfur-containing precipitation agents.* **Water, Air, and Soil Pollution**, 2020, 231.

Polińska, W., Kotowska, U., Kiejza, D., & Karpińska, J. *Insights into the use of phytoremediation processes for the removal of organic micropollutants from water and wastewater; a review.* **Water (Switzerland),** 2021, 13.

Popok, V. N., & Kylián, O. *Gas-phase synthesis of functional nanomaterials.* **Applied Nano**, 2020, 25–58.

Qu, F., Liang, H., He, J., Ma, J., Wang, Z., Yu, H., & Li, G. *Characterization of dissolved extracellular organic matter (dEOM) and bound extracellular organic matter (bEOM) of Microcystis aeruginosa and their impacts on UF membrane fouling.* **Water Research, 46** 46, 2012, 2881–2890.

Sabar, S., Aziz, H. A., Yusof, N. H., Subramaniam, S., Foo, K. Y., Wilson, L. D. and Lee, H. K. *Preparation of sulfonated chitosan for enhanced adsorption of methylene blue from aqueous solution*. **Reactive and Functional Polymers,** 151, 2020, 104584.

Sabzehmeidani, M. M., Mahnaee, S., Ghaedi, M., Heidari, H., & Roy, V. A. L. *Carbon based materials: A review of adsorbents for inorganic and organic compounds.* **Materials Advances,** 2, 2021, 598–627.

Saha, B., Chowdhury, S., Sanyal, D., Chattopadhyay, K., & Suresh Kumar, G. *Comparative study of toluidine blue O and methylene blue binding to lysozyme and their inhibitory effects on protein aggregation*. **ACS omega,** 3(3), 2018, 2588-2601.

Saha, S., Bansal, S., & Khanuja, M. *Classification of nanomaterials and their physical and chemical nature.* **Nano-enabled Agrochem. Agric. (Elsevier, 2022)**, 2022, 7–34.

Saleem, J., Bin Shahid, U., Hijab, M., Mackey, H., & McKay, G. *Production and applications of activated carbons as adsorbents from olive stones.* **Biomass Conversion and Biorefinery**, 9, 2019, 775–802.

Samal, K., Mahapatra, S., & Hibzur Ali, M. *Pharmaceutical wastewater as emerging contaminants (ec): treatment technologies, impact on environment and human health.* **Energy Nexus**, 6, 2022, 100076.

Samuel, J. J., & Yam, F. K. *Photocatalytic degradation of methylene blue under visible light by dye sensitized titania*. **Materials Research Express**, 7(1), 2020, 015051.

Santoso, E., Ediati, R., Kusumawati, Y., Bahruji, H., Sulistiono, D. O., & Prasetyoko, D. *Review on recent advances of carbon based adsorbent for methylene blue removal from waste water.* **Materials Today Chemistry**, 16, 2020, 100233.

Sarma, G. K., Sen, S., Gupta, E., & Bhattacharyya, K. G. *Removal of hazardous basic dyes from aqueous solution by adsorption onto kaolinite and acid-treated kaolinite: kinetics, isotherm and mechanistic study.* **SN Applied Sciences**, 1(3), 2019, 1-15.

Selmi, T., Seffen, M., Celzard, A., & Fierro, V. *Effect of the adsorption pH and temperature on the parameters of the Brouers–Sotolongo models*. **Environmental Science and Pollution Research**, 27, 2020, 23437–23446.

Shakoor, S., & Nasar, A. *Adsorptive treatment of hazardous methylene blue dye from artificially contaminated water using cucumissativus peel waste as a low-cost adsorbent.* **Groundwater for Sustainable Development**, 5, 2017, 152-159.

Sharma, G., Sharma, S., Kumar, A., Lai, C.W., Naushad, M., Shehnaz, Iqbal, J., & Stadler, F.J. *Activated carbon as superadsorbent and sustainable material for diverse applications.* **Adsorption Science & Technology,** 2022, 1–21.

Sheng, L., Zhang, Y., Tang, F., & Liu, S. *Mesoporous/microporous silica materials: preparation from natural sands and highly efficient fixed-bed adsorption of methylene blue in wastewater.* **Microporous and Mesoporous Materials**, 257, 2018, 9-18.

Srivatsav, P., Bhargav, B. S., Shanmugasundaram, V., Arun, J., Gopinath, K. P., & Bhatnagar, A. *Biochar as an eco-friendly and economical adsorbent for the removal of colorants (Dyes) from aqueous environment: A review*. **Water (Switzerland),** 12, 2020, 1–27.

Su, H., Li, W., Han, Y., & Liu, N. *Magnetic carboxyl functional nanoporous polymer: Synthesis, characterization and its application for methylene blue adsorption.* **Scientific Reports**, 2018, 1–8.

Subha, V., Divya, K., Gayathri, S., Jagan Mohan, E., Keerthanaa, N., Vinitha, M., Kirubanandan, S., & Renganathan, S. *Applications of iron oxide nanocomposite in waste water.* **Water, Air, and Soil Pollution,** 2018, 21-22.

Sun, L., Hu, D., Zhang, Z., & Deng, X. *Oxidative degradation of methylene blue via PDS-based advanced oxidation process using natural pyrite.* **International Journal of Environmental Research and Public Health,** 16(23), 2019, 4773.

Tara, N., Siddiqui, S. I., Rathi, G., Chaudhry, S. A., & Asiri, A. M. Nano-*engineered adsorbent for the removal of dyes from water: A review*. **Current Analytical Chemistry**, 16(1), 2020, 14-40.

Tasca, A.L., Clematis, D., Stefanelli, E., Panizza, M., & Puccini, M. *Ciprofloxacin removal: BDD anode coupled with solid polymer electrolyte and ultrasound irradiation.* **Journal of Water Process Engineering,** 33, 2020, 101074.

Tenorio, R., Fedders, A.C., Strathmann, T., & Guest, S.J. *Impact of growth phases on photochemically produced reactive species in the extracellular matrix of algal cultivation systems.* **Environmental Science: Water Research and Technology,** 3, 2017, 1095–1108.

Thabede, P. M., Shooto, N. D., & Naidoo, E. B. *Removal of methylene blue dye and lead ions from aqueous solution using activated carbon from black cumin seeds*. **South African Journal of chemical engineering,** 33(1), 2020, 39-50.

Tian, Y., Zou, J., Feng, L., Zhang, L., & Liu, Y. *Chlorella vulgaris enhance the photodegradation of chlortetracycline in aqueous solution via extracellular organic matters (EOMs): Role of triplet state EOMs.* **Water Research,** 149, 2019, 35–41.

Torres, E. *Biosorption: A review of the latest advances*. **Processes**, 8, 2020, 1–23.

Uddin, M. K., & Nasar, A. *Decolorization of basic dyes solution by utilizing fruit seed powder*. **KSCE Journal of Civil Engineering**, 24(2), 2020, 345-355.

Wammer, K.H., Korte, A.R., Lundeen, R.A., Sundberg, J.E., McNeill, K., & Arnold, W.A. *Direct photochemistry of three fluoroquinolone antibacterials: Norfloxacin, ofloxacin, and enrofloxacin.* **Water Research,** 47, 2013, 439–448.

Wang, L., Huang, X., Han, M., Lyu, L., Li, T., Gao, Y., Zeng, Q., & Hu, C. *Efficient inhibition of photogenerated electron-hole recombination through persulfate activation and dual-pathway degradation of micropollutants over iron molybdate.* **Applied Catalysis B: Environmental,** 257, 2019, 117904.

Wang, Y., Zhou, Y., Jiang, G., Chen, P. & Chen, Z. *One-step fabrication of carbonaceous adsorbent from corncob for enhancing adsorption capability of methylene blue removal.* **Scientific Reports**, 10, 2020, 1–9.

Wang, Z., Gao, M., Li, X., Ning, J., Zhou, Z., & Li, G. *Efficient adsorption of methylene blue from aqueous solution by graphene oxide modified persimmon tannins.* **Materials Science and Engineering**, 108, 2020, 110196.

Wei, L., Li, H., & Lu, J. *Algae-induced photodegradation of antibiotics: a review*. **Environmental Pollution,** 272, 2021, 115589.

Wei, X., Wang, Y., Feng, Y., Xie, X., Li, X., & Yang, S. *Different adsorption-degradation behavior of methylene blue and Congo red in nanoceria/H2O2 system under alkaline conditions*. **Scientific reports,** 9(1), 2019, 1-10.

Xiong, J., Guo, S., Zhao, T., Liang, Y., Liang, J., Wang, S., Zhu, H., Zhang, L., Zhao, J. R., & Chen, G. *Degradation of methylene blue by intimate coupling photocatalysis and biodegradation with bagasse cellulose composite carrier.* **Cellulose,** 27, 2020, 3391–3404.

Xu, L., Zhang, M., Wang, Y., & Wei, F. *Highly effective adsorption of antibiotics from water by hierarchically porous carbon: Effect of nanoporous geometry.* **Environmental Pollution,** 274, 2021, 116591.

Yang, J., Lv, G., Zhang, C., Wang, Z., & Sun, X. *Indirect photodegradation of sulfamethoxazole and trimethoprim by hydroxyl radicals in aquatic environment: Mechanisms, transformation products and eco-toxicity evaluation.* **International Journal of Molecular Sciences,** 21, 2020, 1–14.

Zabłocka-Godlewska, E., Przystaś, W., & Grabińska-Sota, E. *Possibilities of obtaining from highly polluted environments: new bacterial strains with a significant decolorization potential of different synthetic dyes*. **Water, Air, and Soil Pollution,** 2019, 229.

Zamel, D., Hassanin, A.H., Ellethy, R., Singer, G., & Abdelmoneim, A. *Novel bacteria-immobilized cellulose acetate/poly (ethylene oxide) nanofibrous membrane for wastewater treatment.* **Scientific reports**, 9(1), 2019, 1-11.

Zare, N. G., Fallah, Z., Le, V. T., Doan, V. D., Mudhoo, A. W., Joo, S., Vasseghian, Y., Tajbakhsh, M., Moradi, O., Sillanpää, M., & Varma, R. S. *Remediation of pharmaceuticals from contaminated water by molecularly imprinted polymers: a review* **Springer International Publishing**. 2022.

Zhang, Y., An, Y., Wu, L., Chen, H., Li, Z., Dou, H., Murugadoss, V., Fan, J., Zhang, H., Mai, X., & Guo, Z. *Metal-free energy storage systems: combining batteries with capacitors based on a methylene blue functionalized graphene cathode*. **Journal of Materials Chemistry A**, 7(34), 2019, 19668-19675.

Zhao, Q., Wang, J., Li, Z., Guo, Y., Wang, J., Tang, B., Abudula, A., & Guan, G. *Heterostructured graphitic-carbon-nitride-nanosheets/copper(I) oxide composite as an enhanced visible light photocatalyst for decomposition of tetracycline antibiotics.* **Separation and Purification Technology**, 250, 2020, 117238.

Appendices

APPENDIX 1: Determination of λmax for Methylene Blue Solution.

S/N	Wavelength (nm)	Absorbance
1	**600**	**0.341**
2	**610**	**0.432**
3	**620**	**0.502**
4	**630**	**0.651**
5	**640**	**0.736**
6	**645**	**0.851**
7	**650**	**0.866**
8	**655**	**0.802**
9	**660**	**0.478**
10	**664**	**0.172**

11	**668**	**0.036**

APPENDIX 2: Calibration curve for the methylene blue

S/N	Concentration (mg/L)	Absorbance
1	0	0
2	1	0.013
3	2	0.029
4	3	0.042
5	4	0.065
6	5	0.084

7	10	0.138
8	15	0.774
9	20	0.698

APPENDIX 3: Adsorption of methylene blue solution on the snail shell

Time (min)	Initial concentration (ppm)	Ph	Adsorbent dosage (mg)
1	25	3	10
5	50	5	20
10	100	7	30
20	200	9	40
30	250	11	50
40	300	13	100

60	350	15	150
120	400	17	200

Bio-data

A. PERSONAL DATA

Full Names	**Abisoye Abidemi, ADARAMAJA**
Permanent Home Address	7, Arowojolu Street Lodge, Oke-ado, Ibadan, Oyo State.
E-mail Address	bisoye016@yahoo.com
Phone Number	08034129682
Date of Birth	16th August, 1986
Place of Birth	Ogun
Nationality	Nigerian

Next of kin Mrs. Obasuyi Yetunde

B. EDUCATION BACKGROUND

Educational Institutions Attended with Dates and Qualifications

- Lead City University, {**MSc. Industrial Chemistry**} 2021 – till date
- Olabisi Onabanjo University, {**BSc. in Industrial Chemistry**} 2009-2012
- Shamudeen Grammar School, Ijebu-Igbo, Ogun State
- (**Senior Secondary School Certificate**) 1997-2002

C. WORK EXPERIENCE WITH DATES

- Ijebu North Local Government Health Centre 2010-2012

D. PUBLICATION: Thesis and Dissertation

- Photochemical Composition of *Blighia sapida* Leaves

E. REFEREES

1. Dr. A. O. Bamisaye

   Department of Chemical Sciences

   (*Industrial Chemsitry, Chemistry Unit*)

   Lead City University,

   Ibadan, Oyo State.

2. Dr. O. K. Oderinde

   Department of Chemical Sciences

   (*Industrial Chemsitry, Chemistry Unit*)

   Lead City University,

   Ibadan, Oyo State.

---------- ----------

Signature **Date**

The University Compliance Certification

This is to certify that this Thesis written by Abisoye Abidemi, ADARAMAJA with matriculation number LCU/PG/002217 in the Department of Chemical Science, Faculty of Applied Sciences, Lead City University, Ibadan, Oyo State is in full compliance with approved University format and style.

---------- ----------

Signature **Date**